UNIVERSITY OF NATAL

FUZZY LOGIC POWER SYSTEM STABILISER IN MULTI-MACHINE STABILITY STUDIES

by

Geeven Valayatham Moodley

BScEng

Submitted in fulfillment of the academic requirements for the degree of Masters in Science, Engineering, in the School of Electrical and Electronic Engineering, University of Natal, Durban, South Africa

October 2003

I hereby declare that all the material incorporated into this thesis is my own original and unaided work except where specific reference is made by name or in the form of a numbered reference. The work contained herein has not been submitted for a degree at any other university.

Signed: _____

GEEVEN VALAYATHAM MOODLEY

As the candidate's supervisor I have approved this thesis for submission.

Signed: _____ Name: Professor R G Harley Date : 10 May 2003

ABSTRACT

Conventional power system stabilisers (PSS) are designed to eliminate poorly damped, low frequency power oscillations that occur between remote generating pools or power stations, due to different types and settings of the automatic voltage regulators at different power stations. The supplementary control of the PSS is exerted on the power system through a generator's excitation system to which the PSS is attached. In order to design these conventional power system stabilisers, requires accurate system data and an in-depth knowledge of classical control theory. This thesis investigates the use of an intelligent, non-linear PSS that utilises fuzzy logic techniques. Others have proposed the concept of such a PSS, since it does not require accurate system data.

This thesis describes the basic aspects of power system stability. Thereafter the methods of modelling synchronous machines in a multi-machine power system are presented. The sample power system being studied and the simulation packages used in the investigations are introduced and the methods involved to design and tune a conventional power system stabiliser using classical control theory and design methods proposed by others, are discussed.

The general concept of fuzzy logic is introduced and the application of fuzzy logic techniques to controller design is explained. Using the principles of fuzzy logic controller design, a fuzzy logic power system stabiliser utilising 9 rules is designed and tuned for the multi-machine power system under investigation. The fuzzy logic stabiliser is then applied to a synchronous motor in a pump storage scheme. Previous work has applied fuzzy logic stabilisers only to synchronous generators.

To further compare the performance of the 9 rule fuzzy stabiliser, a 49 rule stabiliser developed by other researchers, and adapted to operate on the synchronous motor, is evaluated.

Computer simulated results of each of the stabiliser's performances are presented. The results of the 9 rule fuzzy stabiliser are compared with the performance of a conventional linear stabiliser as well as with a 49 rule fuzzy stabiliser. The robustness properties of the fuzzy stabilisers are evaluated. The results further prove that with proper membership function selection, a simple fuzzy stabiliser that demands very little computational overheads can be achieved to provide adequate system damping.

ACKNOWLEDGEMENTS

The work presented in this thesis was carried out under the supervision of Professor Ronald G Harley of the School of Electrical and Electronic Engineering, University of Natal, Durban. I wish to thank Professor Harley for his support, guidance and patience throughout my postgraduate studies, and for his efforts during the correction of this document.

In addition I would also like to thank:

Dr. Glenn Jennings for his assistance, suggestions and guidance during the investigation phase of this project.

my postgraduate colleagues Dr. Ganesh Kumar Venayagamoorthy, Dr. Bruce Rigby, Messrs Timothy Rae and Bruce van Blerk, for their assistance, encouragement and guidance.

my work colleagues Michael Coker and Kannan Lakmeeharan, for their suggestions, assistance and for initiating this project.

and finally, my wife, Vasinthee, son, Eshen, family and friends for their support, patience and encouragement.

The financial support of the University of Natal and the National Research Foundation, are also gratefully acknowledged.

TABLE OF CONTENTS

LIST OF SYMBOLS

The commonly used symbols and notations adopted in this thesis are listed below. Other symbols used in the text are explained where they first occur.

Acronyms

AC	alternating current
AVR	automatic voltage regulator
DC	direct current
DOM	degree of membership
FLPSS	fuzzy logic power system stabiliser
HVDC	High voltage direct current
MAX	maximum
MIN	minimum
MMF	magneto-motive force
PSS	power system stabiliser
rms	root mean square

Synchronous machine symbols

δ	rotor angle
θ	angular position
Ψ	flux linkage
ω_o	synchronous speed
ω	rotor speed
i	current – instantaneous
u	voltage – instantaneous
d,q	rotor reference frame - direct and quadrature axis respectively
D,Q	Direct and quadrature axes in synchronous reference frame
L_{md}	mutual inductance – d axis
L_{mq}	mutual inductance – q axis
M_e	electrical torque
s	slip
X	reactance

Conventional Stabiliser Symbols

T_w	washout time constant
K_{stab}	stabiliser gain
T_1,T_2,T_3,T_4	phase compensation time constants
V_{smax}	stabiliser maximum output limit
V_{smin}	stabiliser minimum output limit

General

pu	per unit
p	derivative operator d/dt
∂	Partial differential operator
Δ	Small change operator
x_o	Signifies steady state value of variable x
$\dot{x}$	Signifies the time differential of variable x

CHAPTER ONE

INTRODUCTION

1.1 Objectives and historical perspective

The electric power system has grown, over the past century, to become, mathematically modeled, one of the highest order systems created by man to date. A power system is a non-linear, non-stationary system which is continually in a dynamic state, albeit small changes (a kettle drawing load) or large variations (rejection of a large induction motor off the system). There is a continual variance in the power system to match the generated power to the required load and achieve equilibrium, over a large interconnected network. Nevertheless, most power systems are operated with an exceptionally high reliability, due mostly to the large margin of safety included in the designs.

In order to help maintain this equilibrium in the power system, specific control devices have been devised over the years. One such controller is a power system stabiliser. The purpose of a power system stabiliser is to help reduce low frequency power oscillations, which can often be found between a generating station and the network or between groups of generating stations within a network. The power system stabiliser provides a supplementary control signal to the generator's excitation system controller, to help damp out these low frequency oscillations.

Power system stabilisers are therefore found in many generating stations around the world. The method of using classical linear control theory to design and tune power system stabilisers is well documented in many publications. They are tuned for best performance at a selected operating condition of the power system so that the non-linear system equations may be linearised for small changes around this condition. At any other operating condition, the performance of the stabiliser therefore degrades. Even the normal excitation system controller is linear and designed and tuned in the same way, with similar degradation at other operating points. A non-linear power system really needs a non-linear stabiliser and a non-linear excitation system controller.

In recent years there have been studies into using non-linear controllers and stabilisers based on artificial intelligence techniques. The use of neural networks in power system stabilisers has been investigated in an attempt to create smarter controllers [ZHANG1,2, HSU]. [HASSAN1] was one of the earlier attempts to utilise fuzzy logic techniques in a power system stabiliser. Though the use of fuzzy logic techniques for stabiliser design and application was proven successful, the stabiliser was applied to a simple single machine, infinite bus system (SMIB). Further work by [HASSAN2], [SHI], [EL-MET1],[TOLIYAT]

and [CHEN] successfully demonstrated the application of a fuzzy logic power system stabiliser on a single machine, infinite bus system. [HASSAN2], [HIYAMA1] and [EL-MET2] successfully demonstrated the application of a fuzzy logic power system stabiliser (FLPSS) in on a SMIB system in a 3kW laboratory generator (called a "micro-machine"). These practical investigations were performed on a single-machine infinite bus system.

In September 1994, a publication by [HIYAMA2] illustrated the robustness of a fuzzy logic power system stabiliser in a multi-machine power system consisting of 2 generators and an infinite bus. [HIYAMA2] compared the performance of a fuzzy logic stabiliser against the performance of a conventional stabiliser, designed using classical linear control techniques. The results prove the robustness, efficiency and feasibility of utilising a fuzzy logic power system stabiliser.

In all the references presented above, all the fuzzy logic power system stabilisers were tested on a synchronous machine that was operating in generating mode. Often, synchronous machines may be required to operate in motoring mode, as is in the case of pump-storage schemes. The effects of a fuzzy logic power system stabiliser on a synchronous machine in motoring mode have not been published.

The objective of this research is to firstly design and tune a fuzzy logic power system stabiliser (FLPSS) for application on a synchronous motor in a multi-machine environment. Thereafter the performance of the FLPSS is compared to the performance of a stabiliser, designed using classical linear control theory, and optimally tuned at one operating point of the study network. Analysing the performance of the FLPSS, a further aim is to reinforce previous research, illustrating the robustness of a fuzzy logic power system stabiliser.

1.2 Thesis Outline

Any investigation of this nature requires accurate mathematical models of the power system for computer simulation. Essential to the study of the dynamic behavior of power systems is the synchronous machine. Chapter Two of this thesis introduces the concept of power system stability. Thereafter two methods of mathematically modeling synchronous machines in computer simulations are presented along with the methods used to simulate a multi-machine system. The excitation system of the synchronous machine is also an integral part of the machine's operation and contributes to the stability of the power system. The mathematical model of an excitation system used in this investigation is presented. Lastly the power system model used to perform the studies of comparing the performance of the two different types of stabilisers is introduced.

Chapter Three introduces the classical power system stabiliser based on classical linear control theory. The various functions of each part of the classical stabiliser are described. Thereafter a design procedure to tune a conventional stabiliser is followed to create a power system stabiliser tuned for the study system presented in Chapter Two.

Chapter Four introduces the concept of fuzzy logic. The theory involving fuzzy sets and operators is discussed in order to give the reader a greater appreciation for the concept of fuzzy logic. Thereafter a generic method to create a fuzzy controller for any application is presented. This design procedure is then used to design and tune a fuzzy logic power system stabiliser utilising 9 rules. A FLPSS designed in previous research by [EL-MET1] and utilising 49 rules, is adapted for these investigations to operate on a synchronous motor. The aim of introducing the 49 rule FLPSS is to compare the performance of a 9 rule with a 49 rule FLPSS and to establish if a FLPSS using fewer rules to make decisions results in a poorer performing FLPSS.

The different power system stabilisers designed in this thesis are then tested in simulation on the study system. The system is subjected to a pre-selected fault and the response of each stabiliser is recorded. The performances of the stabilisers are compared against each other and the results are presented in Chapter Five.

The conclusions from the results of this research project are discussed in Chapter Six.

1.3 New Contributions

The work contained in this thesis is primarily an extension of theoretical work by researchers [EL-MET1, HASSAN2, HIYAMA2]. The work however does make the following meaningful and original contributions to research in the application of fuzzy logic power system stabilisers to multi-machine stability studies.

(i) The fuzzy logic stabiliser designed in this thesis is applied to a synchronous machine that is in motoring mode of operation. Previous work studied the application of fuzzy logic stabilisers to synchronous machines that are operating in generating mode. In the case of pumped storage schemes, synchronous machines are required to operate in motoring mode during pumping operation.

(ii) The fuzzy logic power system stabiliser designed in this thesis utilises just 9 rules to make decisions. This fuzzy stabiliser utilises two input signals, thus 9 rules are the absolute minimum number of rules that can be used in the decision making process of the FLPSS. The results indicate that the 9 rule FLPSS performs equally as well as a 49 rule FLPSS. The 9 rule FLPSS will also require less computational overheads than a 49 rule FLPSS, when practically implemented.

1.4 Research Publications

Many of the findings of this thesis have already been presented at refereed conferences [MOODLEY1, 2].

CHAPTER TWO

THEORETICAL BACKGROUND

2.1 Introduction

In order to understand the behaviour of a power system requires that the system be adequately modelled (mathematically) so that its dynamic characteristics can be studied. This chapter starts by defining the concept of power system stability, the various areas and the factors that affect power system stability. The one component of the power system that is central to most areas of stability, is the synchronous generator. The physical description of a synchronous machine is given before a mathematical model or description of it is established. The mathematical models developed are both in terms of algebraic equations and state space representation. Thereafter the state space representation of the excitation system for the synchronous generators used in this thesis, is described.

Finally the power system model used for this thesis is presented along with a description of the simulation software used to model the study system.

2.2 Power System Stability

Power system stability is broadly viewed as the ability of a power system to remain in equilibrium during normal operation and to return to an acceptable level of stability after being subjected to a contingency. There are basically three classifications of stability, namely, *angle* (rotor), *frequency* (mid-long term) and *voltage* stability.

Voltage stability is defined as the ability of the power system to maintain acceptable voltages at all buses in the power system under normal operating conditions or after subjected to a system disturbance. *Frequency (Mid-long term) stability* is generally concerned with the dynamic response of a power system after being subjected to a severe disturbance. A severe disturbance causes large changes in the voltage, frequency and power flows in a power system. These large changes cause slower processes and control action, not normally modelled in other stability studies, to be taken into consideration. The time of concern with this type of stability may range from several seconds to several minutes. Frequency and voltage stability are outside of the scope of this thesis and will not be dealt with any further.

Angle (rotor) stability is defined as the ability of a power system to remain in synchronism or the ability of synchronous machines in a system to remain "in-step". The stability of a synchronous machine is

fundamentally a balance between the mechanical and electrical torques of the machine. Under steady state conditions, the rotor of a synchronous machine (driven by the mechanical torque) rotates at synchronous speed creating a field also rotating in space at synchronous speed. The stator (armature) of the machine also has a rotating field that rotates at synchronous speed, hence the term "synchronism". Synchronism in a power system is largely affected by the generator power angle, also called the rotor angle.

Under balanced operation the electrical torque (M_e) is equal to the mechanical torque (neglecting losses) to maintain synchronism. Changes in the mechanical torque would cause corresponding changes in the electrical torque, ΔM_e. These changes can be resolved into two components.

$$\Delta M_e = \left(K_S . \Delta\delta\right) + \left(K_D . \Delta\omega\right) \tag{2.1}$$

where K_s is the synchronising torque coefficient and K_D is the damping torque coefficient [KUNDUR1]. The power system may become unstable due to a lack of damping and/or synchronising torques in the generator. This would result in increasing amplitude rotor angle oscillations and a steady increase in rotor angle respectively.

Angle stability has two main areas of analysis:

Transient stability is concerned with the ability of the power system to maintain synchronism after being subjected to a severe fault. The stability of the system is largely affected by the initial operating condition and the severity of the disturbance. The transient stability is usually concerned with about 1 to 10 seconds after the occurrence of the fault. "First swing" instability, due to a lack of synchronising torque, is also of concern in transient stability studies.

Small-signal stability is defined as the ability of the power system to maintain synchronism whilst being subjected to continuous small disturbances. Synchronism may be lost between a single machine and the system or between groups of machines in the system. The nature of the disturbance is deemed to be small enough to allow the power system model to be linearised around the operating point, hence allowing linear analysis of the stability of the power system. The degree of stability/instability depends on various factors such as the initial operating conditions, transmission line lengths and generator excitation controls.

In power systems studies, the damping of oscillatory instability (power swings) are of major importance. These oscillations can be further classified, depending on the mode of operation;

- *Local modes* are oscillations concerned with the synchronous machine swinging against the rest of the power system.
- *Inter-area modes* are concerned with groups of generators swinging against other group(s) of generators in the power system. This mode is usually caused by groups of closely coupled machines being interconnected by weak transmission systems.
- *Control modes* are associated with the controls on generating units, e.g. poorly tuned exciters and speed governors. HVDC converters and static var compensators can also contribute to this mode.
- *Torsional modes* are associated with the turbine-shaft system of the generator. Interactions between series-capacitor-compensated lines, excitation and governor controls are the primary cause of this type of mode.

It is clear that the synchronous machine is a fundamental component of stability studies and needs to be closely analysed. The next section takes a closer look at the physical nature and operation of a synchronous machine.

2.3 Synchronous Machines

The synchronous machine fundamentally consists of two elements, namely the *armature* or *stator* and the *rotor*. Much like the dc generator, the operation of the synchronous machine is based on Faraday's law of electromagnetic induction and can operate as both motor and generator.

The theory of synchronous machines is primarily based on the relative motion of the two cylindrical parts and the distribution of the flux in the air-gap of the machine. These parts are linked in a magnetic circuit, which is set up by currents in conductors near the surfaces of the elements. An in-depth explanation of the operation of asynchronous machine scan be found in [SAY,SYED]. Basic explanations of the integral part of a synchronous machine are given in the following sections.

2.3.1 Stator (Armature)

In power station generators the armature is contained on the stationary member or the *stator*. The stator is made up of the iron core and the armature windings. The iron core carries the magnetic flux and is laminated to reduce eddy currents and hysteresis losses. On large machines the armature windings are usually copper bars (solid or hollow to allow for cooling) that are placed on the inner periphery of the stator core as illustrated in Figure 2.1.

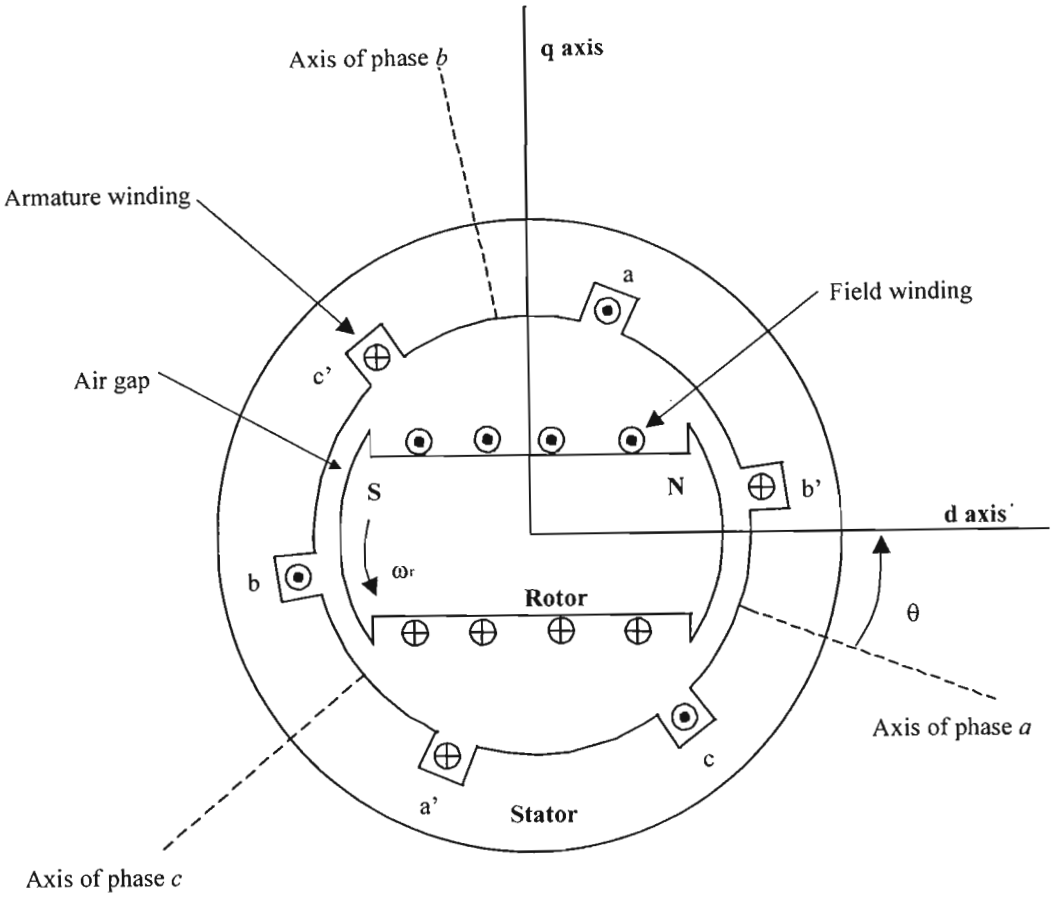

Fig.2.1 – Placement of stator phase coils with axes at 120° displacement within the stator periphery of a two-pole synchronous machine

At balanced operation, the three phase currents in the armature windings produce a magnetic field that rotates at synchronous speed in the air-gap of the machine. The armature also produces a three-phase ac voltage that is 120° apart. These voltages are much higher than those contained in the field circuit, sometimes as high as 33 kV. Therefore the stator circuit must be carefully insulated to ensure safe and efficient operation of the machine.

2.3.2 Rotor magnetic circuit

In order to generate an electric current at synchronous frequency, the stator requires a synchronously moving magnetic field. The dc current carrying rotor provides this magnetic field and is driven at synchronous speed by the turbine.

There are two types of rotors used, namely a round rotor and a salient pole rotor, shown schematically in Figure 2.2. The round rotor is found in high-speed applications such as gas and steam turbines. This rotor is characterised by its axially long shaft with diameters not normally exceeding 1.2 m. The rotor is typically made of forged steel with slots cut into the length of the metal. Copper bars or strips are usually contained in the slots along the periphery length of the rotor forming the windings of the rotor. The

salient pole rotor has a shorter axial length with a much larger diameter than the round rotor. This rotor is used in lower speed applications such as hydroelectric generating stations. Salient pole rotors have projected pole faces with concentrated windings around the pole face.

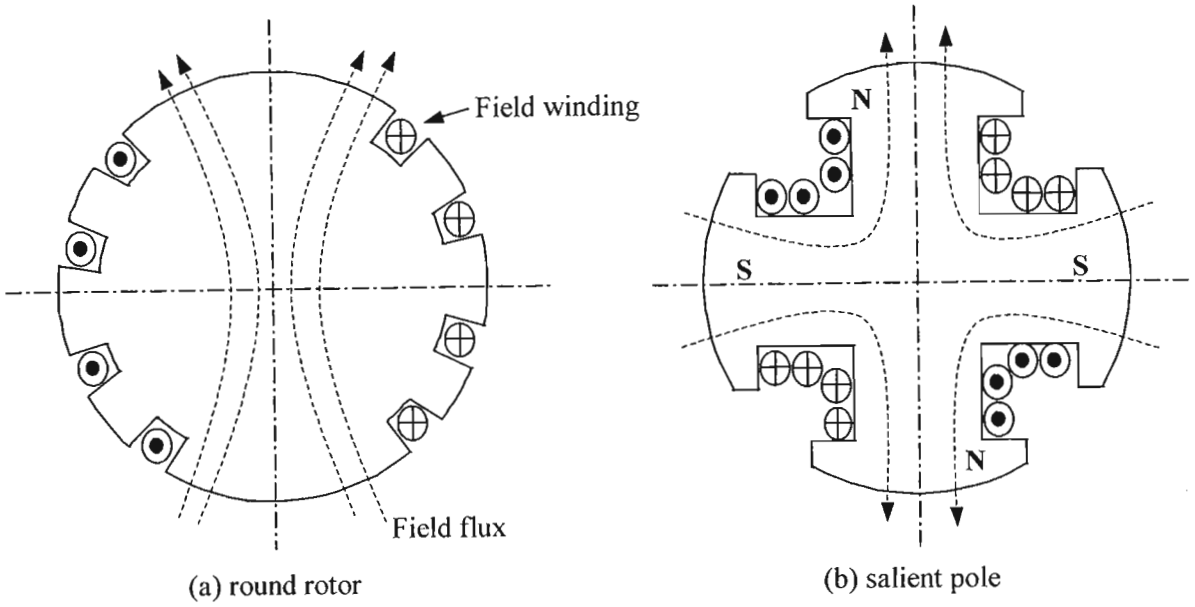

Fig. 2.2 – Field windings and magnetic field paths shown within the (a) round rotor and (b) the salient pole rotor

The rotor winding carries a dc current provided by an exciter. The rotor also contains damper bars, which reduce eddy currents during dynamic conditions of operation.

The next section develops the theory to mathematically model the physical interaction between the armature and rotor of the synchronous.

2.4 Mathematical Modelling of Synchronous Machines

The synchronous machine can be described as an interaction of currents and induced voltages in windings. The interaction of current and flux linkage develops electrical torque, which counteracts the mechanical torque. Therefore a synchronous machine can be mathematically modelled in terms of currents, voltages, flux linkages and torques.

In order to model a synchronous machine, some idealised model needs to be set up. Figure 2.3 shows the idealised synchronous machine, which has a rotating three-phase armature winding. Voltage equations for this machine's windings can be set up from the component voltages of each phase current. These

non-linear equations however are difficult to solve as the coefficients of some components vary with the angle defining the rotor position at any instant in time.

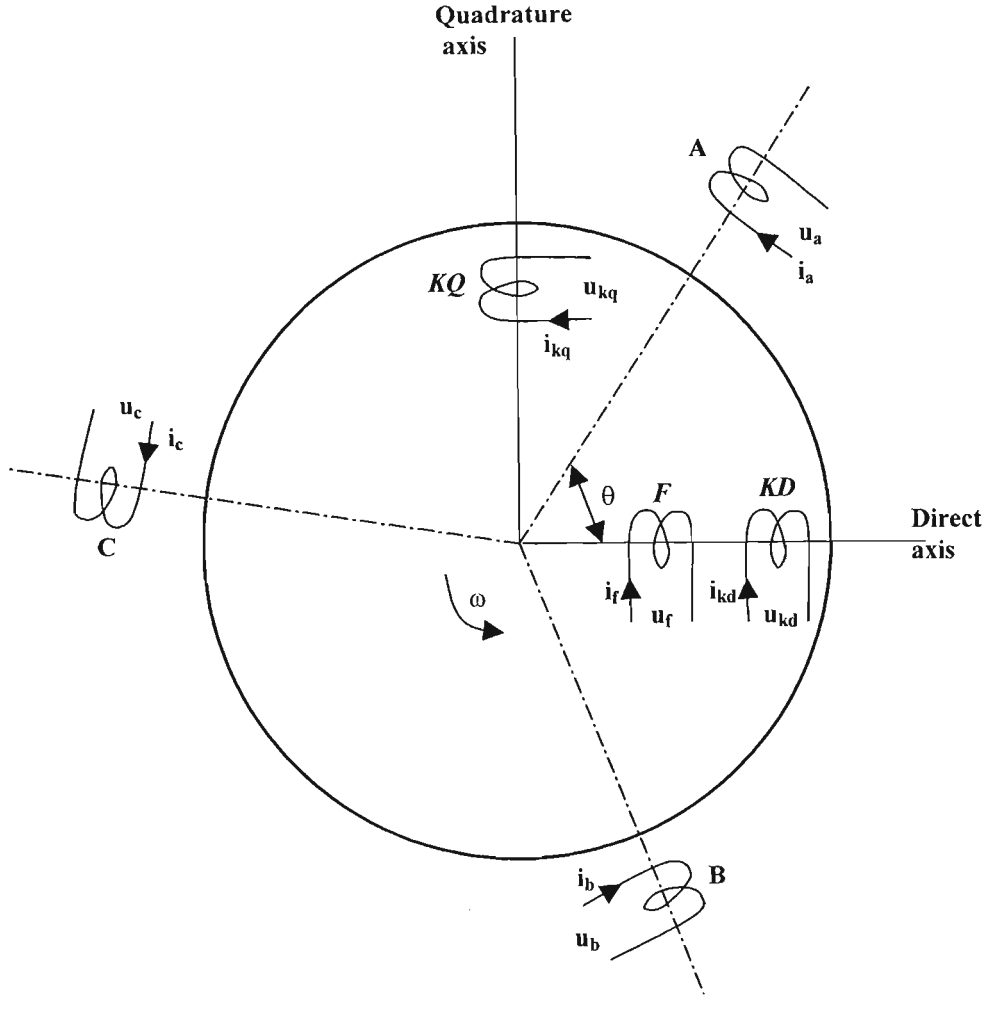

Fig.2.3 – Diagram of an idealised synchronous machine showing actual coils

Park first suggested replacing or transforming the three-phase abc armature windings by a new set of two fictitious windings (dq) [PARK1,2]. These new windings have current and voltage quantities that are different from, but related to the actual abc quantities. The method of analysis of synchronous machines by the transformed equations is known as the two-axis theory and is adopted in this thesis

To further simplify the derivation of the equations, all equations are derived in the per unit system, explained in Appendix A and using the following assumptions [ADKINS];

(a) The machine windings produce a sinusoidally distributed flux density wave.

(b) Magnetic saturation is neglected.

(c) Eddy currents are neglected.

(d) Inductance and resistance values are constant.

(e) Frictional losses are neglected.

(f) The machine construction is symmetrical with respect to the d and q axes.

(g) The d,q axes are located on the main reluctance axes of the rotor.

2.4.1 Two-axis equations of the synchronous machine

Figure 2.4 shows the idealised machine with the three-phase windings replaced by windings (d,q) on the direct (d) and quadrature (q) axes. The fictitious d,q windings carry the currents i_d and i_q which are located on the d,q axes and have the same number of turns each as a phase winding that would set up the same magneto-motive force (MMF) wave as the actual currents i_a, i_b, i_c. Since three windings are replaced by two axis windings, the base value of current in the d,q axis windings is changed to one and a half times the base value of current in the abc phase windings.

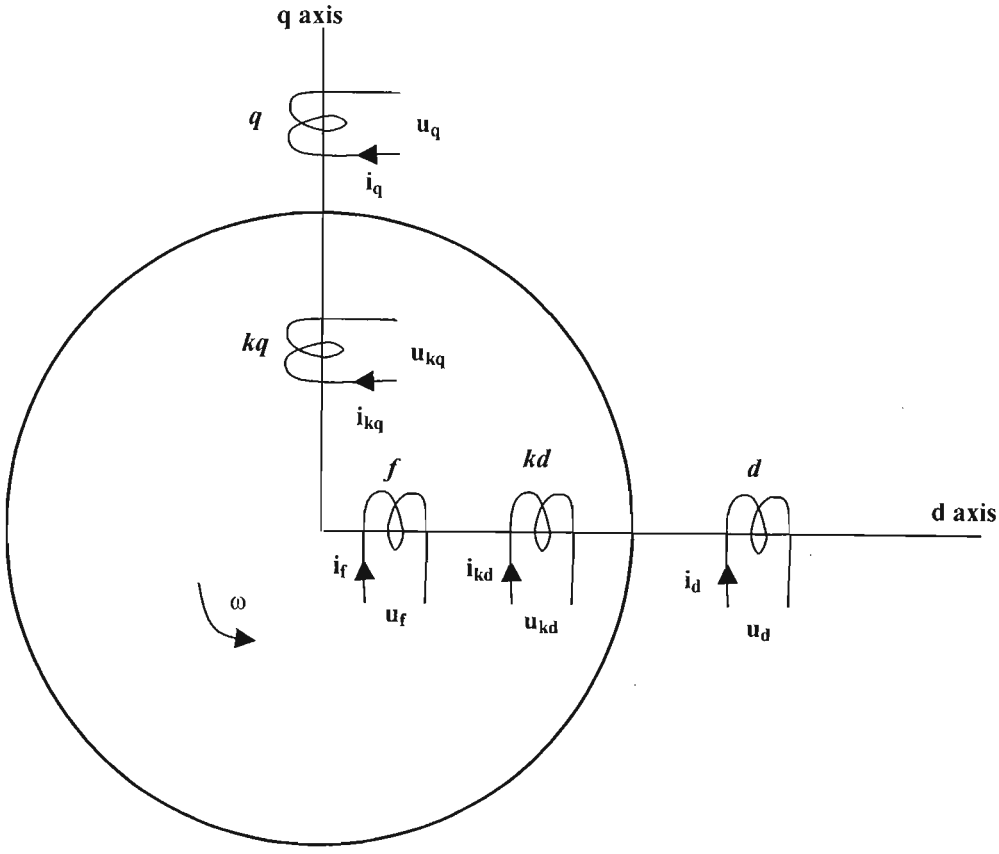

Fig.2.4 – Two-axis representation of a synchronous machine with one damper winding on each axis

The MMF due to current i_a in phase A is sinusoidal and proportional to i_a,. The maximum occurs at angular position θ (axis of the coil). The MMF may be resolved along both the direct and quadrature axes. The amplitude of the resultant MMF of all three phase currents along the direct axis is

$$k_m\left\{i_a\cos\theta + i_b\cos\left(\theta-\frac{2\pi}{3}\right) + i_c\cos\left(\theta-\frac{4\pi}{3}\right)\right\} \qquad (2.2)$$

where k_m is a constant. The amplitude of the MMF wave due to the current i_d, and taking into account the change of the unit explained earlier, is given by

$$\frac{3}{2}k_m i_d \tag{2.3}$$

Equating eqns (2.2) and (2.3) yields

$$i_d = \frac{2}{3}\left\{i_a \cos\theta + i_b \cos\left(\theta - \frac{2\pi}{3}\right) + i_c \cos\left(\theta - \frac{4\pi}{3}\right)\right\} \tag{2.4}$$

Similarly i_q is given by

$$i_q = \frac{2}{3}\left\{i_a \sin\theta + i_b \sin\left(\theta - \frac{2\pi}{3}\right) + i_c \sin\left(\theta - \frac{4\pi}{3}\right)\right\} \tag{2.5}$$

Allowing for any zero sequence current in the phases, the following relationship is used;

$$i_z = \tfrac{1}{3}\left(i_a + i_b + i_c\right) \tag{2.6}$$

The transformation equations giving axis currents, i_d, i_q, i_z, in terms of the actual currents, i_a, i_b, i_c, are given in matrix form by;

$$\begin{bmatrix} i_d \\ i_q \\ i_z \end{bmatrix} = \frac{2}{3}\begin{bmatrix} \cos\theta & \cos\left(\theta - \frac{2\pi}{3}\right) & \cos\left(\theta - \frac{4\pi}{3}\right) \\ \sin\theta & \sin\left(\theta - \frac{2\pi}{3}\right) & \sin\left(\theta - \frac{4\pi}{3}\right) \\ \frac{1}{2} & \frac{1}{2} & \frac{1}{2} \end{bmatrix} \begin{bmatrix} i_a \\ i_b \\ i_c \end{bmatrix} \tag{2.7}$$

The voltage equations can be derived in the same manner as the current equations and are given by;

$$\begin{bmatrix} u_d \\ u_q \\ u_z \end{bmatrix} = \frac{2}{3}\begin{bmatrix} \cos\theta & \cos\left(\theta-\frac{2\pi}{3}\right) & \cos\left(\theta-\frac{4\pi}{3}\right) \\ \sin\theta & \sin\left(\theta-\frac{2\pi}{3}\right) & \sin\left(\theta-\frac{4\pi}{3}\right) \\ \frac{1}{2} & \frac{1}{2} & \frac{1}{2} \end{bmatrix}\begin{bmatrix} u_a \\ u_b \\ u_c \end{bmatrix} \tag{2.8}$$

Eqns (2.7) and (2.8) are known as the current and voltage transforms respectively. The inverse of the transforms are given by;

$$\begin{bmatrix} i_a \\ i_b \\ i_c \end{bmatrix} = \begin{bmatrix} \cos\theta & \sin\theta & 1 \\ \cos\left(\theta-\frac{2\pi}{3}\right) & \sin\left(\theta-\frac{2\pi}{3}\right) & 1 \\ \cos\left(\theta-\frac{4\pi}{3}\right) & \sin\left(\theta-\frac{4\pi}{3}\right) & 1 \end{bmatrix}\begin{bmatrix} i_d \\ i_q \\ i_z \end{bmatrix} \tag{2.10}$$

and

$$\begin{bmatrix} u_a \\ u_b \\ u_c \end{bmatrix} = \begin{bmatrix} \cos\theta & \sin\theta & 1 \\ \cos\left(\theta-\frac{2\pi}{3}\right) & \sin\left(\theta-\frac{2\pi}{3}\right) & 1 \\ \cos\left(\theta-\frac{4\pi}{3}\right) & \sin\left(\theta-\frac{4\pi}{3}\right) & 1 \end{bmatrix}\begin{bmatrix} u_d \\ u_q \\ u_z \end{bmatrix} \tag{2.11}$$

At any instant the sinusoidal flux density wave existing in the air-gap can be defined by a magnitude and an angle. This flux density wave can be resolved into components on the direct and quadrature axes and expressed by flux linkages ψ_{md} and ψ_{mq} respectively. Assuming these quantities are known, the voltage equation for the armature circuit can be derived and the induced voltage in the armature circuit determined. The voltage induced in winding A depends on the angular position θ and the flux linkage components. The voltage induced by ψ_{md} is $-p(\psi_{md}\cos\theta)$ and by ψ_{mq} is $-p(\psi_{mq}\sin\theta)$ where p is the operator indicating the differential with respect to time, d/dt . The total internal voltage opposing the voltage induced by the main air-gap flux is given by;

$$p\left(\psi_{md}\cos\theta + \psi_{mq}\sin\theta\right) \tag{2.12}$$

The air-gap flux is a combination of all the actions of currents in windings in both the rotor and armature. The armature currents produce fluxes which do not cross the air-gap but nevertheless link phase A. The leakage reactance drop by i_a is $L_l p i_a$ where L_l is the leakage inductance of winding A. Currents i_b and i_c produce drops $-L_m p i_b$ and $-L_m p i_c$ in winding A where L_m is the part of the mutual inductance between two coils due to the flux that does not cross the air gap. To a good approximation, the terms L_l and L_m are independent of rotor position.

The phase A voltage, u_a, is equal to the sum of the internal voltage due to the main air-gap flux, the drops due to local armature fluxes, and the resistance drop, and is expressed as;

$$u_a = p(\psi_{md}\cos\theta + \psi_{mq}\sin\theta) + (R_a + L_l p)i_a - L_m p(i_b + i_c) \tag{2.13}$$

Using eqn (2.6) and the value of i_a from eqn (2.10), eqn (2.13) can be expressed as;

$$\begin{aligned} u_a &= p\left[\psi_{md}\cos\theta + \psi_{mq}\sin\theta\right] + (L_l + L_m)p(i_d\cos\theta + i_q\sin\theta + i_z) - 3L_m p i_z + R_a i_a \\ &= p\left[(\psi_{md} + L_a i_d)\cos\theta + (\psi_{mq} + L_a i_q)\sin\theta\right] + L_z p i_z + R_a i_a \\ &= p\left[\psi_d\cos\theta + \psi_q\sin\theta\right] + R_a i_a + L_z p i_z \end{aligned} \tag{2.14}$$

where the following quantities are introduced;

$$L_a = L_l + L_m \tag{2.15}$$

$$L_z = L_a - 3L_m \tag{2.16}$$

$$\psi_d = \psi_{md} + L_a i_d \tag{2.17}$$

$$\psi_q = \psi_{mq} + L_a i_q \tag{2.18}$$

The voltage equations for u_d, u_q and u_z can now be found by using eqn (2.14) as well as the terms for i_a and u_a from eqn (2.10) and eqn (2.11). The product terms in the square brackets of eqn (2.14) are differentiated, and using $p\theta = \omega$, results in;

$$\begin{aligned} &(u_d - R_a i_a)\cos\theta + (u_q - R_a i_q)\sin\theta + (u_z - R_a i_z - L_z p i_z) \\ &\qquad = \cos\theta(p\psi_d + \omega\psi_q) + \sin\theta(p\psi_q - \omega\psi_d) \end{aligned} \tag{2.19}$$

Eqn (2.19) must hold for all values of θ and equating coefficients on both sides results in;

$$u_d = p\psi_d + \omega\psi_q + R_a i_d \tag{2.20}$$

$$u_q = -\omega\psi_d + p\psi_q + R_a i_q \tag{2.21}$$

$$u_z = (R_a + L_z p) i_z \tag{2.22}$$

For the purpose of this thesis, the synchronous machine is modelled as containing one damper winding on the direct axis and one damper winding on the quadrature axis. Based on Figure 2.4 the direct and quadrature axis flux linkages can be expressed as, [ADKINS];

$$\psi_d = L_{fd} i_f + L_{dkd} i_{kd} + L_d i_d \tag{2.23}$$

$$\psi_q = L_{akq} i_{kq} + L_q i_q \tag{2.24}$$

The field and damper winding voltage equations can be expressed as;

$$u_f = (R_f + L_{ff} p) i_f + L_{fkd} p i_{kd} + L_{fd} p i_d \tag{2.25}$$

$$u_{kd} = 0 = L_{fkd} p i_f + (R_{kd} + L_{kkd} p) i_{kd} + L_{dkd} p i_d \tag{2.26}$$

$$u_{kq} = 0 = (R_{kq} + L_{kkq} p) i_{kq} + L_{qkq} p i_q \tag{2.27}$$

Eqns (2.23) to (2.27) hold true for both actual and per-unit values. It is found [ADKINS] that eqns (2.23) to (2.27) are much easier to handle if the per-unit system (Appendix A) is adopted. To further simplify the eqns (2.23) to (2.27) it is assumed that the mutual inductances on the direct axis are equal, that is;

$$L_{dkd} = L_{fd} = L_{fkd} = L_{md} \tag{2.28}$$

Also

$$L_{qkq} = L_{mq} \tag{2.29}$$

and L_{mq} and L_{md} are known as the mutual or magnetising inductances.

The self inductance of each winding is the sum of the mutual and leakage inductance hence;

$$L_d = L_{md} + L_a \tag{2.30}$$

$$L_{ff} = L_m + L_f \tag{2.31}$$

$$L_{kkd} = L_{md} + L_{kd} \tag{2.32}$$

$$L_q = L_{mq} + L_a \tag{2.33}$$

$$L_{kkq} = L_{mq} + L_{kq} \tag{2.34}$$

where L_a, L_f, L_{kd} and L_{kq} are the per-unit leakage inductances and the armature leakage inductance L_a is given by eqn (2.15). Eqns (2.23) to (2.27) can now be written in terms of per unit inductances;

$$\psi_d = (L_{md} + L_a)i_d + L_{md}i_f + L_{md}i_{kd} \tag{2.35}$$

$$\psi_q = (L_{mq} + L_a)i_q + L_{mq}i_{kq} \tag{2.36}$$

$$u_f = L_{md}pi_d + [R_f + (L_{md} + L_f)]i_f + L_{md}pi_{kd} \tag{2.37}$$

$$u_{kd} = 0 = L_{md}pi_d + L_{md}pi_f + [R_{kd} + (L_{md} + L_{kd})p]i_{kd} \tag{2.38}$$

$$u_{kq} = 0 = L_{mq}pi_q + [R_{kq} + (L_{md} + L_{kq})p]i_{kq} \tag{2.39}$$

Substitution of ψ_d and ψ_q terms in eqns (2.20) and (2.21) leads to a matrix defining the two-axis equations for the synchronous machine in (2.40);

$$\begin{bmatrix} u_f \\ u_{kd} \\ u_d \\ u_q \\ u_{kq} \end{bmatrix} = \begin{bmatrix} R_f + (L_{md} + L_f)p & L_{md}p & L_{md}p & 0 & 0 \\ L_{md}p & R_{kd} + (L_{md} + L_{kd})p & L_{md}p & 0 & 0 \\ L_{md}p & L_{md}p & R_a + (L_{md} + L_a)p & (L_{mq} + L_a)\omega & L_{mq}\omega \\ -L_{md}\omega & -L_{md}\omega & -(L_{md} + L_a)\omega & R_a + (L_{mq} + L_a)p & L_{mq}p \\ 0 & 0 & 0 & L_{mq}p & R_{kq} + (L_{mq} + L_{kq})p \end{bmatrix} \begin{bmatrix} i_f \\ i_{kd} \\ i_d \\ i_q \\ i_{kq} \end{bmatrix} \tag{2.40}$$

The definitions and values of the fundamental machine constants or the parameters that are required to study a synchronous machine can be found in Appendix B1-B4.

2.4.2 Torque equation and sign convention for the synchronous machine

The instantaneous torque of a machine is dependent on the current flowing in the machine windings. The torque developed by the interaction between the currents and the flux is known as the electrical torque. The difference between this torque and the externally applied torque, is due to acceleration or deceleration. The machine is regarded as generating with positive electrical torque, when the mechanical power is passing into the machine (at positive speed) from the outside. When positive voltage and current are applied to the terminals of the machine, the machine is regarded as motoring. This sign convention was adopted by [ADKINS] and is used in this thesis.

The electrical torque can be expressed in equation form as;

$$M_t = M_e + J\frac{d\omega}{dt} + K\omega \tag{2.41}$$

where M_t and M_e are the instantaneous applied shaft and electrical torques respectively and K represents a constant coefficient of friction. The electrical torque developed by a machine represented by the two armature windings D and Q, can be determined from rotational voltage terms in the armature equations. In the per-unit system, the electrical power input to a machine should have a value approximately unity when all the voltages and currents in the individual circuits have unit values. The power P for the three phase generator, if u_a, u_b, u_c, i_a, i_b and i_c are unity, is given by eqn (2.42).

$$P = \tfrac{1}{3}\left(u_a i_a + u_b i_b + u_c i_c\right) \tag{2.42}$$

Using the current and voltage inverse transform eqns of (2.10) and (2.11), eqn (2.42) can be shown to be;

$$P = \tfrac{1}{2}\left(u_d i_d + u_q i_q\right) + u_z i_z \tag{2.43}$$

Under balanced operation, the zero sequence terms u_z and i_z are equal to zero hence

$$P = \tfrac{1}{2}\left(u_d i_d + u_q i_q\right) \tag{2.43}$$

Taking each part of eqn (2.43) separately and substituting u_d and u_q from eqns (2.20) and (2.21) results in;

$$P_d = \tfrac{1}{2} u_d i_d = \tfrac{1}{2}\left(i_d p\psi_d + \omega\psi_q i_d + R_a i_d^2\right) \tag{2.44}$$

$$P_q = \tfrac{1}{2} u_q i_q = \tfrac{1}{2}\left(i_q p\psi_q - \omega\psi_d i_q + R_a i_q^2\right) \tag{2.45}$$

The $ip\psi$ and Ri^2 terms in eqns (2.44) and (2.45) represent the rate of change of stored energy and ohmic power losses in the machine respectively. The electrical power (which develops torque) is given by the remaining rotational voltage terms and is expressed as;

$$P_e = \tfrac{1}{2}\omega\left(\psi_q i_d - \psi_d i_q\right) \tag{2.46}$$

The torque equation in per-unit is expressed in eqn (2.47). The negative sign appears since P_e is derived from the electrical power passing into the terminals, whereas M_e is defined as a torque applied to the shaft.

$$\begin{aligned} M_e &= -\left(\frac{\omega_o}{\omega}\right)P_e \\ &= \frac{\omega_o}{2}\left(\psi_d i_q - \psi_q i_d\right) \end{aligned} \tag{2.47}$$

2.4.3 Modified two-axis machine equations in terms of rotor angle δ

Synchronous machines operate in power systems in conjunction with other machines. In many cases, for the purpose of modelling machines, the external power system supply voltage is regarded as a fixed reference with respect to magnitude and phase and is known as the *swing* or *infinite* bus. The reference axis of the system can be assumed to be rotating inside the machine and indicates the position of the d-axis of the machine if the machine were at no load. The position of the rotor during any operating condition of the machine can be measured by its displacement relative to this reference axis.

When the machine is operating under loaded steady state conditions, the speed is synchronous speed ω_o and the angular position of the rotor is displaced from the reference position by a constant rotor angle δ known as the *load angle*. This angle varies with load on the machine and is regarded as positive if the rotor lags behind the reference position and thus the machine is regarded as acting as a motor, developing motoring torque which causes the rotor to accelerate. A leading rotor angle is negative and causes the machine to act like a generator and has the opposite effect.

The position θ_r of the reference axis with respect to any stationary point in space is given at any time by;

$$\theta_r = \omega_0 t \tag{2.48}$$

It is often customary to choose t=0 when the reference axis coincides with that of phase A of the armature. The rotor position can at any instant be given by;

$$\theta = \omega_o t - \delta = \theta_r - \delta \tag{2.49}$$

Differentiating eqn (2.49) with respect to time yields the rotor speed ω, which is given by

$$\omega = \omega_0 - p\delta \tag{2.50}$$

The instantaneous slip is given by;

$$s = \frac{p\delta}{\omega_0} \tag{2.51}$$

The second derivative of eqn (2.49) with respect to time yields the rotor acceleration as

$$p^2\theta = -p^2\delta = p\omega \tag{2.52}$$

The torque eqn of (2.41) is now modified using eqns (2.47) and (2.52) to give

$$\begin{aligned} M_t &= M_e - Jp^2\delta - Kp\delta \\ &= \frac{\omega_0}{2}\left(\psi_d i_q - \psi_q i_d\right) - Jp^2\delta - Kp\delta \end{aligned} \tag{2.53}$$

Using eqn(2.50) to substitute for ω in eqns (2.20) and (2.21) gives the following armature voltage equations for a balanced three-phase supply

$$u_d = p\psi_d + \omega_0\psi_q + R_a i_d - \psi_q p\delta \tag{2.54}$$

$$u_q = p\psi_q - \omega_0\psi_d + R_a i_q + \psi_d p\delta \tag{2.55}$$

If the machine is connected to an infinite bus, the axis voltages u_d, u_q in eqn (2.55) are determined as follows. Assume that the phase A terminal voltage of a balanced three-phase supply of frequency $\omega_o/2\pi$ is

$$u_a = U_m \sin\omega_0 t \tag{2.56}$$

but $\omega_0 t = \theta + \delta$, hence

$$u_a = U_m \sin\delta\cos\theta + U_m \cos\delta\sin\theta \tag{2.57}$$

Using the transform of eqn (2.11) this results in

$$u_a = u_d \cos\theta + u_q \sin\theta \tag{2.58}$$

The two values for u_s given by eqns(2.57 and (2.58) must be equal for all θ, hence

$$u_d = U_m \sin\delta \tag{2.59}$$

$$u_q = U_m \cos\delta \tag{2.60}$$

Substituting eqns (2.59) and (2.60) into eqns (2.54) and (2.55) respectively yields

$$U_m \sin\delta = p\psi_d + \omega_0\psi_q + R_a i_d - \psi_q p\delta \tag{2.61}$$

$$U_m \cos\delta = p\psi_q - \omega_0\psi_d + R_a i_q + \psi_d p\delta \tag{2.62}$$

2.4.4 State space modelling of the synchronous machine

The state of a system represents the minimum necessary amount of information about the system at any instant in time t_0, so that its future behaviour can be determined without reference to the input before t_0. The system state may be represented in an n-dimensional Euclidean space called the *state space* [OGATA].

The behaviour of any dynamic system can be described by a set of *n* first order non linear ordinary differential equations of the form

$$\dot{x}_i(t) = f_i(x_1, x_2, \ldots, x_n, u_1, u_2, \ldots, u_r) \qquad i = 1,2,\ldots,n \tag{2.63}$$

where **n** is the order of the system and **r** is the number of inputs. Eqn (2.63) can be expressed in the general state space form as

$$\dot{x} = Ax + Bu + F(x) \tag{2.64}$$

where F(x) represents any non-linear terms.

The choice of state variables for a synchronous machine is not unique. The intention is to choose the least number of states that best describe the system. The choice of flux linkages or currents, or combinations thereof, as state variables leads to the direct derivation of the state space equations.

State space representation using flux linkages as states

Choosing the flux linkages as the electromagnetic states and the load angle and its derivative as the mechanical states, the state variable vector is given by;

$$\begin{bmatrix} x_1 \\ x_2 \\ x_3 \\ x_4 \\ x_5 \\ x_6 \\ x_7 \end{bmatrix} = \begin{bmatrix} \delta \\ \dot{\delta} \\ \omega_0 \psi_d \\ \omega_0 \psi_f \\ \omega_0 \psi_{kd} \\ \omega_0 \psi_q \\ \omega_0 \psi_{kq} \end{bmatrix} \tag{2.65}$$

and the input variables are given by the vector

$$\begin{bmatrix} u_1 \\ u_2 \end{bmatrix} = \begin{bmatrix} M_t \\ u_f \end{bmatrix} \tag{2.66}$$

where M_t is the mechanical torque and u_f is the field voltage.

Re-arranging eqns (2.35) to (2.39) and (2.54), (2.55) results in eqns (2.67), (2.68), (2.69) and (2.70).

$$\dot{\psi}_d = u_d - \omega_0 \psi_q - R_a i_d + \psi_q \dot{\delta} \tag{2.67}$$

$$\dot{\psi}_q = u_q + \omega_0 \psi_d - R_a i_q - \psi_d \dot{\delta} \tag{2.68}$$

$$\dot{\psi}_f = u_f - R_f i_f \tag{2.69}$$

$$\dot{\psi}_{kd} = u_{kd} - R_{kd} i_{kd} \tag{2.70}$$

$$\dot{\psi}_{kq} = u_{kq} - R_{kq} i_{kq} \tag{2.71}$$

Additional flux linkage variables ψ_f, ψ_{kd} and ψ_{kq} have been introduced and $u_{kd} = u_{kq} = 0$. These flux linkage terms are derived by expressing eqns (2.37) to (2.39) in an alternate form. The field equation of (2.37) can be expressed as

$$u_f = R_f i_f + p\psi_f \tag{2.72}$$

where

$$\psi_f = L_{md} i_d + (L_{md} + L_f) i_f + L_{md} i_{kd} \tag{2.73}$$

The terms ψ_{kd} and ψ_{kq} can be derived in a similar manner.

The currents in the windings are related to the flux linkages by the following two sets of linear equations in matrix form as

$$\begin{bmatrix} \omega_0\psi_d \\ \omega_0\psi_f \\ \omega_0\psi_{kd} \\ \omega_0\psi_q \\ \omega_0\psi_{kq} \end{bmatrix} = \begin{bmatrix} X_{md}+X_a & X_{md} & X_{md} & 0 & 0 \\ X_{md} & X_{md}+X_f & X_{md} & 0 & 0 \\ X_{md} & X_{md} & X_{md}+X_{kd} & 0 & 0 \\ 0 & 0 & 0 & X_{mq}+X_a & X_{mq} \\ 0 & 0 & 0 & X_{mq} & X_{mq}+X_{kq} \end{bmatrix} \begin{bmatrix} i_d \\ i_f \\ i_{kd} \\ i_q \\ i_{kq} \end{bmatrix} \tag{2.74}$$

The reactance terms X are defined in Appendix B2. The inverse of eqn (2.74) is given by

$$\begin{bmatrix} i_d \\ i_f \\ i_{kd} \\ i_q \\ i_{kq} \end{bmatrix} = \omega_o \begin{bmatrix} Y_{1d} & Y_{4d} & Y_{5d} & 0 & 0 \\ Y_{4d} & Y_{2d} & Y_{6d} & 0 & 0 \\ Y_{5d} & Y_{6d} & Y_{3d} & 0 & 0 \\ 0 & 0 & 0 & Y_{1q} & Y_{3q} \\ 0 & 0 & 0 & Y_{3q} & Y_{2q} \end{bmatrix} \begin{bmatrix} \psi_d \\ \psi_f \\ \psi_{kd} \\ \psi_q \\ \psi_{kq} \end{bmatrix} \tag{2.75}$$

The state variable equation is derived by substituting the currents of eqns (2.74) and (2.75) into eqns (2.67) to (2.71) and (2.53)

$$\begin{bmatrix} \dot{x}_1 \\ \dot{x}_2 \\ \dot{x}_3 \\ \dot{x}_4 \\ \dot{x}_5 \\ \dot{x}_6 \\ \dot{x}_7 \end{bmatrix} = \begin{bmatrix} \dot{\delta} \\ \ddot{\delta} \\ \omega_0 \dot{\psi}_d \\ \omega_0 \dot{\psi}_f \\ \omega_0 \dot{\psi}_{kd} \\ \omega_0 \dot{\psi}_q \\ \omega_0 \dot{\psi}_{kq} \end{bmatrix} = \omega_0 \begin{bmatrix} 0 & \frac{1}{\omega_0} & 0 & 0 & 0 & 0 & 0 \\ 0 & -\frac{K}{J\omega_0} & 0 & 0 & 0 & 0 & 0 \\ 0 & 0 & -Y_{1d}R_a & -Y_{4d}R_a & -Y_{5d}R_a & -1 & 0 \\ 0 & 0 & -Y_{4d}R_f & -Y_{2d}R_f & -Y_{6d}R_f & 0 & 0 \\ 0 & 0 & -Y_{5d}R_{kd} & -Y_{6d}R_{kd} & -Y_{3d}R_{kd} & 0 & 0 \\ 0 & 0 & 1 & 0 & 0 & -Y_{1q}R_a & -Y_{3q}R_a \\ 0 & 0 & 0 & 0 & 0 & -Y_{3q}R_{kq} & -Y_{2q}R_{kq} \end{bmatrix} \begin{bmatrix} \delta \\ \dot{\delta} \\ \omega_0\psi_d \\ \omega_0\psi_f \\ \omega_0\psi_{kd} \\ \omega_0\psi_q \\ \omega_0\psi_{kq} \end{bmatrix}$$

$$+ \begin{bmatrix} 0 \\ \frac{M_e}{J} \\ \omega_0\psi_q\delta + \omega_0 u_d \\ 0 \\ 0 \\ -\omega_0\psi_d\delta + \omega_0 u_q \\ 0 \end{bmatrix} + \begin{bmatrix} 0 & 0 \\ -\frac{1}{J} & 0 \\ 0 & 0 \\ 0 & \omega_o \\ 0 & 0 \\ 0 & 0 \\ 0 & 0 \end{bmatrix} \begin{bmatrix} M_t \\ u_f \end{bmatrix} \qquad (2.76)$$

The general method to calculate the initial conditions for eqn (2.76) is described in Appendix C.

The electrical torque given in eqn (2.47) can be expressed as follows in terms of flux linkages if eqn (2.75) is used.

$$M_e = \frac{\omega_0^2}{2}\left[Y_{1d}\psi_d\psi_q + Y_{3q}\psi_d\psi_{kq} - Y_{1d}\psi_q\psi_d - Y_{4d}\psi_q\psi_f - Y_{5d}\psi_q\psi_{kd}\right] \qquad (2.77)$$

2.4.5 Representation in a multi-machine system

In power system simulations each machine is represented by the state variables given in section 2.4.4 and its voltages and currents are expressed in a reference frame fixed to its direct and quadrature axes. However modern power systems are made up of many machines and it becomes necessary to represent more than one machine (multi-machine) in the study. During transients the machine speeds differ and each has its own rotor angle with respect to some reference. The d,q reference frame of each machine, tied to the rotor of that machine, therefore rotates at speeds different from the reference frame of all other machines. These separate reference frames can become quite tedious to keep track of, hence the need to refer all quantities to a *common reference frame* or the (D,Q) reference frame. The d,q and D,Q frames of reference are related by the frame transformation. It can also be shown that by neglecting the

ψ_d and ψ_q terms in the machine equations developed thus far, the computational burden is greatly simplified [ADKINS]. The transformation to the common reference frame is unaffected by the above simplifications.

In general any alternating current may be expressed in phasor form by;

$$i = I_m \cos(\omega t + \alpha) \tag{2.78}$$

where ω is equal to 2π times the frequency and α is the phase angle of the current. Eqn (2.78) can be expressed in terms of its real and imaginary components with the real component being expressed as

$$i = \sqrt{2}\left(\frac{I_m}{\sqrt{2}}\varepsilon^{j\alpha}\right)\varepsilon^{j\omega t} \tag{2.79}$$

or

$$i = \sqrt{2}I\varepsilon^{j\omega t} \tag{2.80}$$

where I in eqn (2.80) is expressed as

$$I = \frac{I_m}{\sqrt{2}}\varepsilon^{j\alpha} \tag{2.81}$$

Eqns (2.79), (2.80) and (2.81) give the transformation of a quantity, i, between instantaneous function of time, and I, the complex number. If the frequency ω is a constant then eqn (2.79) may be expressed as;

$$i(t) = \left\{\sqrt{2}\left[I_D(t) + jI_Q(t)\right]\varepsilon^{j\omega t}\right\} \tag{2.82}$$

The current components I_D and I_Q in a new D,Q reference frame which rotates at synchronous speed and is tied to the supply frequency as a common reference frame. This method of transformation applies equally to the voltage quantities. In any machine the angle between its d,q axis reference frame and the common D,Q reference frame is the rotor angle δ of that machine relative to the infinite bus.

The transformation for the i^{th} machine in an m-machine system is

$$\left(u_{Di} - ju_{Qi}\right) = \left(u_{di} - ju_{qi}\right)\varepsilon^{-j\sigma i} \tag{2.83}$$

The transforms of one machine are independent of all other machines. Eqns (2.84) and (2.85) are related by the network equation;

$$U_{DQ} = Z_{DQ} I_{DQ} + L_{DQ} \dot{I}_{DQ} \tag{2.86}$$

where Z_{DQ} is the matrix of self and transfer complex impedances of the system and L_{DQ} is the matrix of network inductances.

The mathematical representation of the synchronous machine in multimachine studies has been established in this section. It is now necessary to establish the mathematical representation of any controllers that may be attached to each of the synchronous machines. The next section investigates excitation systems and their mathematical modelling for representation in stability studies.

2.5 Excitation Systems

2.5.1 Overview of excitation systems

The excitation system which includes the voltage regulator, is used to provide dc current to the field winding of the synchronous machine and thereby controls reactive power flow and machine terminal voltage. During network disturbances, this system is used to provide a rapid response of the field current, thus enhancing the transient and small signal stability of the power system. Apart from the control nature of the excitation system, it also ensures that the machine operates within its specified operational limits, thus serving as a protective device.

The fundamental components of an excitation system are shown in Figure 2.5 below.

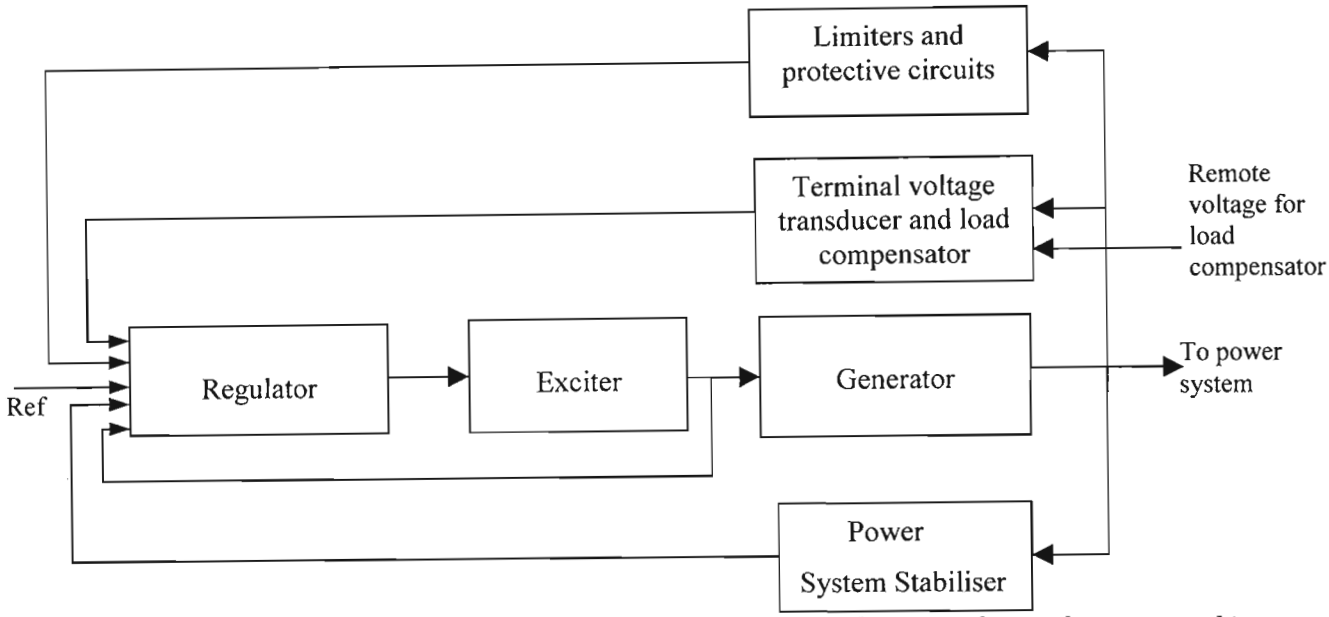

Fig. 2.5 – Fundamental block diagram of the excitation control system of a synchronous machine (KUNDUR1).

The function of each component is explained as follows;

- The exciter provides the dc power to the field winding.
- The regulator ensures that the input signal is of an appropriate level and form for use by the controller (usually a phase lead/lag or proportional/integral) contained in it.
- The terminal voltage transducers are used to rectify and filter the terminal voltage to a dc quantity. The load compensator is used to control the voltage of a remote terminal, away from the terminals of the generator.
- The power system stabiliser provides an auxiliary signal to damp out system power oscillations.
- Limiters and protective circuits are used to ensure that the excitation system and generator operate within specified limits

Nowadays three types of exciters are in use, namely dc, ac, and static.

- *Dc* systems use a dc generator to directly provide the dc power to the field winding. The system has high maintenance costs due to the slip-rings and brush-gear employed and has been phased out over the years.
- The *ac* system uses an ac machine (alternator) to achieve the power necessary for the field winding. The ac output from the alternator is rectified by either controlled or non-controlled rectifiers. The rectifiers can be either stationary or rotating.
- *Static* systems use power electronic devices to provide the power to the field winding through slip rings or brushes. Recent developments in the field of power electronics have made these exciters more reliable with little maintenance required.

In recent years, great advances have been made in *digital* control technology. The digital systems essentially provide the control, protective and logical functions of the excitation system with the power conversion stages done by static power electronic devices. Digital technology allows for complex yet reliable control algorithms to be effortlessly employed.

2.5.2 State space modelling of excitation system used for this study

For the purpose of this study, the machines in the multimachine system use the excitation system shown in Figure 2.6.

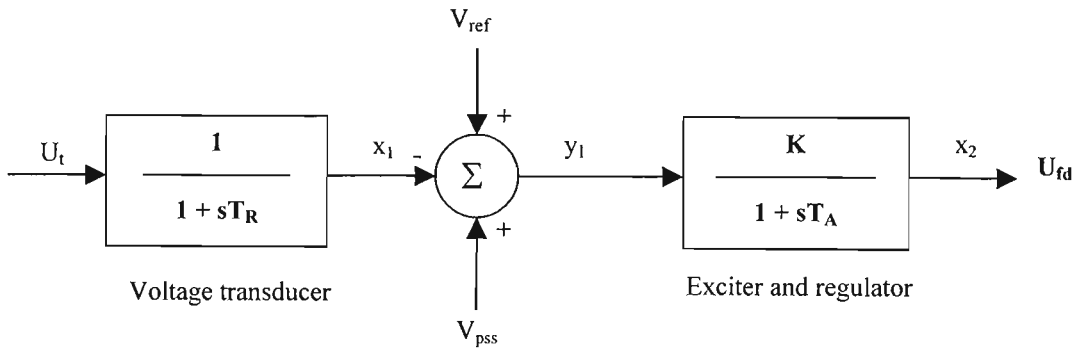

Fig. 2.6 – Block diagram of the simplified excitation system used for this study

This excitation system is a simplified system using the terminal voltage U_t , as input and U_{fd} as output, fed directly to the field windings. All quantities are in per unit and are listed in Table B.4 in Appendix B5. The transfer function of the voltage transducer is given by;

$$\frac{x_1(s)}{U_t(s)} = \frac{1}{1+sT_R} \tag{2.87}$$

The state space model is given by

$$\dot{x}_1 = \frac{1}{T_R} U_t - \frac{1}{T_R} x_1 \tag{2.88}$$

From the initial steady state conditions, the state variable x_1 is equal to U_t.

The transfer function of the exciter/regulator term is given by

$$\frac{x_2(s)}{y_1(s)} = \frac{K}{1+sT_A} \tag{2.89}$$

and the state space equation given by

$$\dot{x}_2 = \frac{1}{T_A} K y_1 - \frac{1}{T_A} x_2 \tag{2.90}$$

The initial conditions are x_2 equal to U_{fd} and y_1 equal to U_{fd}/K.

The reference signal U_{ref} is calculated, upon initialisation by;

$$U_{ref} = \frac{U_{fd}}{K} + x_1 - U_{pss} \tag{2.91}$$

where U_{pss} is the output signal from the power system stabiliser.

2.6 Multi-machine System Model and Simulation Packages Used

The system model chosen to investigate the performance of the power system stabilisers is shown in Figure 2.7. This model is a simplified model of an actual network that includes a pumped storage scheme (synchronous motor).

The system contains two synchronous machines, a generator and a motor. The machine data is given in Table B3 of Appendix B5. These machines are connected through a balanced transmission line L_{12}. Each machine is connected to the infinite bus via balanced transmission lines L_{13} and L_{23} respectively. The transmission line data is given in Table B2 of Appendix B5. The generator supplies a local static load LD_1 and there is a local static load LD_2 at the motor's terminals. The machines are assumed to have round rotors and are fitted with simplified exciters as shown in Figure 2.6. No turbine governing systems are modelled for either the generator or the motor, that is, the mechanical torque M_t is assumed to be constant, although it would be more realistic to assume turbine power to be constant for investigations of small disturbance around a steady operating point. The infinite bus is modelled as a voltage source behind a Thévenin equivalent impedance. This is done to represent the rest of the electrical network and with the assumption that the dynamics of the rest of the network can be neglected. The power system stabilisers designed in this thesis are fitted to the synchronous motor.

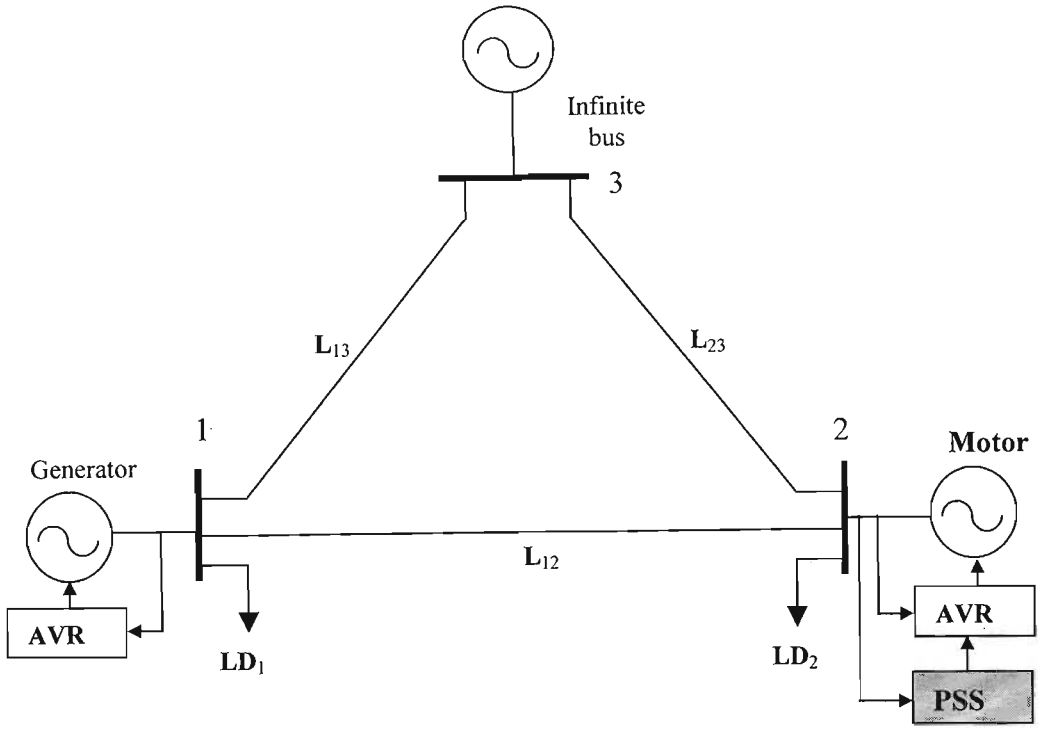

Fig. 2.7 – Diagram showing the multimachine system model used for the studies

The data for the exciters are given in Table B4 of Appendix B5 and the operating point chosen for the system is given in Table B1 of Appendix B5. The conventional stabiliser and fuzzy logic power system stabiliser are to be designed and tuned, in Chapters 4 and 5, to improve the overall system stability and increase post disturbance damping of the system.

The synchronous machine, exciters, loads and transmission system are modelled using Matlab® (Version 4.2c) and the Power System Toolbox (Version 1.0) [CHOW]. The Power System Toolbox is also used along with user-defined code to design and tune the conventional power system stabiliser. The fuzzy logic power system stabilisers are designed and implemented in simulations using the Fuzzy Logic Toolbox [ROGER] and a Simulink® block representation which is interfaced with the Power System Toolbox operating in Matlab.

The synchronous machine model pre-programmed into the Power System Toolbox was used in the simulation studies. This model can be adapted to represent the synchronous machine model explained in Chapter 2, by using the required parameters and neglecting certain parameters. The toolbox also has a built in model of the simplified exciter used in these studies. The model derivations explained in Chapter 2 are done in order to establish an understanding of mathematically modelling electrical equipment in computer simulations. Assumptions are often made in modelling of electrical equipment in order to create mathematical models that are computationally less demanding. These assumptions and the level

of detail required needs to be understood in order to represent electrical networks as accurately as possible.

2.7 Conclusion

This chapter introduced the various areas of power system stability and the factors that affect it. The area of angle stability is of direct concern to this thesis and the synchronous machine plays an important role in this area of power system stability. A description of the synchronous machine and its physical operation was given. A mathematical model for the synchronous machine was derived and the state space representation of the synchronous machine was established

The excitation system that is used to control the field current was also described. Excitation systems play an important role in the control of a synchronous machine and directly affect the power system stability. The power system stabiliser uses the excitation system to modulate the field current to help introduce additional damping to a power system. The mathematical model and state space representation of an excitation system was established.

The aim of the chapter thus far was to establish the mathematical models for the synchronous machine and related control systems. Once established, a software platform to simulate the power system, with these components, had to be chosen. The choice of Matlab and associated toolboxes as the preferred simulation platform was briefly described.

This chapter introduced the power system that is used in this study to enable a performance comparison between the fuzzy logic stabilisers and the conventional power system stabiliser to be done.

Chapters Three and Four give a theoretical understanding of the conventional and fuzzy logic power system stabilisers respectively and the procedures undertaken to design each type of stabiliser.

Chapter Five presents the performance results of the stabilisers at different operating points in order to establish robustness of the stabilisers.

Chapter Six then draws conclusions on the applicability and performance of a fuzzy logic power system stabiliser in a multi-machine environment, based on the results presented in Chapter Five.

CHAPTER THREE

CONVENTIONAL POWER SYSTEM STABILISERS

3.1 Introduction

Since the late 1950's and early 1960's most generating units were being fitted with continuously-acting voltage regulators. With these regulators and the increasing size of the power system networks, these networks were being operated closer to their stability limits, particularly during periods of prolonged low frequency power oscillations, which were being noticed in power systems around the world. Research revealed that continuous supplementary control of excitation systems could be used to improve system stability and was rigorously investigated by [DEMELLO] and many others. From this type of research the power system stabiliser was developed to help damp these low frequency power oscillations. Over the years the power system stabiliser has evolved and has become almost commonplace in most large power system networks. Various techniques for designing and tuning such power system stabilisers have been developed.

This chapter deals with the fundamental theory surrounding the purpose and the components of a power system stabiliser. The design and tuning process of a conventional power system stabiliser, for the system model given in Figure 2.7, is explained.

The term *conventional* power system stabiliser is used to differentiate the between power system stabilisers tuned by classical linear control techniques, and those utilising fuzzy logic techniques.

3.2 Fundamental Theory of a Conventional Power System Stabiliser

Small signal stability studies can be performed on a linearised power system model to ascertain the level of system instability and damping. In chapter 2, the concept of representing the nonlinear synchronous machine as a state-space representation was introduced. Often in small signal studies, the state matrix is linearised around one operating point to allow modal analysis techniques to be performed on the system. These techniques can help describe the dynamic characteristics of a system. The concept of linearisation of a state matrix is explained in Appendix D1.

From the linearised state matrix a block diagram representation of the synchronous machine and controllers can be set up. [DEMELLO] used the concept of the block diagram, with great effect, to introduce the concept of supplementary excitation control. [KUNDUR1] gives a detailed description of

the derivation of the block diagram for the synchronous machine connected to an infinite bus through a transmission line and the block diagram's relation to the linearised state matrix. The primary use of the block diagram in this thesis is to explain the fundamental purpose of the power system stabiliser. The block diagram showing a power system stabiliser, $G_{pss}(s)$, connected to a synchronous machine (with no damper windings modeled) and excitation system $G_{ex}(s)$, is shown in Figure 3.1. The K terms are constants derived from machine and operating terminal parameters. A detailed derivation of the K terms can be found in [KUNDUR1].

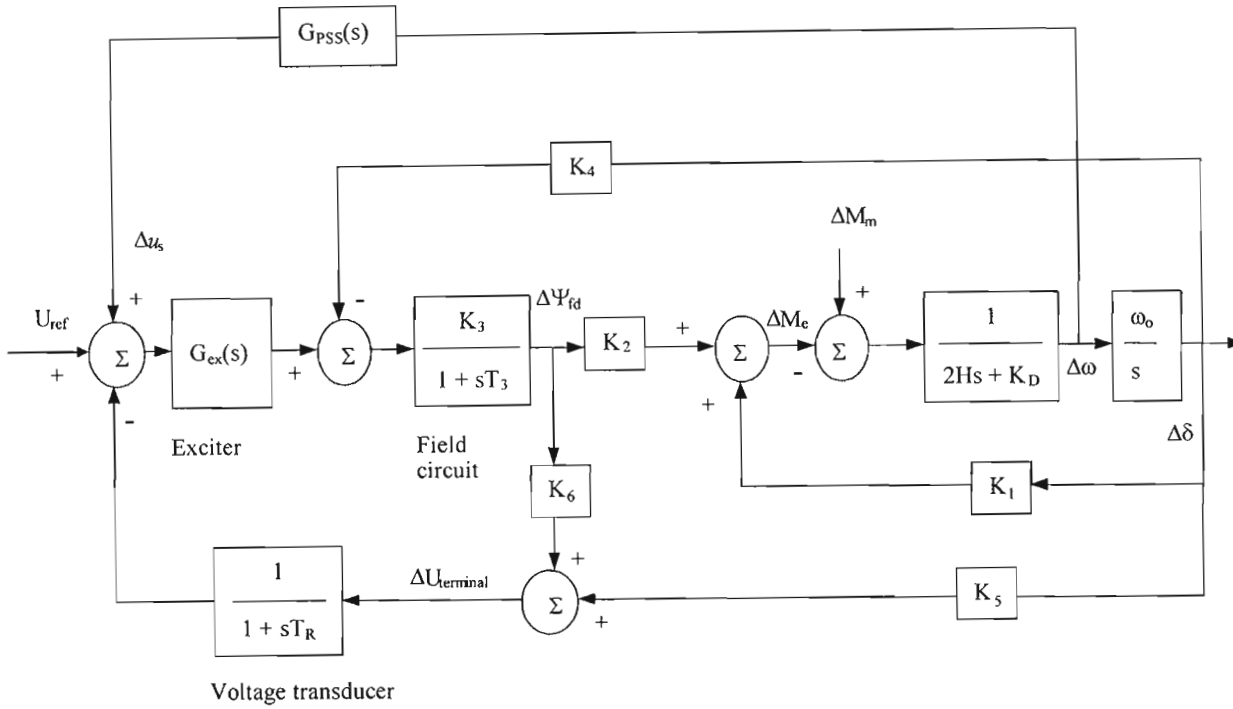

Figure 3.1 – Block diagram with a PSS feeding an auxiliary signal into the excitation system of a synchronous machine with no damper windings modeled.

The purpose of the power system stabiliser is to add damping to the generator rotor oscillations by controlling the excitation using auxiliary stabilising signals [KUNDUR1]. In order to provide the required damping, the stabiliser must produce a component of electrical torque in phase with the rotor speed deviations. From Figure 3.1, it is clear that if the stabiliser is to inject a component of electrical torque T_e in phase with the rotor speed deviations, it must compensate for the phase lag introduced by the exciter and field circuit of the machine.

There are essentially two modes of oscillation that a power system stabiliser is typically designed to enhance the damping of, namely ***local plant mode*** and ***inter-area*** *mode.* The *local plant mode* is associated with a synchronous machine or the units at a power station swinging against the rest of the power system. The mode has a typical frequency range of 0.8 Hz to 2.0 Hz. The *inter-area mode* is associated with many machines in one part of the system swinging against other machines in other parts

of the system. This type of mode has a characteristic frequency range of 0.1 to 0.8 Hz. Other modes that may be influenced by the power system stabiliser include torsional modes and control modes, such as the "*exciter mode*" associated with the exciter and field circuit [KUNDUR1]. In modal analysis techniques, the eigenvalues of the system indicate the inherent damping and frequency of modes in a system. The derivation of the eigen-properties of a state matrix and modal analysis techniques are explained in Appendix D2.

The block diagram of typical components found in the conventional power system stabiliser $G_{pss}(s)$, is shown in Figure 3.2. The stabiliser contains a washout term, stabiliser gain, phase lead compensation and output limiters. The role of each component of the stabiliser is explained further in the following sections.

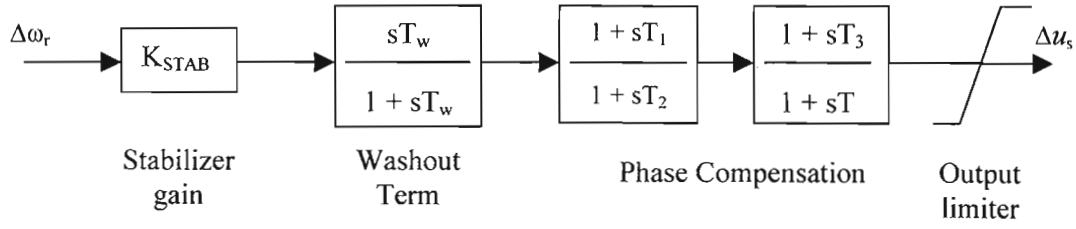

Figure 3.2 – Basic PSS showing washout, phase lead, gain and output limiter blocks

3.2.1 Phase Lead Compensation Blocks

To compensate for the inherent phase lag introduced from the exciter input to the electrical torque, the power system stabiliser must introduce phase lead. Two first-order phase compensation blocks are shown in Figure 3.2, but if the compensation required is small, then only one block may be used. For machines with low d-axis open circuit time constants (T_{do}'), the phase compensation may be neglected.

The phase compensation required to provide optimal damping, changes with system conditions. A compromise is often made and a characteristic acceptable for a desired range of frequencies (normally 0.1 to 2.0 Hz), and for different system conditions, is selected. This may result in less than optimum damping at any one frequency, but there is an increased bandwidth of operation of the stabiliser. Slight under-compensation is often preferred such that there is an increase in both the damping and the synchronising torque components of the electrical torque.

3.2.2 Stabiliser Washout term

The stabiliser washout term is a high pass filter that removes dc signals but the value of T_w is set high enough to allow signals associated with the rotor speed oscillations to pass unchanged. Caution must be exercised not to set the value of T_w too high so that it leads to generator voltages exceeding operational limits, as a result of stabiliser action, during system-island conditions. Without this term, a change in speed would modify the terminal voltage, for example as found during islanding conditions.

3.2.3 Stabiliser Gain

The value of stabiliser gain has a significant effect on the damping of the rotor oscillations. Ideally the stabiliser gain should be set to the value yielding maximal damping. Beyond this point further increases in the gain value causes a decrease in damping [KUNDUR2], [LARSEN2]. The gain must also be set to a value that does not cause excessive amplification of signal noise.

3.2.4 Stabiliser Limits

The stabiliser limits are imposed to restrict the level of generator terminal voltage fluctuations during transient conditions. Too high stabiliser signals will cause the excitation system to saturate and defeat the purpose of voltage regulation. To date there is no fixed procedure to determine the values of the limits of the stabiliser, though various methods have been used, [KUNDUR2], [LARSEN2] based on actual stabiliser applications.

3.3 Design of a Conventional Power System Stabiliser

The design procedure followed to calculate the parameters for the conventional power system stabiliser used in this study is explained below. The stabiliser has the basic form shown in Figure 3.2. The parameters for each control block are calculated using techniques used in [KUNDUR2] and [LARSEN2]. Other techniques to tune a power system stabiliser have been proposed by [BOLLING] and [FARMER].

3.3.1 Identification of the system modes

The very first question to be asked, though very simplistic, but very important, "Is there a need for a power system stabiliser or can the problem be solved by some other means". So the first step is to identify the problem. One of the best ways to identify any system parameters that may cause undamped oscillations in a power system, is to calculate an eigenvalue scan of the system. The procedure to calculate the eigenvalues of a system matrix is explained in Appendix D2.

The eigenvalues for the system model shown in Figure 2.7 in Chapter 2 are given in Table 3.1. There are 16 eigenvalues presented in Table 3.1 due to the fact that each synchronous machine unit is modeled

using eight state variables. There are six state variables for the generator and two state variables for the excitation system. From Table 3.1 it can be clearly seen than there is a poorly damped eigenvalue which has the complex value of -0.05 ± j5.69. This eigenvalue has a damping ratio of +0.0096 and a natural frequency of 0.91 Hz. The damping ratio and natural frequency of this mode are calculated using eqns (D.52) and (D.51) respectively in Appendix D2. From a calculation of the participation matrix, it is found that the unstable eigenvalue is associated with the rotor angle and speed of the synchronous motor. The participation matrix yields normalised contributions of each state variable to a particular mode of oscillation. Using the participation matrix, the contribution of the synchronous motor's rotor angle and speed state variables are identified as having the largest contribution to the eigenvalue of complex value -0.05 ± j5.69 and a PSS should be placed at this motor.

Table 3.1 – Eigenvalues of the system with no stabiliser

Eigenvalue	Damping Ratio	Frequency
-2.46 + j3.17	0.6125	0.5053
-2.46 – j3.17	0.6125	0.5053
-0.05 + j5.69	**0.0096**	**0.9060**
-0.05 – j5.69	**0.0096**	**0.9060**
-2.50 – j5.33	0.4249	0.8478
-2.50 + j5.33	0.4249	0.8478
-0.54 – j8.30	0.0645	1.3215
-0.54 + j8.30	0.0645	1.3215
-11.94	1.00	0
-17.34	1.00	0
-98.48 – j4.63	0.9989	0.7375
-98.48 + j4.63	0.9989	0.7375
-103.67 – j2.00	0.9998	0.3184
-103.67 + j2.00	0.9998	0.3184
-134.99	1.00	0
-163.71	1.00	0

3.3.2 Choice of input signal for the stabiliser

One of three types of signals is commonly used as an input to the power system stabiliser, namely speed deviation, frequency, and a combination of shaft speed and electrical power. The choice of input signal depends on the type of generating unit (thermal, hydraulic) to which the stabiliser will be fitted [KUNDUR1], and the practical applicability of the measuring and processing of the input signal. The advantages and disadvantages of each signal are further discussed in the following subsections.

For the modeling of the synchronous machine, the rotor is modeled as a lumped single mass representation throughout these studies. The speed deviation is used as the input signal for the conventional power system stabiliser, with no torsional filters needed.

3.3.2.1 Speed deviation

The use of speed deviation as an input signal to stabilisers has been successfully used as far back as 1969 [KUNDUR1]. However a number of limitations have been found with stabilisers utilizing this type of signal as input. One major drawback is the use of torsional filters. Torsional filters have been found to add further phase lag hence causing a destabilising effect on the exciter. This in turn limits the maximum allowable stabiliser gain, which also limits the stabiliser's damping contribution to the system.

3.3.2.2 Shaft speed and electrical power

This type of stabiliser uses a signal that is proportional to the rotor speed deviations derived from the accelerating power [KUNDUR1]. The problem arises to measure the integral of change of mechanical power, free of torsional modes. The integral of mechanical power is related to the shaft speed and electrical power as follows;

$$\int \Delta P_m \, dt = M\Delta w + \int \Delta P_e \, dt \tag{3.1}$$

Eqn (3.1) is used to simulate a signal proportional to the integral of mechanical power change by adding signals proportional to the change in shaft speed and integral of electrical power change. Torsional frequencies can be removed with a simple low-pass filter.

The overall transfer function for deriving the equivalent rotor speed deviation is given by;

$$\Delta\omega_{eq}(s) = \frac{\Delta P_e}{Ms} + G(s)\left[\frac{\Delta P_e(s)}{Ms} + \Delta\omega(s)\right] \tag{3.2}$$

where G(s) is the transfer function of the low-pass torsional filter. This type of stabiliser has two advantages over the stabiliser utilizing the speed signal as input [KUNDUR1], namely;

(i) The ΔP_e signal has a high degree of torsional attenuation hence there is generally no need for a torsional filter in the main stabilising path. The exciter mode problem is eliminated allowing higher stabiliser gains to be used which result in better system damping.

(ii) An end-of-shaft speed-sensing arrangement with a simple torsional filter can be used together with electrical power to derive the mechanical power signal. This allows the use of a standard design for all generator units irrespective of their torsional characteristics.

3.3.2.3 Frequency

Terminal frequency has also been used in many power system stabiliser applications and, as with speed based stabilisers, torsional filters are required [LARSEN2]. However frequency based stabilisers have been found to be more sensitive to inter-area modes hence producing better damping contribution for these modes. These stabilisers however do have a few shortcomings. Firstly, during a rapid transient, the terminal frequency signal undergoes a phase shift, which causes a spike in the field voltage that is seen directly on the generator's outputs. Secondly, industrial loads such as arc furnaces cause noise on the power system that is "seen" by the frequency based stabiliser.

3.3.3 Calculation of time constants for the phase lead blocks

In order to calculate the time constants for the phase lead blocks of the stabiliser, the phase lag introduced between exciter input and the electrical torque has to be calculated first. In order to do this, the inertia of the machine at which the stabiliser is to be added should be increased by 100 times. This is done to ensure that the generator angle remains constant during modulation of the generator excitation system by the PSS. During modulation, the resulting change in electrical torque causes variations in the rotor speed and a large inertia prevents these changes taking place.

Furthermore, the other machines in the system are represented as infinite buses since the frequency response of the machine is sensitive to the Thévenin equivalent impedance at its terminals but relatively independent of the dynamics of other machines in the system.

Generally, slight under-compensation is preferred to cater for uncertainties in the system model. A value of 10° is suggested by [KUNDUR1] over the entire frequency range of 0.2 to 2.0 Hz.

Figure 3.3 shows the calculated phase lag from the exciter input to the electrical torque component for the synchronous motor. The phase lead introduced by the stabiliser is also shown on the diagram. The phase lead introduced by the stabiliser is obtained by selecting time constants for the phase compensation terms (T_1,T_2,T_3,T_4). As can be seen the stabiliser cannot fully compensate for the phase lag over the entire frequency range. As much phase lead as possible is therefore introduced around the frequency of the unstable or poorly damped mode (0.91Hz) whilst maintaining approximately 15° under-compensation at this frequency. Unfortunately the disadvantage is that at lower frequencies, there is overcompensation taking place.

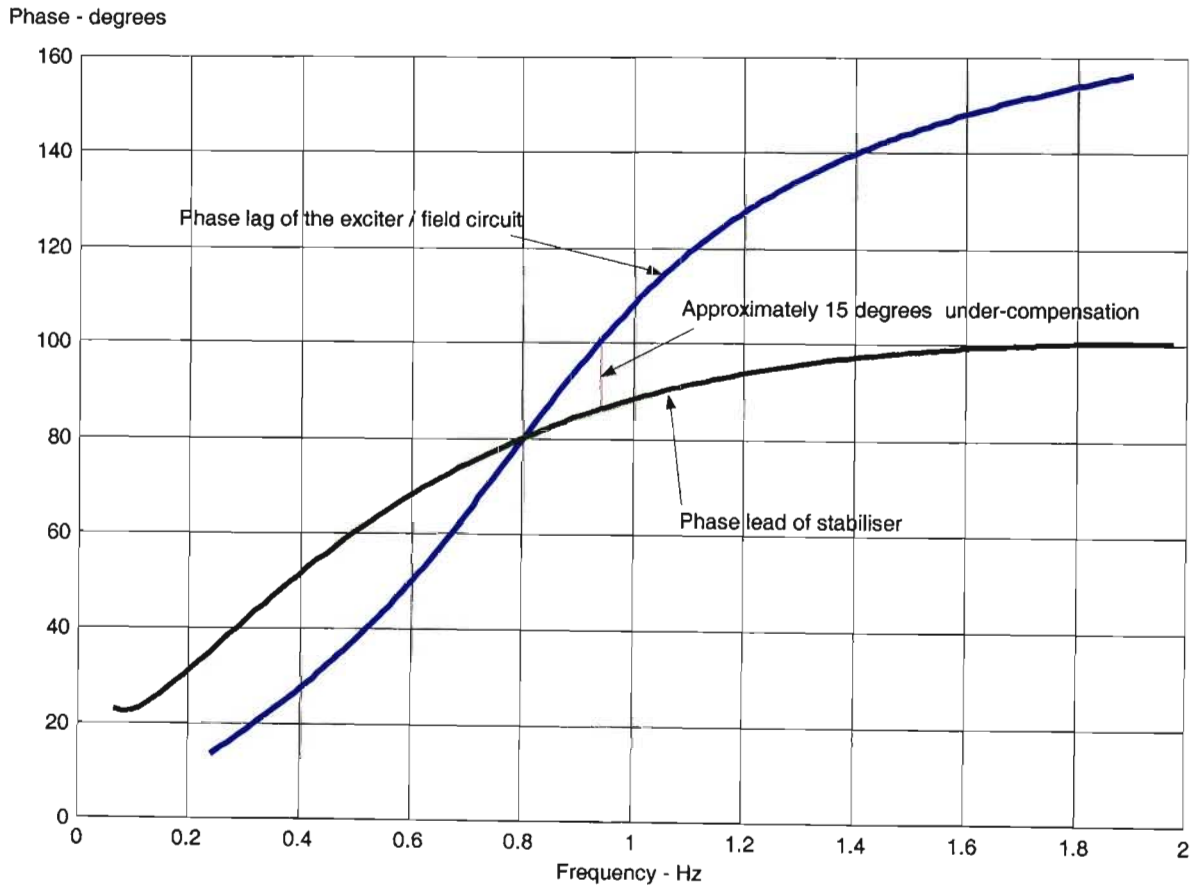

Figure 3.3 – Phase compensation of the stabiliser against the phase lag of the exciter/generator

Eigenvalue scans at a later stage will help determine if this overcompensation at lower frequencies is acceptable and does not pose a threat to the system stability. If required, the phase compensation can then be reduced to yield slight under-compensation at lower frequencies by manipulating the time constants in the phase compensation blocks of the stabiliser.

3.3.4 Selection of the Washout Term

The choice of the washout term is not a critical decision, though a few guidelines are adhered to ensure optimal system stability. A value of 1.5 seconds is satisfactory for local mode oscillations between 0.8 to 2.0 Hz. For lower frequency inter-area oscillations between 0.2 Hz and 0.8Hz, a value of 10 seconds or higher may be chosen. Lower time constants result in increased phase lead at lower frequencies. This must be compensated for as it may lead to significant instability in inter-area modes, due to the desynchronizing effect it introduces.

Figure 3.4 shows a graph with the effect of various washout time constants. As can be seen, at lower frequencies (0.1Hz – 0.2Hz), there is a significant difference in the phase lead introduced by the stabiliser for washout time constants less than 10 seconds. A value of 10 seconds is chosen for the washout time constant for the conventional PSS. This value for the washout term also aids in providing less compensation at the lower frequencies.

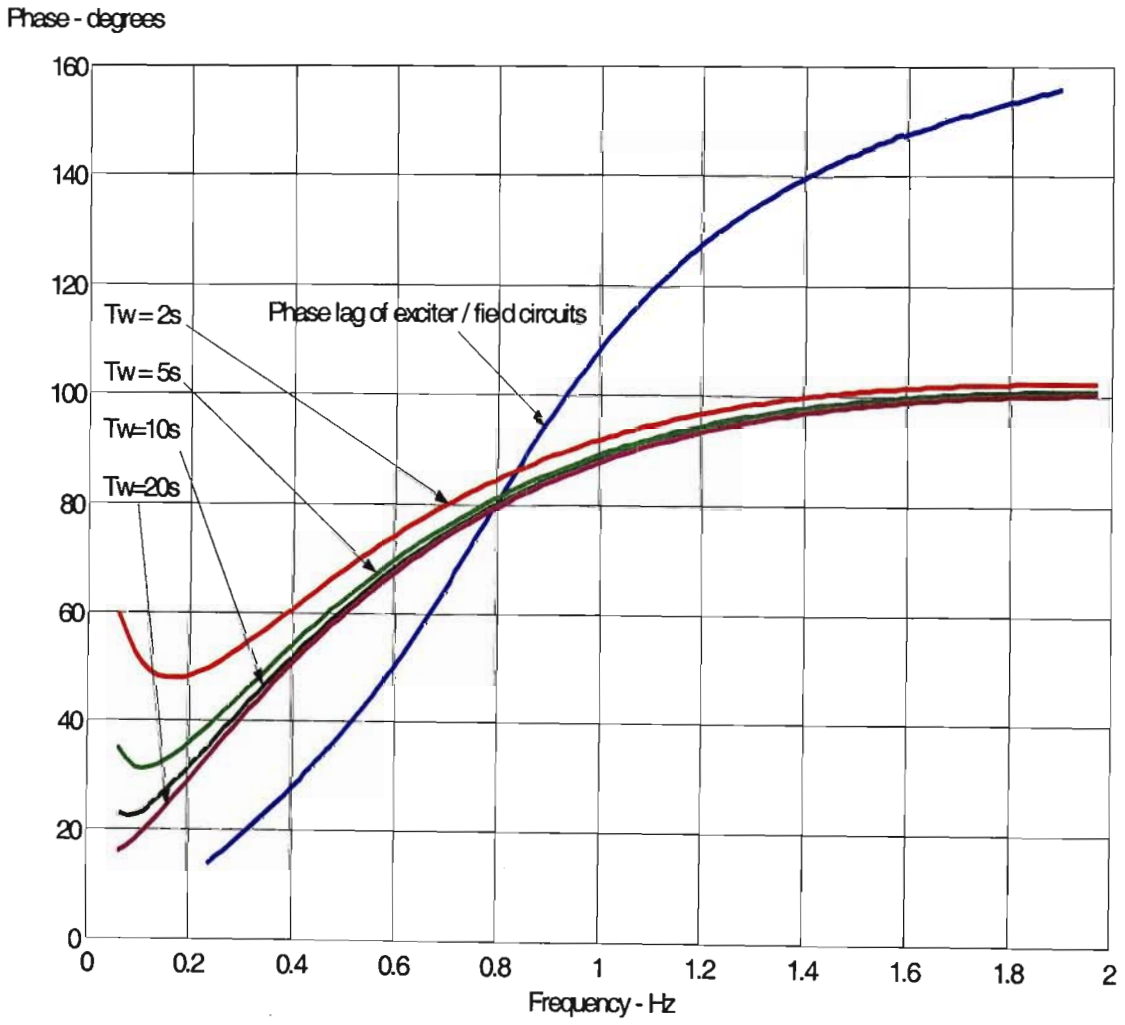

Figure 3.4 – Phase angle properties of different values for T_w on the lower end of the frequency response of the stabiliser

3.3.5 Calculation of Stabiliser Gain

The stabiliser gain is chosen done by examining the effect of various gains on the damping ratio of the rotor oscillations. The damping of the oscillation increases with increasing gain up to a certain point and then decreases. The value of the stabiliser gain is generally set to the value yielding the highest damping ration of the critical system modes without compromising the stability of the other system modes.

Table 3.2 shows the effect of varying the gain of the stabiliser on the poorly damped mode associated with the motor's rotor angle. From the table it can be seen that the damping ratio (defined in Appendix D, eqn (D.52)) increases with the stabiliser gain increasing from 0 up to 35 and, thereafter it starts to decrease as the stabiliser gain is increased above 35.

Table 3.2 - Effect of stabiliser gain on the damping ratio of the eigenvalue associated with the rotor angle of the motor

Stabiliser Gain	Eigenvalue	Damping Ratio
0	$-0.05 \pm j5.69$	0.0096
5	$-0.08 \pm j5.72$	0.0139
10	$-0.22 \pm j5.75$	0.0386
15	$-0.38 \pm j5.79$	0.0650
20	$-0.55 \pm j5.84$	0.0939
25	$-0.75 \pm j5.94$	0.1253
30	$-0.94 \pm j6.13$	0.1518
34	$-1.02 \pm j6.32$	0.1589
35	**$-1.03 \pm j6.36$**	**0.1591**
36	$-1.03 \pm j6.41$	0.1589
40	$-1.04 \pm j6.56$	0.1558

To ensure that the stabiliser gain is not adversely affecting any other system modes, an eigenvalue scan of the system with a stabiliser gain of 35, is given in Table 3.3 which indicates that all the eigenvalues of an oscillatory nature in the system are stable and well damped with the inclusion of the stabiliser into the system.

Table 3.3 – Eigenvalues of the system with a stabiliser having a gain of 35 included

Eigenvalue	Damping ratio	Frequency (Hz)
-0.0010	1.0000	0
-0.0010	1.0000	0
-2.31 – j3.12	0.5955	0.4961
-2.31 + j3.12	0.5955	0.4961
-1.55 – j5.13	0.2890	0.8166
-1.55 + j5.13	0.2890	0.8166
-1.03 – j6.36	0.1591	1.0128
-1.03 + j6.36	0.1591	1.0128
-1.04 – j8.63	0.1195	1.3730
-1.04 + j8.63	0.1195	1.3730
-0.1192	1.0000	0
-0.1720	1.0000	0
-0.2633	1.0000	0
-0.4209	1.0000	0
-0.9091	1.0000	0
-0.9091	1.0000	0
-98.42 – j4.63	0.9989	0.7374
-98.42 + j4.63	0.9989	0.7374
-103.60 - j2.14	0.9998	0.3407
-103.60 + j2.14	0.9998	0.3407
-1.3499	1.0000	0
-1.6371	1.0000	0

3.3.6 Selection of output limits for the stabiliser

The positive output limit for the stabiliser is set to a relatively high value to allow a large contribution from the stabiliser during power swings. This value is typically between 0.1 and 0.2 p.u. When selecting the value, attention must be paid to the value not being too high so that it may cause large terminal voltage values. A terminal voltage limiter should be fitted to the excitation system or the positive output limit value should be decreased so as to not to cause excessively high terminal voltages. From transient simulations it is found that an upper limit value of 0.2 p.u. is adequate for the conventional stabiliser designed for these studies.

[KUNDUR1] suggests a value between -0.05 p.u. and -0.1p.u for the negative limiter. To allow for maximum possible effort from the stabiliser, a value of -0.1p.u. is chosen.

3.4 Conclusion

The value of the time constants and parameters of the conventional power system stabiliser are summarised in Table 3.4. The results of performance simulations of the conventional stabiliser, when the system is subjected to a fault, are compared with the performance results of the fuzzy logic stabiliser in Chapter Five.

Table 3.4 – Final settings for the conventional power system stabiliser

Tw	T1	T2	T3	T4	K_{stab}	V_{smax}	V_{smin}
10s	0.219s	0.029	0.219s	0.029s	35	0.2	-0.1

CHAPTER 4

FUZZY LOGIC POWER SYSTEM STABILISER

4.1 Introduction

In 1965 a professor from the University of California in Berkley, Lotfi A.Zadeh, first introduced the concept of making precise decisions from imprecise data [ZADEH1]. In 1975 Zadeh introduced the concept of a linguistic variable, which contains words as its value and not numbers [ZADEH2]. These variables along with logical operators were to form the basis for fuzzy logic. Today fuzzy logic is used in almost every aspect of human life from cameras to washing machines and cement kilns.

Fuzzy logic is as much a part of human beings as is the skin on our bodies and the hair on our heads, yet we are often intimidated by the concept of fuzzy logic. Simply put, fuzzy logic is a convenient method of mapping an input space to an output space. Furthermore fuzzy logic uses "imprecise" data to make "precise" decisions

In the real world, human dependence on precise data is often negligible, yet people function reasonably well in making decisions. Consider a person walking across a street and a car came hurtling around the corner heading for this person. What would be the more significant thing for you to say to this person;

(a) " A car of 756 kg is approaching you at 78 km/h from a north-easterly direction" or

(b) "LOOK OUT!"

As a human being, there was no need for precise data in order to make a decision to warn the person, as quickly as possible, of the impending danger. It is on this same principle that the concept of fuzzy logic is derived.

Based on the above example it is apparent that the decision taken to warn of the danger quickly was based on having previous experience/exposure involving fast moving cars. This principle of applying expert knowledge to imprecise data to make decisions is the fundamental thinking behind fuzzy logic controllers. Unlike conventional controllers, which require a deep understanding of the system, exact mathematical equations and precise data, fuzzy logic controllers apply an abstract form of thinking to make decisions. Furthermore, fuzzy logic allows expert knowledge to be applied in a subjective manner, such as, short, tall, very tall, which is mapped onto numeric ranges.

This chapter outlines the basic fuzzy set theory and the three main processes involved in the design of a fuzzy logic controller, namely, fuzzification, inference and defuzzification. The design criterion applied to design a fuzzy logic power system stabiliser is then explained.

4.2 Theory of Fuzzy Logic

This section outlines the basic theory of fuzzy logic and fuzzy sets. The application of fuzzy theory to controller design explained in the next section.

4.2.1. Fuzzy Sets

A fuzzy set is a set that has no clearly defined boundary. It may contain elements that may only be partially associated with the set or contain only a partial degree of membership to the set. In classical set theory, elements of sets either are a part of the set or not.

This classical set theory does not allow any partial membership to a set. This however is not the way humans tend to operate. In order to understand the concept of partial membership of a set, consider the four different seasons and the months of the year. In South Africa, the winter months are generally around May, June, July and August and summer months are around November, December, January and February. If one was asked the question, "Is September a winter month?" and applied only classical set theory to answer the question, then the answer will be no, as September is not a member of the winter months set. Though from human experience, many South Africans know that a severe winter may run into September.

This partial belonging of September to the winter season and spring season cannot be represented by classical set theory. Fuzzy sets however cater for such "in-between" or intermediate values by giving absolute truth or belonging a numerical value of one (1) and absolute falseness or non-belonging a value of zero (0). Any partial belonging is assigned a value between zero and one depending on the amount of "belonging" an element has to a set.

Now consider the question, "Is July a winter month?". Based on past experience, one can answer with a great degree of certainty that July is a winter month and can be assigned a value of 1. Likewise, the question "Is December a winter month?", can be answered with a great degree of certainty that December is NOT a winter month and be assigned a value of 0. The in-between values become very useful for a question such as "Is September a winter month?'. Such a question cannot be answered absolutely, hence a person may answer that about 60% of September is winter, hence a value of 0.6 can be assigned to such a question. This assignment of a certain percentage of belonging of a value to a set, is often referred to as a degree of membership (DOM).

The concepts of classical set theory and fuzzy set theory can be graphically displayed, as shown in Figure 4.1. Figure 4.1(a) shows the classical representation of the four different season sets. It is quite clear that such sets are not a realistic representation of what happens in nature as on the 1st September, the season does not change abruptly from winter to spring. Figure 4.1(b) is a much more realistic

representation of the seasonal behavior, as the 1st September has both the "feel" of winter as well as spring.

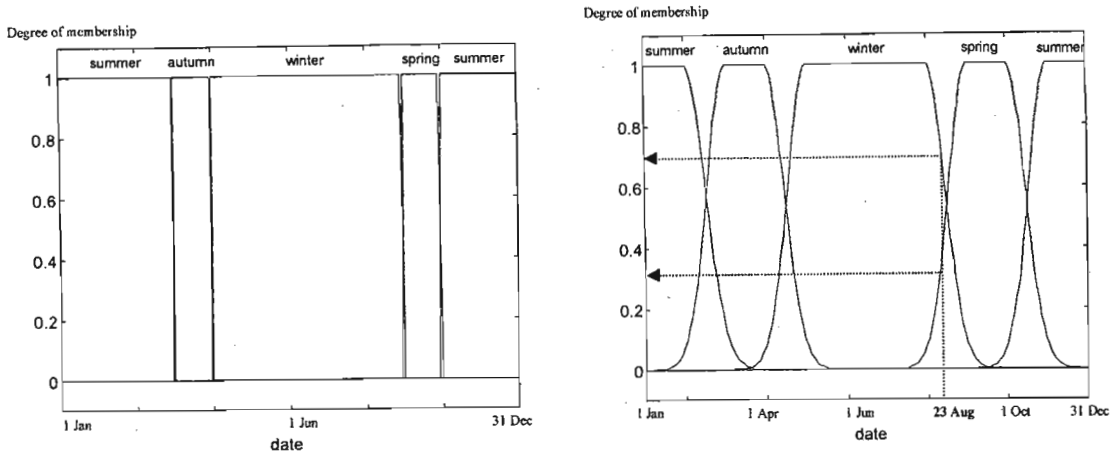

Figure 4.1 – Illustration of classical and fuzzy set theory

4.2.2. Fuzzy Operators

The fuzzy operators employed in fuzzy theory form the logic or the reasoning for fuzzy controllers. The important point to remember about fuzzy logical reasoning is that it forms a superset of standard Boolean logic. If the fuzzy variables were restricted to the bounds of 0 (completely false) and 1 (completely true), then the standard logical operation would hold. Consider the standard truth tables shown in tables 4.1 (a),(b) and (c).

Table 4.1 – Standard Boolean logic tables

X	Y	X **AND** Y
0	0	0
0	1	0
1	0	0
1	1	1

(a)

X	Y	X **OR** Y
0	0	0
0	1	1
1	0	1
1	1	1

(b)

X	**NOT** X
0	1
1	0

(c)

Fuzzy logic is the truth of any statement, and is a matter of degree. The values (degree of membership) are any real value including and between 0 and 1. Thus fuzzy logic must employ logical functions that will preserve the results of the AND, OR and NOT X operators in standard logic.

These functional results are preserved by use of the MIN (minimum), MAX (maximum) and 1-X functions. Tables 4.2 (a), (b) and (c) illustrate the usefulness of using the MIN, MAX and 1-X functions for fuzzy logic.

Table 4.2 – Preservation of the AND, OR, NOT X functions by the MIN, MAX, 1-X functions.

X	Y	**MIN** (X,Y)
0	0	0
0	1	0
1	0	0
1	1	1

(a)

X	Y	**MAX** (X,Y)
0	0	0
0	1	1
1	0	1
1	1	1

(b)

X	**1-X**
0	1
1	0

(c)

The tables illustrated in Table 4.2 (a), (b) and (c) can be applied to any real value between 0 and 1. These truth tables hold true for both two-valued logic and multi-valued logic. Figures 4.2 (a), (b) and (c) illustrate the application of the logical functions to multi-valued systems or fuzzy sets.

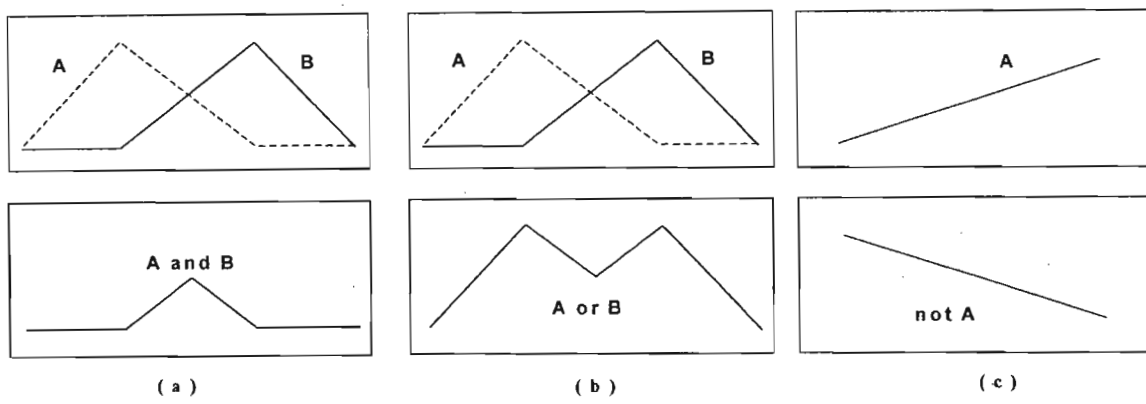

Figure 4.2 – Illustration of multi-valued logic

Tables 4.2 (a), (b) and (c), respectively represent the general definition of the fuzzy intersection or conjunction (AND), fuzzy union or disjunction (OR) and fuzzy complement (NOT). These definitions are the classical operators of these functions: AND = min, OR=max, and NOT = additive compliment (1-X). A more general definition of fuzzy intersection operators is given in Appendix E and an in-depth description can be found in [BANDEM].

Since fuzzy logic variables or sets can be assigned subjective names, the full benefit of the logic can be extracted by using these variables in conditional statements

A single fuzzy *if-then* rule assumes the form of;

If *x* is A, then *y* is B

Where A and B are the linguistic variables defined by the ranges (universe of discourse) X and Y, respectively. The rule has two parts, namely the antecedent ("if x is A') and the consequent ("then y is B"). The use of many of these fuzzy if-then statements or rules, forms the mapping between fuzzy input

sets to fuzzy output sets. Each rule defines a fuzzy patch in the Cartesian product A x B (system state space)

The antecedent is an interpretation that returns a single value between 0 and 1, whereas the consequence is an assignment that assigns the entire fuzzy set B to the output variable y.

In the case of two-valued or binary logic, if-then rules are simple. If the premise is true, then the conclusion is true. However if the premise is a fuzzy statement, then the affect on the conclusion is as follows; if the antecedent is true to a certain degree of membership, then the consequent is also true to the same degree of membership. In other words, assuming r and s are variables, where r is the antecedent and s is the consequent;

In binary logic: $r \rightarrow$ s (r and s can be either true or false)

In fuzzy logic: $0.6r \rightarrow 0.6s$ (partial antecedents imply partial conclusions).

The antecedent of a rule may also have many parts. In such a case all the parts of the antecedents are calculated simultaneously and resolved into a single number using logical operators. In the case of the consequent having multiple parts then all consequences are affected equally by the result of the antecedent

The affect on the consequent by the antecedent is done by the *implication function*. The consequent specifies the fuzzy set to be assigned to the output and the implication function then modifies that fuzzy set to the degree specified by the antecedent. The most common ways used to truncate output fuzzy sets is by the use of the *min* function (where the set is chopped off) or the *prod* function (where the set is 'squashed").

4.3 Application of Fuzzy Theory to Controller design

The application of fuzzy logic to control systems is not as extravagant or outrageous, as the concept may first be perceived to be. The design of any fuzzy controller follows three general stages, namely, fuzzification, inference and defuzzification. These steps are illustrated in Figure 4.3. The input and output signals are discrete values that are respectively available from, and to, the system being controlled.

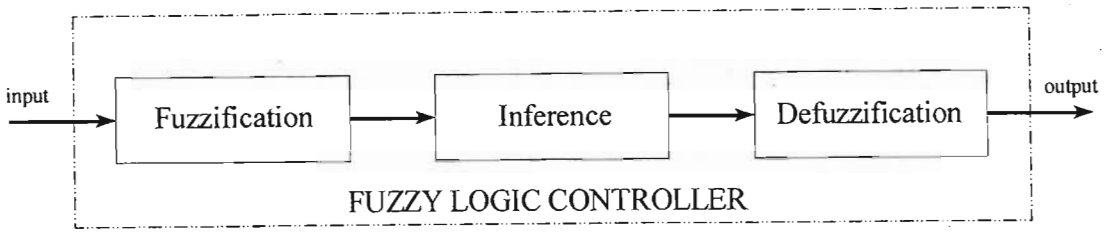

Figure 4.3 – Basic processes employed by a fuzzy logic controller

4.3.1 Fuzzification

Fuzzification is defined as the process of associating discrete (crisp) value variables with *fuzzy variables* (fuzzy sets) and assigning a *degree of membership* (DOM) of the crisp variable to the fuzzy variable or fuzzy set. Fuzzy variables are often referred to as linguistic variables due to their subjective description of an actual discrete value. For example, to describe a person's height, various categories or fuzzy variables can be chosen, for example, short, tall and very tall. The choice of which category a person's height may fall into is subjective. If a man's height is 6 ft then that man may be described as either average or tall. Due to their subjective nature, fuzzy variables can cater for this "fuzziness".

Consider the example when a fuzzy controller samples discrete values from the system to be controlled. The fuzzy controller makes decisions based on fuzzy variables, so some form of association between the discrete (crisp) value variables and the fuzzy variables is needed. The membership function is a function that associates the discrete input variable to the fuzzy variables. Each discrete input variable can be associated with one or more fuzzy variables. Each fuzzy variable may have its own unique membership function shape and this membership function is used to associate a DOM of a discrete variable to a fuzzy variable. The only condition that a membership function must satisfy is that it must be between 0 and 1.

Membership functions can take on an arbitrary curve though often shapes like those of a rectangle, triangle, generalised bell shape or trapezoid are used. Membership functions can also take on more elaborate shapes like the Gaussian curve or sigmoidal curves (open and closed). Often certain applications will require asymmetry hence sigmoidal shapes can be used. Where smoothness and non-zero points are required, bell shape and Gaussian curves can be applied. Triangle, trapezoidal and rectangular shapes are simpler and often easier to implement and are used to improve controller speed and efficiency.

To illustrate the concept of fuzzification, consider the design of a fuzzy identifier to determine the season of the year based on the day of the year. The day of the year is the crisp input variable and the variables, *summer, spring, winter* and *autumn* are subjective descriptions of the seasons of the year. The

membership function shapes are arbitrarily chosen as shown in Figure 4.1(b). The ranges of the fuzzy variables are the period of one year. Often the range of the discrete input variable needs to be defined and the fuzzy variable's membership functions need to be spread out over this range.

If the date, 31 December is given as input, then using Figure 4.1(b), shows that the date falls within the *summer* fuzzy variable or fuzzy set. This is confirmed by the DOM, which is assigned to the fuzzy variable a value of 1. In other words this states that the date the 13 December has 100% certainty of being in the *summer* season. Consider however the 23 August. This date falls into a period that is neither 100% true to be *winter* nor 100% true to be *spring*. In this case the single discrete input is associated with two fuzzy variables, namely *winter* and *spring*. How much this discrete value (date) belongs to each of these fuzzy variables is determined by the DOM. Based on the membership function shapes chosen in Figure 4.1(b), the DOMs associated with the *winter* and *spring* fuzzy variables are 0.7 and 0.3 respectively. This can be translated into, the 23 August is about 70% true to be *winter* and 30% true to be *spring*. The mapping of the discrete variable to the fuzzy variable or subset, with the association of a degree of membership can also be viewed as the truth of a statement. Thus the date 23 August can also be viewed as being 30% true to the *spring* fuzzy subset and 70% true to the *winter* fuzzy subset.

Though this discrete date cannot be mapped into a specific season, it is the nature of the fuzzy variables in association with the degree of membership, which enables the "fuzziness" of the input data to be captured and processed to produce a meaningful output.

The next section outlines the processes that the fuzzy variables undergo in order to effect decision-making.

4.3.2 Inference

Input fuzzy variables (sets) are mapped to output fuzzy variables (sets) by fuzzy rules. These rules form the relationship between input and output fuzzy variables. Section 4.2.2 introduced the use of if...then rules to enable logical decisions to be made on fuzzy variables.

The question often arises, as to where the knowledge is derived from to formulate the rules for a fuzzy controller. Fuzzy controllers are often referred to as expert systems, since the knowledge of an expert operator (human) has been captured in the controller. This expert knowledge is based on an understanding of the behavior of the system. Sometimes knowledge of the system being controlled is derived from off-line dynamic simulations of the system. Extensive effort has been devoted to the creation of fuzzy rules and recent studies have shown the successful application of artificial intelligence, such as neural networks, to help generate fuzzy rules [KOSKO].

Consider the identifier in section 4.2.1. The specifications of this identifier are now extended to include the following requirement, "based on the day of the year, calculate a typical average temperature for that day". The fuzzy inputs have already been derived, i.e. the day of the year has been mapped to some season. Now based on the season, some decision needs to be made as to what type of average temperature can be experienced. Remember the emphasis is on type, i.e. a subjective description of the temperature. Fuzzy input variables can only be mapped to fuzzy output variables by the rules.

Typical words to describe the temperature would be, very cold, cold, mild, hot, very hot. Using these five descriptions as the fuzzy output variables, a set of rules needs to be established to map the seasons (fuzzy input variables) to these output variables. Based on expert knowledge of the typical temperatures in Southern Africa, Table 4.3 can be derived;

Table 4.3 – Set of rules for the fuzzy controller

	Fuzzy Input variable		**Fuzzy Output Variable**
IF	Summer	THEN	Hot
	Autumn		Mild
	Winter		Cold
	Spring		Mild

Table 4.3 has mapped fuzzy input variables to fuzzy output variables for a simple, one input (discrete), one output (discrete) system. Fuzzy controllers may often have more than one discrete input value. These inputs are mapped to different sets of linguistic variables in each fuzzy input range. Hence if there are two discrete inputs mapped to 5 linguistic variables each, then a 5X5 table (25 rules) needs to be generated. This table is often referred to as a rule-based table.

With multi-input fuzzy controllers, the handling of the different degrees of membership to each fuzzy input variable needs to be addressed. Using min-max inference, the activation of the *i*th rule consequent is a scalar value, which equals the minimum of the two antecedent conjuncts' values.

To illustrate this concept, consider the introduction of a second discrete input to the identifier defined above, the time of day. The specifications of this identifier are now extended to state, "based on the day of the year and time of the day, calculate a typical temperature for that time of the day".

The time of day is mapped to 4 arbitrarily chosen fuzzy variables, i.e. midday, afternoon, night and morning. The range of these fuzzy variables covers 24 hours or an entire day. The arbitrarily chosen membership functions are shown in Figure 4.4. The choice of the number of fuzzy input variables can be based on the resolution of the discrete input variable's range that is required, though the more input fuzzy variables chosen, the more rules need to be generated. The new rule-based table has 16 rules and is shown in Table 4.4. The output fuzzy variables chosen to describe the temperature are *very cold, cold, mild, hot* and *very hot*.

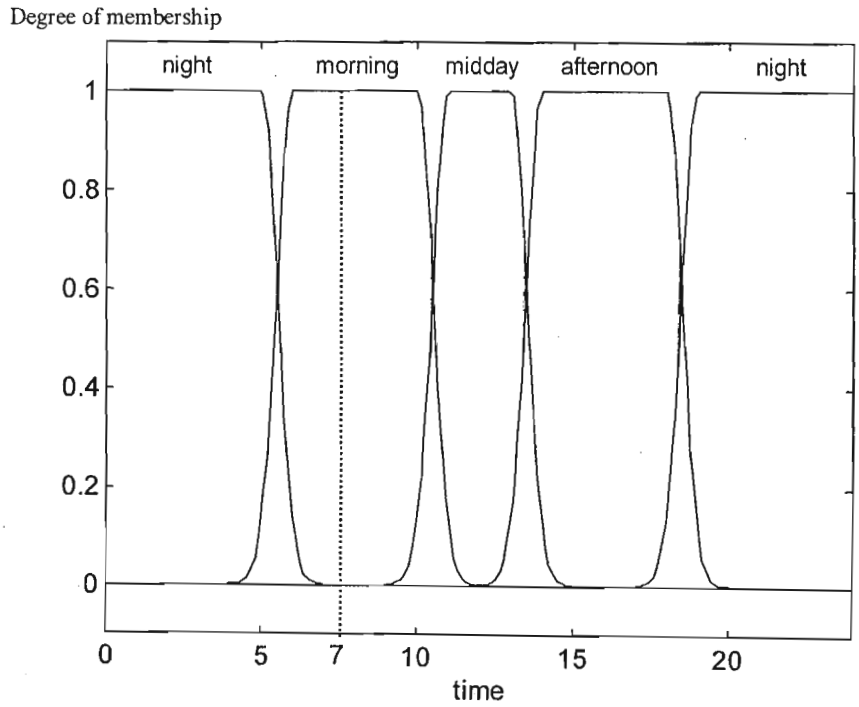

Figure 4.4 – Membership functions for second controller input, time of day.

Table 4.4 – Rule based table for the temperature calculating fuzzy controller.

Day of year	**Time of Day**			
	night	*morning* (1.0)	*midday*	*afternoon*
summer	Mild	Mild	Very Hot	Very Hot
autumn	Cold	Mild	Hot	Mild
winter (0.7)	Very Cold	Cold (0.7)	Mild	Cold
spring (0.3)	Cold	Mild (0.3)	Hot	Mild

Consider two discrete inputs to the system, the date, 23 August and the time 07h00. The date is fuzzified to *spring* (0.3) and *winter*(0.7) and is illustrated in Figure 4.1(b). The time of day is fuzzified to *morning* (1) and the association is illustrated in Figure 4.4. Based on Table 4.4, two rules are activated, i.e., IF time of day is *morning*(1) AND day of year is *spring*(0.3) THEN the temperature is *Mild* and IF time is *morning*(1) AND day of year is *winter*(0.7) THEN the temperature is *Cold*. Using the minimum of the

two degrees of memberships of the antecedents, the output variable, *mild*, is assigned a degree of membership of 0.3, i.e. min(1.0,0.3) = 0.3 and the output fuzzy variable *cold* is assigned a degree of membership of 0.7. Furthermore, the fuzzy input variables have been mapped to a region in the fuzzy output space.

This region in the fuzzy output space is illustrated by the shaded area in Figure 4.5. The range of the output fuzzy space is based again on expert knowledge of temperature variations of Southern Africa. Consider the output membership function *cold*, which is triangular in shape and assigned a DOM of 0.7. When a straight line is projected across the triangle at a value of 0.7, a quadrangular area between the base of the triangle, and the straight line is formed. This area is the area in output fuzzy space that will be used to derive a discrete output variable. The same principle is applied to the membership function, *mild*, in order to get an area in output fuzzy space using the DOM of 0.3 assigned to the membership function. Where two or more regions of output fuzzy space exist, then the MAX function is used to get an overall output fuzzy space. The total shaded area illustrated in Figure 4.5 represents the output fuzzy space derived using the MAX function. This inference method of mapping an input fuzzy space to an output fuzzy space, is commonly known as the MIN-MAX inference method. This method is easily explained as follows;

- where two or more degree of membership values are assigned to the same output fuzzy variable (from the antecedents), then the minimum of these DOM values is assigned to that specific output fuzzy variable.
- the MAX function is then applied to all the output fuzzy variables that have DOMs assigned to them, in order to derive a region in fuzzy output space. Where overlaps in adjacent membership functions that have DOMs assigned to them occur, then the maximum of the DOM values is used. In Figure 4.5, the output fuzzy variable *cold* and *mild* have both been assigned DOMs. In the region where the membership functions of *cold* and *mild* overlap, the MAX function is used to derive the upper limit of fuzzy output region, hence a value 0.7 is used.

Once the output fuzzy region has been defined, a discrete output needs to be derived from this region. The next section explains how to obtain the discrete output by defuzzification.

4.3.3 Defuzzification

Defuzzification is a method of deriving a discrete output variable from fuzzy output variables. In section 4.3.2 a region in the fuzzy output space was calculated based on rules and degrees of memberships. The fuzzy output region for the fuzzy controller defined above is shown in Figure 4.5 as the shaded area, for the given date and time of the year. Often a fuzzy output variable may be assigned two degrees of membership. Using the min-max inference rule the minimum value of the two values is chosen as the degree of membership associated with this output fuzzy variable.

The choice of membership function shapes is once again arbitrary with each fuzzy output variable able to have its own unique function. The range for the fuzzy output variables, in this case temperature, must be chosen to be reflective of the typical discrete values. Typical temperatures over an entire year may vary from –5°C to +35°C in Southern Africa. In order to cater for extreme cases, a range of –10°C to +40°C is chosen as the range for the fuzzy variables.

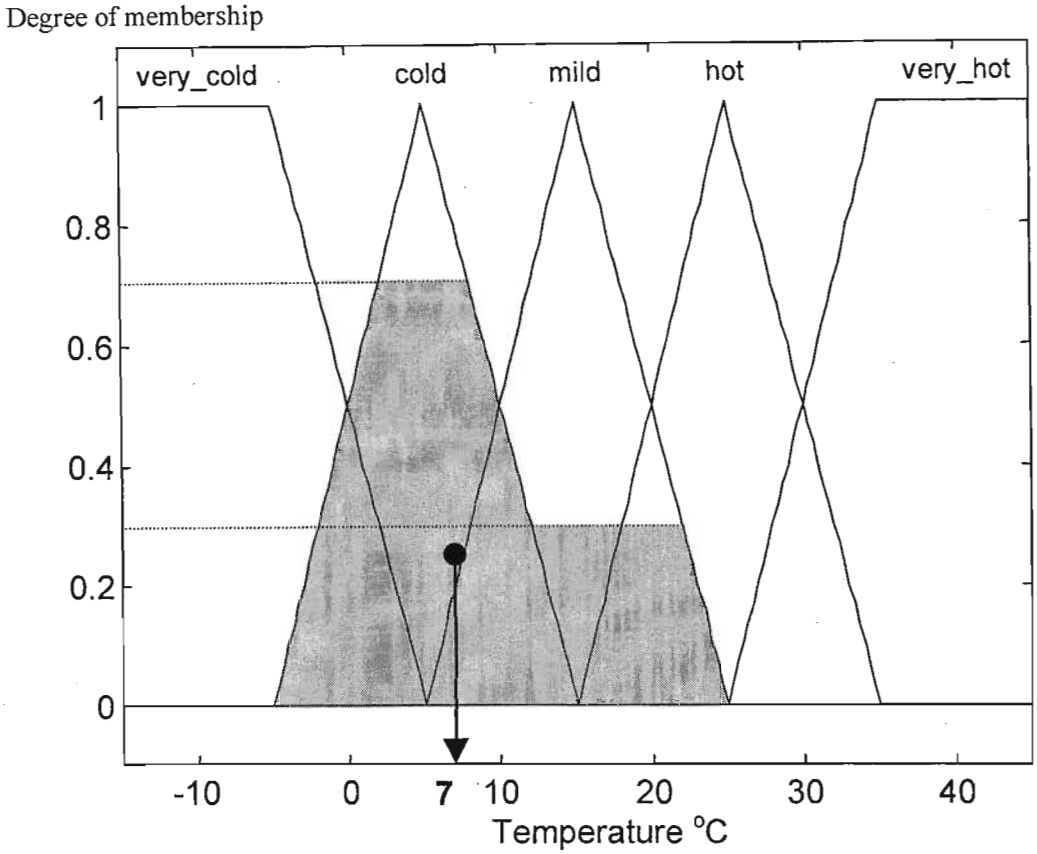

Figure 4.5- Membership functions for the output fuzzy variables and the output fuzzy region.

The final stage is to calculate a discrete value from this fuzzy output region. Various methods exist to derive a discrete value from the fuzzy output region, namely centroid, bisector, middle of maximum (average of the maximum value of the output set), largest of the maximum and smallest of the minimum. The names of the methods are self-explanatory and a detailed explanation of each method can be found in [BANDEM]. The most popular method for defuzzification is the centroid method, i.e. the center of gravity, C, of the shaded area in Figure 4.5. The abscissa of the centroid is the discrete output value of the controller.

In the case of the identifier used to calculate the temperature, for the date 23 August, at 7h00 in the morning a typical temperature would be about +7°C.

4.4 Design of a Fuzzy Logic Power System Stabiliser (9 Rules)

The design of a fuzzy logic power system stabiliser (PSS) is not as complex as it may seem at first. A fuzzy PSS is essentially the conversion of expert knowledge of power system stabilisers, power system behavior and power system control, into an expert controller. The process followed to design a fuzzy PSS is similar to the process of designing any fuzzy controller.

4.4.1 Choice of input signals

The choice of input signals to the fuzzy PSS is of vital importance. The signal/s used must contain enough information of the generator and the power system characteristics and behavior, in order to allow proper control decisions to be executed. [LARSEN1] and [LARSEN2], conducted a rigorous study of the various signals from the power system that are available to the PSS and the limitations and benefits of using each type of signal. [HASSAN1, HASSAN2] made use of the speed deviation and acceleration state of the generator in the phase plane, as inputs to a fuzzy stabiliser. [EL-MET1] made use of the speed and power deviations as inputs to the fuzzy stabilizer whereas [TOLIYAT] used the speed deviation and acceleration as inputs to a fuzzy stabiliser. Based on the above references and the work published by [MALIK], the speed and power deviations, at the generator terminals, are chosen in this investigation as input signals to the fuzzy logic PSS.

4.4.2 Fuzzification

Once the input quantities have been identified, the next step is to define a range over which these signals are to be sampled. In order to establish a range for the speed and power deviation signals, the power system introduced in section 2.6, is subjected to various types of system faults with no stabiliser action on the system. The worst case speed and power deviations are noted and these values are used as the range over which the input signals are to be sampled. These ranges are illustrated in Figure 4.6.

The next step is to establish the number of linguistic variables to map this discrete input range. After investigating the effects of using first 9, then7, then 5 and then 3 linguistic variables, it was established by the author that 3 linguistic variables per discrete input variable gave almost the same result as higher numbers of linguistic variables and was simpler to implement. The linguistic variables associated with the speed deviation are, *speed negative* (*SN*), *speed zero* (*SZ*) and *speed positive* (*SP*). The linguistic variable associated with the power deviation are power negative (*PN*), *power zero* (*PZ*) and *power positive* (*PP*).

Once the linguistic variables are established, the membership functions have to be chosen for these linguistic variables. Various different membership function shapes were used and the fuzzification of the

input monitored. Though most membership functions such as triangular, trapezoidal, Gaussian, Sigmoidal and Pi were evaluated by the author and gave similar results, the Gaussian bell function was chosen due to its inherent smoothness and ease of implementation

The Gaussian shaped membership functions for the speed and power deviation signals appear in Figure 4.6.

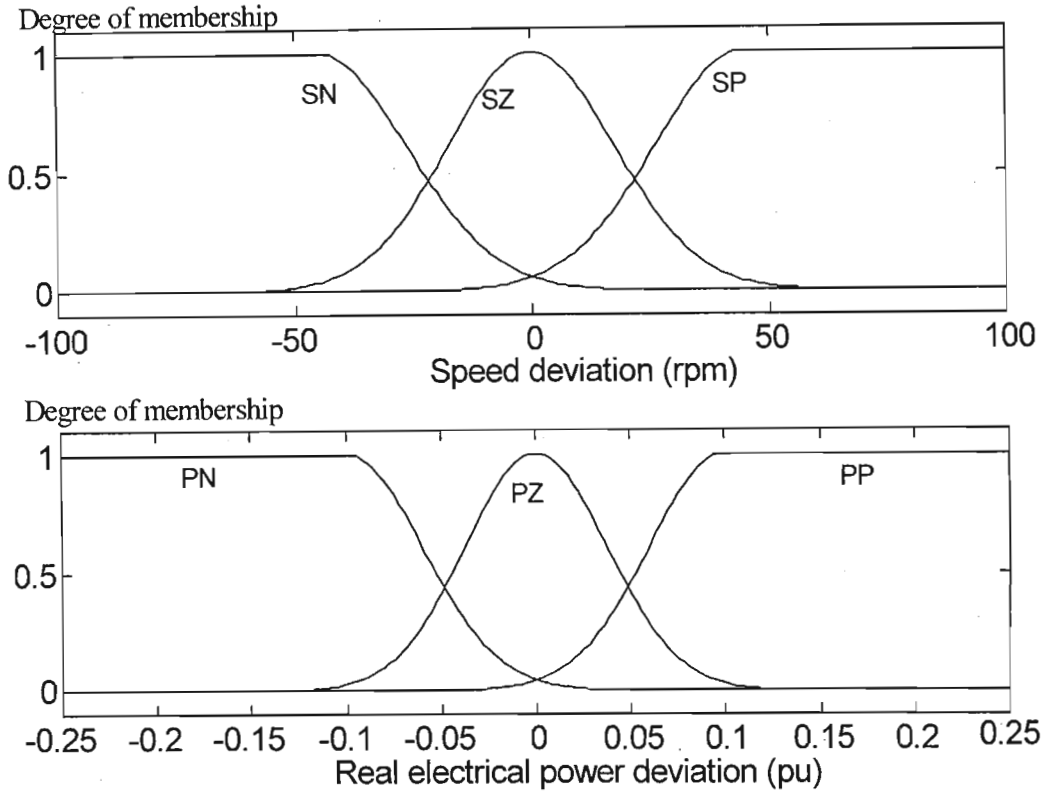

Figure 4.6 – Membership functions for the input variables speed deviation and power deviation

4.4.3 Rule-Based Table (Inference Table)

Rule definition is based on expert knowledge of a system. In the case of a power system, an operator can provide valuable information about the system performance and an engineer can provide expert information about the behavior and performance of a stabiliser in a power system. This expert knowledge is used to form the rule table for the fuzzy logic power system stabiliser.

Due to each input variable having only three linguistic variables associated with it, Table 4.5 is made up of only nine rules (3X3). The rules are derived from previous research [EL-MET1] on fuzzy logic power system stabilisers and theoretical knowledge of classical stabiliser control actions. These rules are the bare minimum set of rules that can be used to control a generator with two discrete inputs to the fuzzy controller. For example, if $\Delta\omega$ is SN and ΔPe=PZ then the rules say that output = OZ. What this

physically means is that if the change in speed is negative (SN), this means the machine is slowing down or decelerating and the change in electrical power is very small (almost zero), then the fuzzy logic power system stabiliser must send an output signal that is very small (almost zero). This output signal value will fall within the range of the OZ membership function. The net effect is that the FLPSS does not issue any supplementary signal to the AVR to exert any further effect on the synchronous machine

Table 4.5 – Rule table used by the fuzzy logic power system stabiliser

$\Delta Pe \rightarrow$ $\Delta\omega \downarrow$	PN	PZ	PP
SN	OP	OP	OZ
SZ	OP	OZ	ON
SP	OZ	ON	ON

4.4.4 Defuzzification

Once the fuzzy decision has been inferred and the corresponding degrees of membership have been transferred to the output variables, a discrete output value needs to be derived. As with each of the discrete input variables, three linguistic variables are associated with the discrete output signal from the fuzzy logic PSS. The linguistic variables are *output negative* (ON), *output zero* (OZ) and *output positive* (OP).

The membership functions chosen for these linguistic variables are also Gaussian shaped curves, due to the smoothness of the curves and are shown in Figure 4.7. The centroid method is employed to derive a crisp signal from the fuzzy output region.

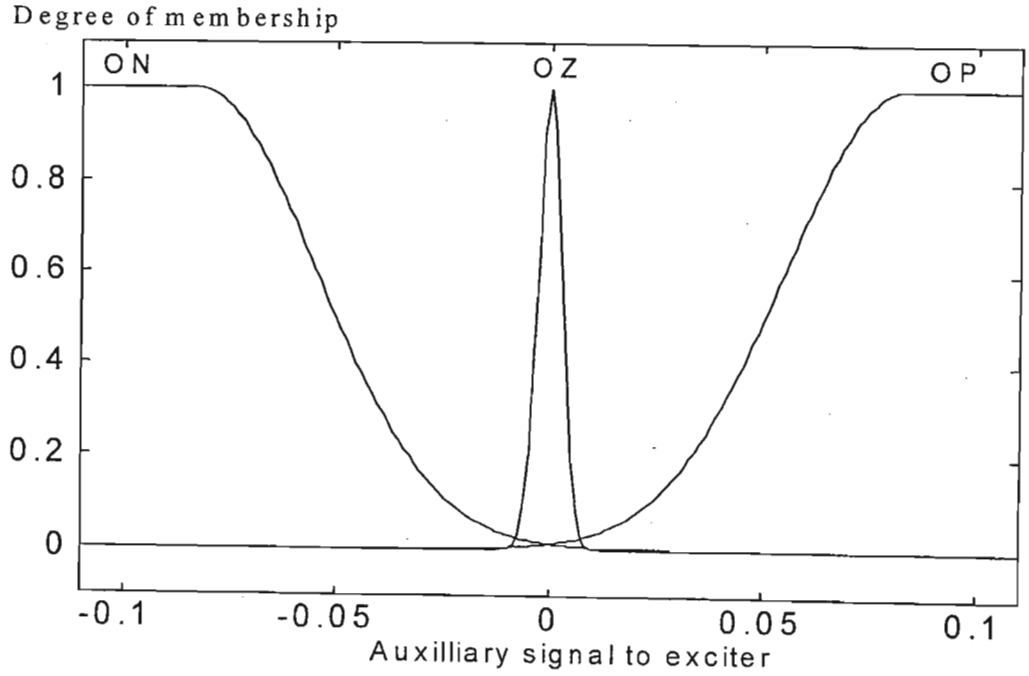

Figure 4.7 – Output membership functions for the auxiliary from the PSS output signal to the exciter

The output range for the fuzzy stabiliser is established by firstly setting the range to ±0.5. A gain function is added to the output of the fuzzy stabiliser. Various tests on the study system introduced in Figure 2.7, with the fuzzy stabiliser in operation, are performed, and the gain function adjusted until an acceptable performance from the fuzzy stabiliser is realised. A good indication of the ideal gain is when the PSS drives the AVR into limits quick enough without compromising small signal stability. When any further increase in gain shows no improvement in the damping of the synchronous machine, this gain is chosen to determine the output range. This gain for this investigation was found to be 0.2 and using this value, the output range for the fuzzy controller is adjusted to ±0.1. Due to the nature of the membership functions, no limiter needs to be added to the output signal, as the discrete output of the FLPSS will never exceed ±0.1.

4.4.5 Optimising the Fuzzy Logic Power System Stabiliser (FLPSS)

The optimisation of the FLPSS is done by evaluating the effects of different membership functions shapes and output ranges in order to achieve improved performance from the FLPSS.

[HASSAN1] and [CHEN] propose methods for a self-tuning FLPSS and with the ability to learn which typically would adjust membership function ranges to provide desired performance. The purpose of this investigation was not to evaluate self-tuning techniques hence no implementation of such techniques is used.

In order to establish the effectiveness of the fuzzy logic power system stabiliser utilising 9 rules, another fuzzy logic power system stabiliser utilising 49 rules is also implemented and evaluated. This 49 rule fuzzy stabiliser was based on work by [El-MET1] and is adapted for application on a synchronous motor. The adaptation of the 49 rule based fuzzy logic stabiliser is explained in the next section. In order to distinguish between the two stabilisers, the stabiliser utilising 9 rules in the rule table will be referred to as the 9 rule fuzzy stabiliser.

4.5. 49 Rule Fuzzy Logic Power System Stabiliser

Previous research work by [EL-MET1], showed a fuzzy logic power system stabiliser employing 49 rules to effectively damp out low frequency power oscillations. That fuzzy stabiliser employed 7 membership functions for each of the two input variables (speed deviation and electrical power deviation) and 7 membership functions for the output variable. The rule table contained 49 rules. The aim of introducing that stabiliser into these studies, is to establish whether a reduction in the number of

rules of a fuzzy logic power system stabiliser, will have any effect on the overall performance of the stabiliser.

In order to perform this comparison, the fuzzy logic power system stabiliser designed by [EL-MET1] for a generator, is adapted by inverting the output signal of the stabiliser so that the stabiliser can be applied to the synchronous motor, for these studies. This adapted stabiliser will be referred to as the 49-rule fuzzy logic stabiliser. The 9 rule and 49 rule fuzzy stabilisers, both utilise the speed and power deviations as inputs.

The 49 rule fuzzy stabiliser uses seven triangular membership functions for each of the input variables and each membership function overlaps the adjacent functions by 50%. The linguistic variables associated with the membership functions for the speed deviation is *speed negative big(SNB), speed negative medium (SNM), speed negative small (SNS), speed zero (SZ), speed positive small (SPS), speed positive medium (SPM) and speed positive big (SPB).* For the power deviations the linguistic variables are, *power negative big (PNB), power negative medium (PNM), power negative small (PNS), power zero (PZ), power positive small (PPS), power positive medium (PPM) and power positive big (PPB).* Figure 4.8 shows the membership functions for the discrete input variables of the 49 rule fuzzy stabiliser. The ranges for the speed and power deviations are set exactly to the same ranges as used by the 9 rule fuzzy stabiliser.

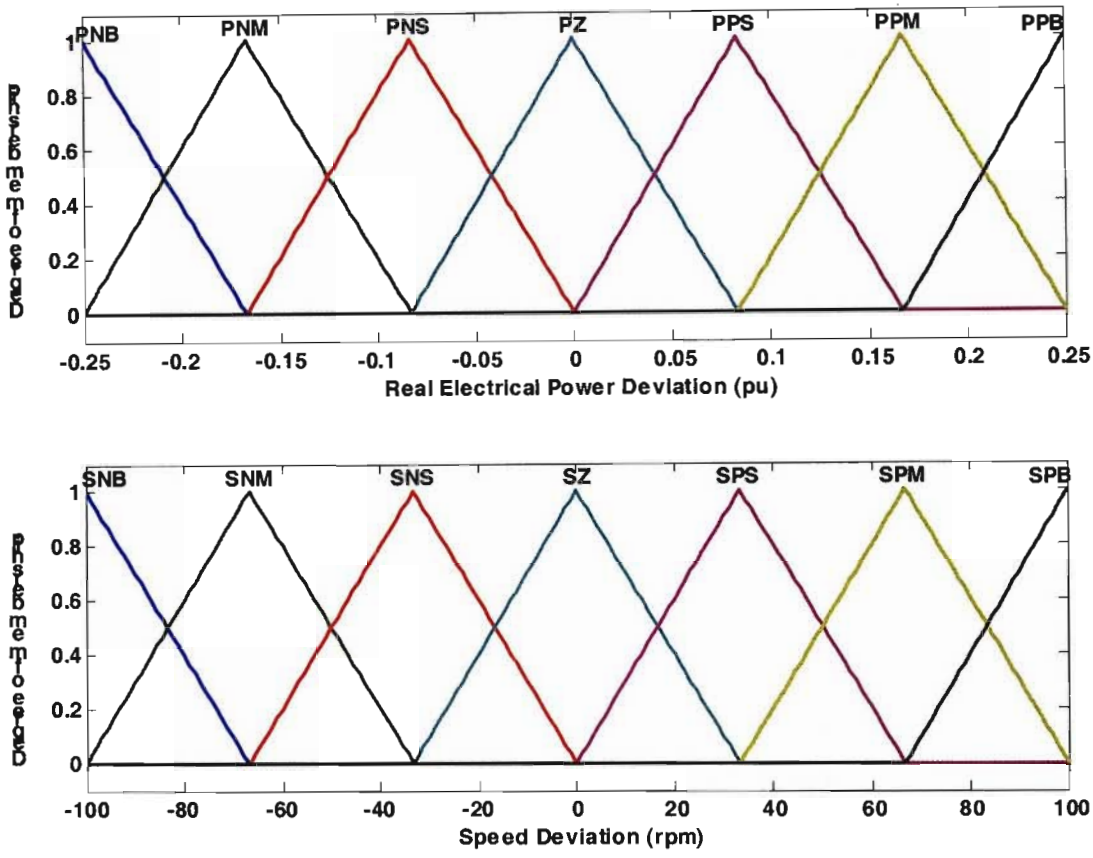

Figure 4.8 – Input variables and membership functions for a 49 rule stabiliser

The 49 rule based table established in [EL-MET1], is now adapted to operate on a synchronous motor. The resulting rule table is given in Table 4.6. A closer examination of the table indicates that the 49 rule table gives a greater resolution to the output membership functions than the 9 rule table.

Table 4.6 – Rule Based table used by the 49 rule fuzzy stabiliser

Speed Deviation	Power Deviation						
	PNB	**PNM**	**PNS**	**PZ**	**PPS**	**PPM**	**PPB**
SNB	OPB	OPB	OPB	OPM	OPM	OPS	OZ
SNM	OPB	OPB	OPM	OPM	OPS	OZ	ONS
SNS	OPB	OPM	OPM	OPS	OZ	ONS	ONM
SZ	OPM	OPM	OPS	OZ	ONS	ONM	ONM
SPS	OPM	OPS	OZ	ONS	ONM	ONM	ONB
SPM	OPS	OZ	ONS	ONM	ONM	ONB	ONB
SPB	OZ	ONS	ONM	ONM	ONB	ONB	ONB

The output variable also has seven triangular membership functions with a 50% overlap between adjacent membership functions. The range of the output signal from the fuzzy stabiliser to the excitation system is limited to the same range as the 9 rule fuzzy stabiliser [-0.1 to 0.1]. The linguistic variables associated with the output membership functions are *output negative big (ONB), output negative medium (ONM), output negative small (ONS), output zero (OZ), output positive small (OPS), output positive medium (OPM) and output positive big (OPB).* Figure 4.9 shows the membership functions for the output signal of the 49 rule fuzzy stabiliser. The centroid method is employed to derive a discrete signal from the fuzzy output region.

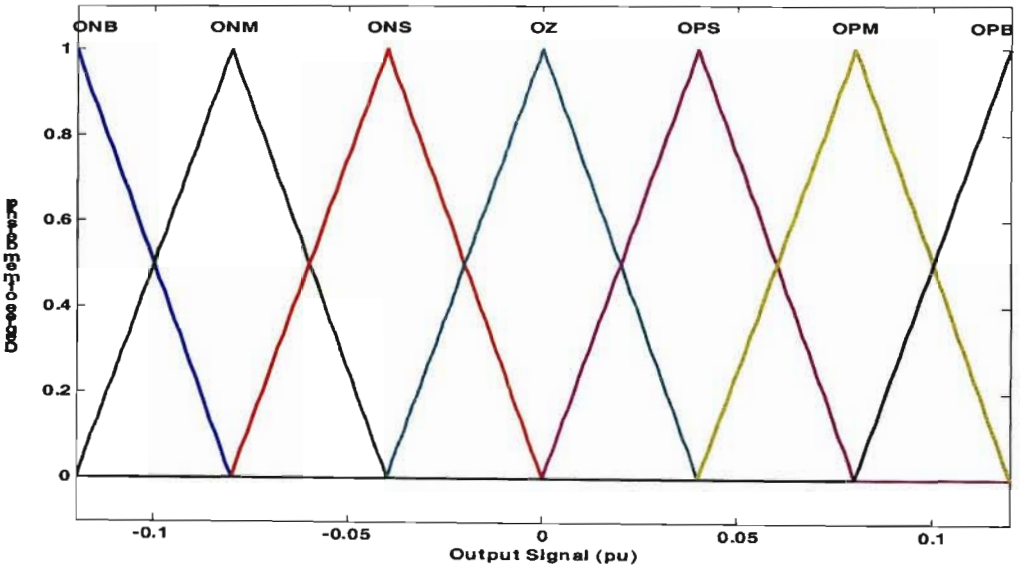

Figure 4.9 – Membership functions used to derive the output signal from the 49 rule stabiliser.

4.6. Conclusion

This chapter explained the basic method employed to design a controller using fuzzy logic techniques. This method was then applied to design and tune two fuzzy power system stabilisers, one utilising 9 rules (3 fuzzy variables for each of the two input and one output variables) and another utilising 49 rules (7 fuzzy variables for each of the two inputs and one output variables). The tuning of the parameters of a conventional PSS is based on linearised equations at a particular operating condition of the power system as well as knowledge of all system parameters. Once the operating condition changes, the PSS performance is expected to degrade. A fuzzy PSS does not require prior knowledge of the system parameters and its performance therefore does not degrade with changing conditions, hence it should be easier to commission, as a CPSS would require on-site re-testing.

The performance results of both the fuzzy power system stabilisers, when the test system of Figure 2.7 is subjected to a fault, is presented in Chapter 5 along with the performance results of the conventional stabiliser. Based on these results, various conclusions as to each stabiliser's robustness and performance are drawn in Chapter 6. The viability of applying a fuzzy PSS to a synchronous motor in a multi-machine environment is also concluded in this chapter.

CHAPTER FIVE

SIMULATION RESULTS

5.1 Introduction

This chapter presents simulated performance results of the conventional power system stabiliser and the fuzzy logic power system stabilisers (9 rule fuzzy stabiliser and the 49 rule fuzzy stabiliser). The study system, introduced in section 2.6 and shown in Figure 2.7 (repeated below in Figure 5.1 for convenience) is used to provide a platform for the simulations. The performance of each stabiliser is evaluated using the same system model. In each case, each type of stabiliser is subjected to different initial operating conditions and the system is subjected to a loss of line fault. The performance of the machines when no stabiliser is present in the system is also presented in order to determine if the stabilisers provide additional damping and to what extent the system stability has been improved.

5.2 Study cases

Three cases are chosen in order to compare the performance of the fuzzy logic power system stabiliser against that of the conventional stabiliser designed in Chapter 3. The first case examines the performance of the stabilisers for the given operating point in Table B1 of Appendix B5, repeated below in Table 5.1 for convenience. This is regarded as the *nominal operating point* and the parameters given in Table 5.1 are measured at the terminals of the machines. The operating point of the motor is then changed in cases 2 and 3 in order to examine the robustness of the fuzzy logic stabiliser under different operating conditions.

Table 5.1 – Nominal operating point parameters of the study system

Quantity	Magnitude (pu)	Angle (degrees)
Voltage – generator (U_{gen})	1.03	9.3
Voltage - motor (U_{mot})	1.03	-3.9
Voltage – Infinite bus (U_{inf})	1.03	0
Real electrical power - generator (P_{gen})	0.67	
Reactive electrical power - generator (Q_{gen})	0.04	
Real electrical power - motor (P_{mot})	-0.42	
Reactive electrical power - motor (Q_{mot})	0.06	
Load LD_1 – real electrical power	0.05	
Load LD_2 – real electrical power	0.05	

In all three cases, in order to create a low frequency power oscillation, the system is subjected to a loss of transmission line contingency. The line tripped, in all three cases, is the line L_{23} in Figure 5.1. The

system was subjected to various other types of faults in order to establish the worst case contingency. It was found that the loss of line L_{23} was a worst case scenario for the test system as when this line is kept out of service indefinitely, the power system is required to settle to a new operating point with very poor damping (no stabilisers present in the system). Furthermore it is assumed that the transmission lines that remain in service after the contingency (lines L_{12} and L_{13}), have enough capacity to carry any extra loading that may occur as a result of the loss of line L_{23}.

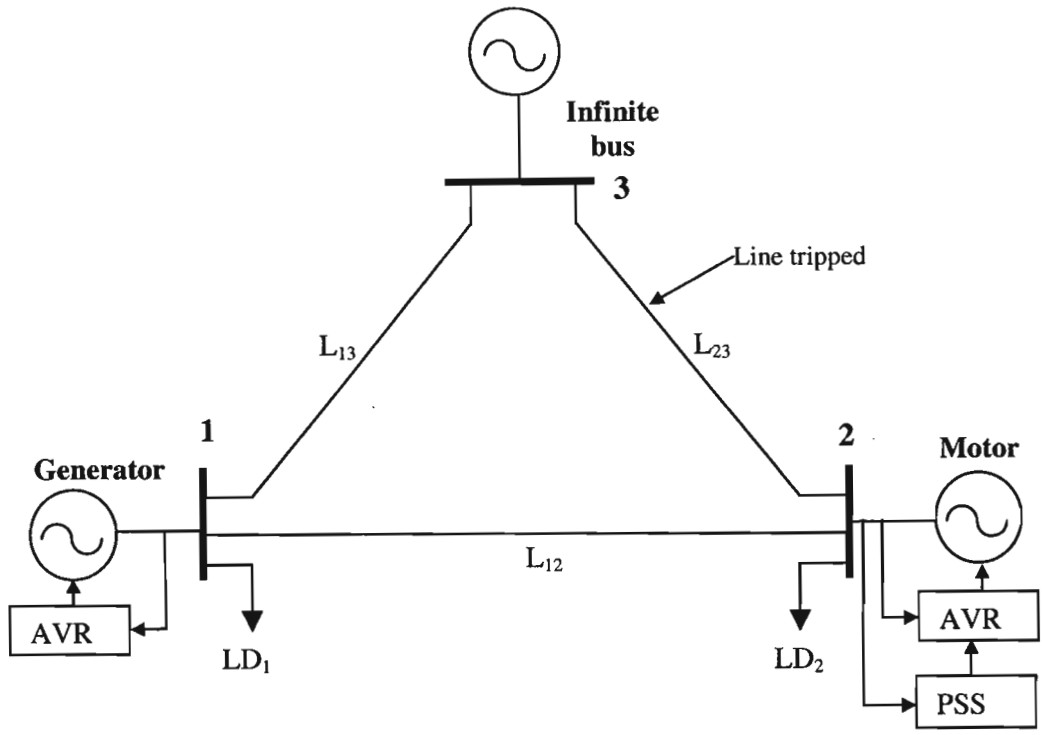

Figure 5.1 – Power system model used to evaluate the performance of the stabilisers

The results presented in this chapter are results of cases that most appropriately indicate the performance of the fuzzy logic and conventional stabilisers when the system is subjected to the worst case fault, under different operating conditions. Numerous simulations, involving different types of faults or system disturbances were conducted during this research project. These results are not presented, as they do not contribute any additional value to the performances of the different PSSs in the power system. The different types of faults, other than the loss of line L_{23}, that the system was subjected to were;

(i) loss of the generator.

(ii) loss of lines L_{13} and L_{12} (separate cases).

(iii) 5% step increase and decrease in the generator's mechanical input power (separate cases).

(iv) 5% step increase and decrease in the motor's mechanical output power (separate cases).

(v) loss of loads LD_1 and LD_2 (separate cases).

(vi) a 15% step increase in loads LD_1 and LD_2 (separate cases).

5.2.1 Case 1 – Operation at Nominal Operating Point

The first case uses the pre-fault operating conditions given in Table 5.2 as a starting point. These quantities are indicated at the terminals of the machine. The conventional power system stabiliser has been tuned at the pre-fault operating point for case 1, in Chapter 3. The line currents flowing in the transmission network are given in Table 5.3. A steady state phasor representation of the terminal voltage and currents of the machines under pre and post fault conditions are shown in Figure 5.2. Figure 5.2 also shows each machine's internal voltage phasor with respect to the infinite bus voltage phasor and the voltage phasor due to the internal inductance of the machines. The angle between the internal voltage of the machine and the infinite bus voltage phasor is the rotor angle of the machine. The machines' rotor angles (with respect to the infinite bus) following the permanent removal of the line L_{23}, are shown in Figure 5.2. The real electrical power at the terminals of each machine, in response to the network fault, appears in Figure 5.3.

Table 5.2 – Pre-and post fault steady state operating conditions for case 1

Quantity	Pre-fault		Post-fault	
	Magnitude (pu)	Angle (degrees)	Magnitude (pu)	Angle (degrees)
Voltage - generator	1.03	9.3	1.03	5.3
Voltage - motor	1.03	-3.9	1.03	-12.1
Current - generator	0.67	5.67	0.67	5.1
Current - motor	-0.42	169	-0.42	168.5
P generator	0.67		0.67	
Q generator	0.04		0.06	
Power factor - generator	0.998		0.996	
P motor	-0.42		-0.42	
Q motor	0.06		0.09	
Power factor - motor	0.99		0.98	
Load LD_1 – real electrical power	0.05		0.05	
Load LD_2 – real electrical power	0.05		0.05	

Table 5.3 – Pre and Post fault currents flows on the transmission network for case 1

From bus	To bus	Line currents – pre-fault		Line currents – post fault	
		Real	Imaginary	Real	Imaginary
1	2	0.36	0.05	0.47	0.09
1	3	0.26	0.03	0.15	0.01
2	3	-0.16	-0.01	0	0

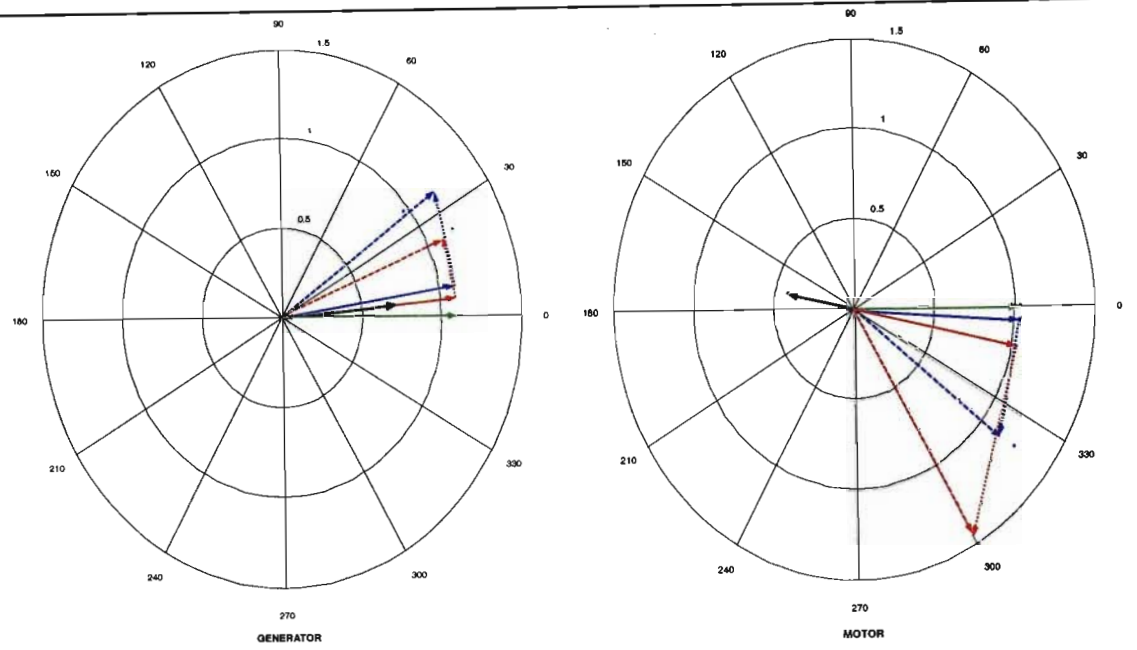

→	Terminal voltage – pre-fault	→	Terminal voltage – post-fault
- - - →	Internal machine voltage – pre-fault	- - - →	Internal machine voltage – post-fault
····· →	Voltage due to machine inductance – pre-fault	····· →	Voltage due to machine inductance – post-fault
→	Machine current – pre-fault	- - - →	Machine current – post-fault
→	Infinite bus voltage		

Figure 5.2 – Steady state phasor representation of the voltages and currents for the synchronous motor and generator for case 1.

Figure 5.2 illustrates that the angular position of the pre and post fault current phasors for both machines does not change significantly. The internal machine voltages change to accommodate the changes to the network configuration as seen from the machine terminals looking into the network. Resistive losses are neglected in the machine models, hence there are no voltage phasors indicating internal machine voltage due to resistance,

Both Figure 5.3 and Figure 5.4 illustrate the poorly damped nature of the power system when no stabiliser is present in the system. The fuzzy stabilisers and the conventional stabiliser have a profound effect on the damping of both machines by reducing the magnitude of the first swing and ensuring a quick settling time (±3 seconds) of the oscillations. The performance of all stabilisers is similar, as all the stabilisers have damped the oscillations in the machines' rotor angles to within ±2.5% of their post-fault values within 3 seconds, as shown in Figure 5.3. The 9 rule fuzzy stabiliser shows a similar performance to the 49 rule fuzzy stabiliser. The performance of the 9 rule fuzzy stabiliser is also comparable to the performance of the conventional stabiliser.

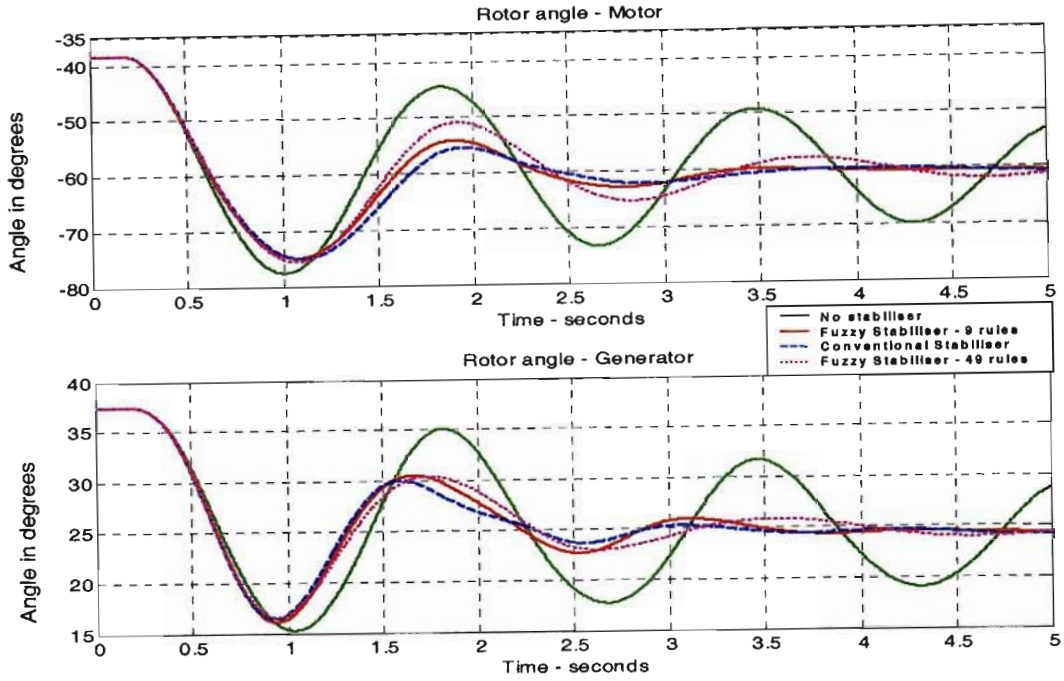

Figure 5.3 – Effects on the rotor angles of both machines for each type of stabiliser for case 1.

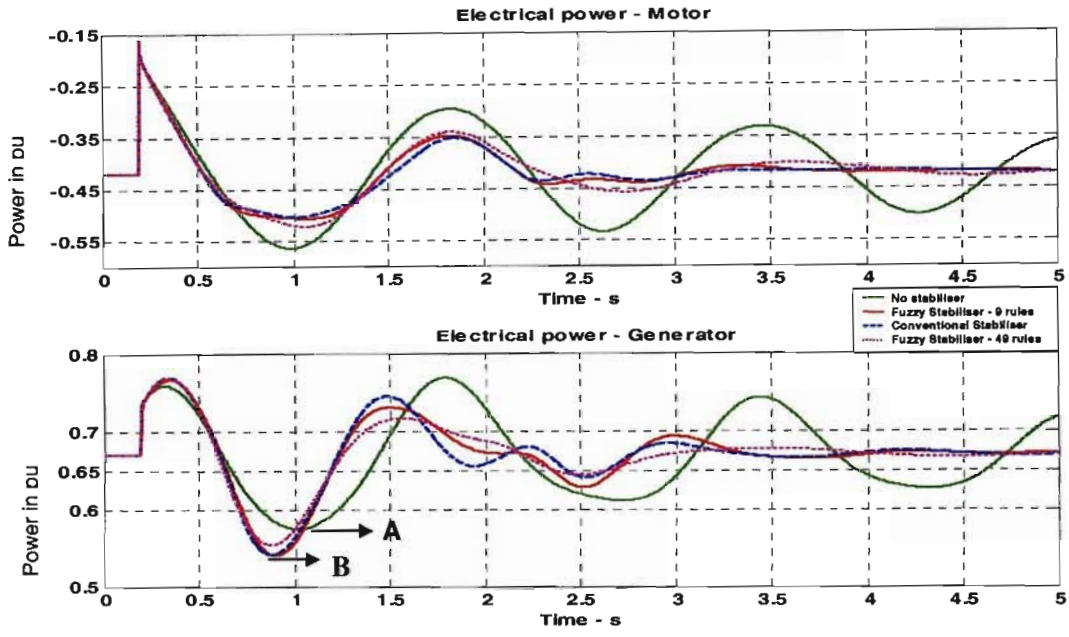

Figure 5.4 – Real electrical power at each machine's terminals for Case 1.

The electrical power oscillations for Case 1 are shown in Figure 5.4. The actions of the fuzzy stabilisers and the conventional stabiliser clearly damp out the power flow oscillations in Figure 5.4. With the PSSs applied at the motor, a slightly greater electrical power swing of the generator in the initial period is noticed as compared to the system with no stabiliser. With no stabiliser present the electrical power of the generator swings to point A. With stabilisers present, the electrical power of the generator swings to point B, which is approximately 0.03 pu greater than point A. In spite of this slightly poorer response in

the initial period, all stabilisers adequately damp out the power oscillations of the generator. The electrical power at the terminals of both machines in the system is damped to within ±2.5% of their post-fault values within 4 seconds.

The effect of all stabilisers on the system is carried out through the motor's excitation system, which in turn affects the field voltage. Figure 5.5 illustrates the effects of all stabilisers on the field voltage of the motor and the generator. In the case of the motor there are clear signs of saturation caused by the PSS driving the AVR to its limits.

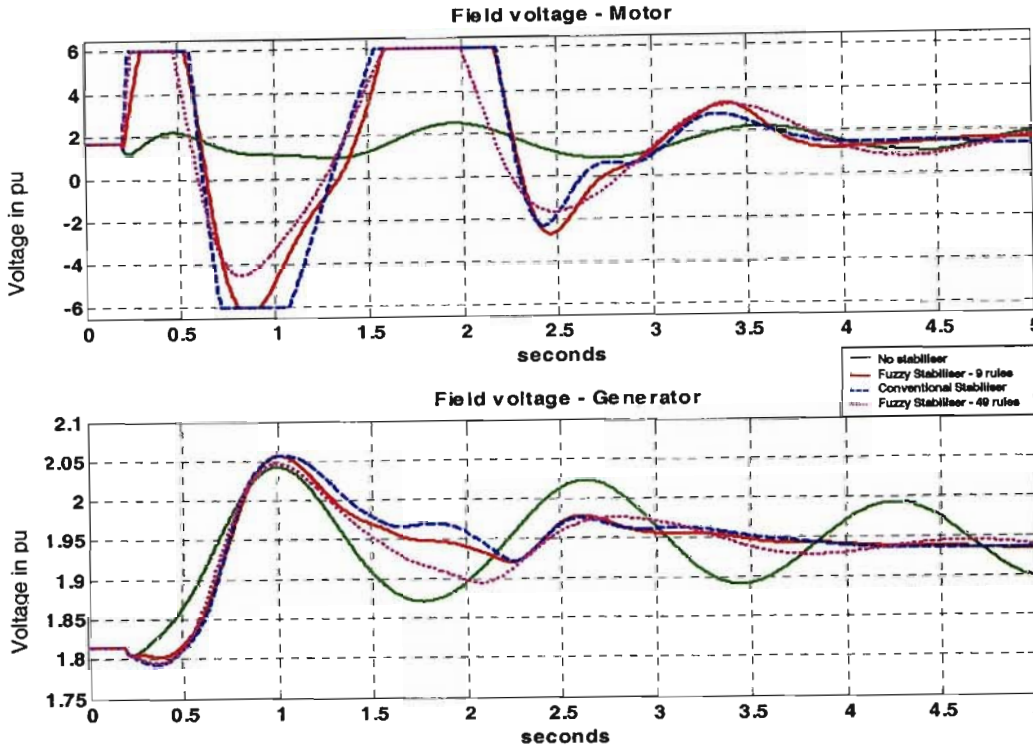

Figure 5.5 – Effects of the stabilisers on the field voltage of the motor.

The effects on the field voltage are similar for all three stabilisers, though the conventional stabiliser illustrates a slightly stronger control action as compared to the fuzzy stabilisers. This is illustrated by the fact that the conventional stabiliser stays at the voltage limits, during the initial period of the disturbance, for slightly longer than the fuzzy logic stabiliser. The slightly slower response of the 49 rules fuzzy stabiliser is clearly shown in Figure 5.5, as this stabiliser does not exert as much control over the field voltage as the other two stabilisers (9 rule fuzzy stabiliser and conventional stabiliser)

The responses of all the stabilisers in this case are similar, with very little to distinguish one performing better than the other. The performance of all the stabilisers is acceptable, illustrated by the quick damping of the oscillations. Even with fewer rules, the 9 rule fuzzy stabiliser produces the same desired effect as the conventional stabiliser, which has been designed and tuned for this operating point.

Without a PSS the field voltage variation for both the motor and generator are much lower than the assigned limits of the AVR. This means that the AVR gain could have been increased to effect more damping by having longer excursions of field voltage however this could lead to small signal instability. It is for this reason that PSSs are used to improve damping rather than high gain AVRs.

5.2.2 Case 2 – Motor operating under leading power factor

For Case 2 the motor's initial operating point is changed so that the motor's reactive power is changed from 0.06 pu lagging (Case 1) to 0.03 pu leading, by reducing the motor's terminal voltage to 1.0 pu. This causes the motor's initial rotor angle to be 54° (Shown in Figure 5.7). The new pre-fault operating condition data appears in Table 5.4. The current flows in the transmission network are given in Table 5.5. The aim of changing the power factor is to investigate the robustness of the fuzzy stabilisers. Figure 5.6 illustrates the current and voltage phasors for both machines in the network, under pre and post fault steady state operating conditions. The effect of the auxiliary control of all the stabilisers on the machines' rotor angles is illustrated in Figure 5.7 when the same line L_{23} is taken out of service. The performance of both the fuzzy stabilisers is acceptable and similar.

Table 5.4 – Pre and post fault steady state operating point parameters for case 2

Quantity	Pre-fault		Post-fault	
	Magnitude (pu)	Angle (degrees)	Magnitude (pu)	Angle (degrees)
Voltage - generator	1.03	9.4	1.03	5.3
Voltage - motor	1.00	-4.0	1.00	-12.6
Current - generator	0.67	1.7	0.67	-4.3
Current - motor	-0.42	171.6	-0.42	161.7
P generator	0.67		0.67	
Q generator	0.09		0.11	
Power factor - generator	0.991		0.986	
P motor	-0.42		-0.42	
Q motor	-0.03		0.04	
Power factor - motor	0.997		0.995	
Load LD_1 – real electrical power	0.05		0.05	
Load LD_2 – real electrical power	0.05		0.05	

Table 5.5 – Current flows in the transmission network for case 2.

From bus	To bus	Line currents – pre-fault		Line currents – post fault	
		Real	Imaginary	Real	Imaginary
1	2	0.36	0.08	0.47	0.11
1	3	0.26	0.03	0.15	0.01
2	3	-0.17	-0.08	0	0

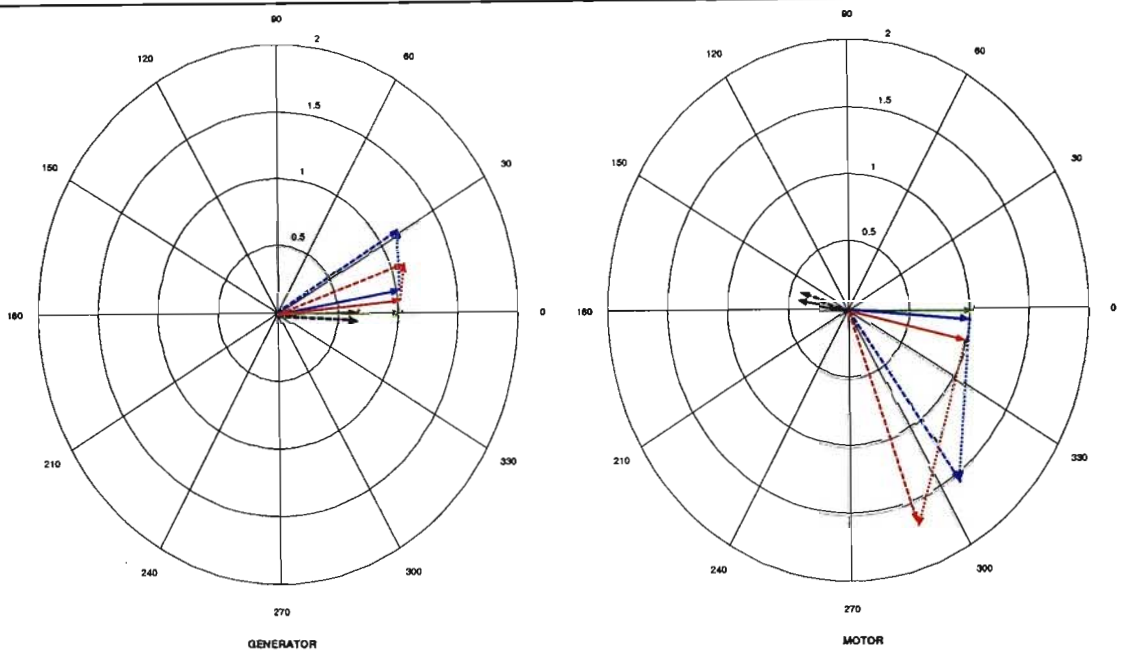

→	Terminal voltage – pre-fault	→	Terminal voltage – post-fault
- - →	Internal machine voltage – pre-fault	- - →	Internal machine voltage – post-fault
····→	Voltage due to machine inductance – pre-fault	····→	Voltage due to machine inductance – post-fault
→	Machine current – pre-fault	- - →	Machine current – post-fault
→	Infinite bus voltage		

Figure 5.6 – Phasor representation of the steady state voltage and currents phasors of both machines for case 2.

From Figure 5.6 it can be seen that the current phasors have changed by 6° and 10° for the generator and motor respectively. The internal machine voltage (for both machines) has also changed to accommodate the change in the network configuration. Resistive losses are neglected in the machine models.

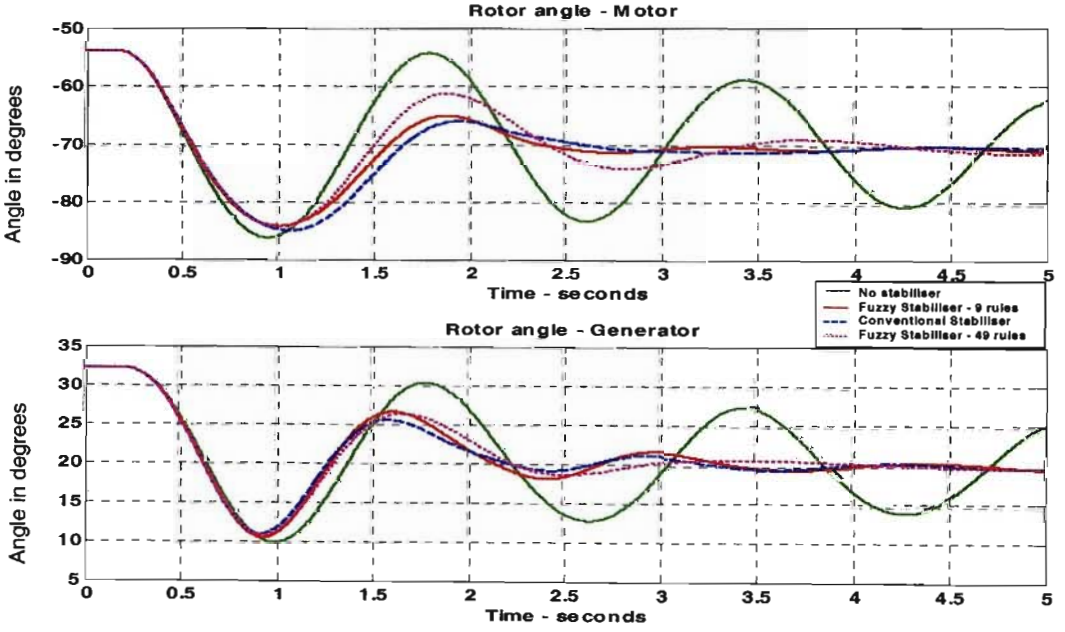

Figure 5.7 – Rotor angle of both machines for each type of stabiliser when the motor is operating at leading power factor.

Even at this new operating condition of case 2, the response of the conventional stabiliser shown in Figure 5.7, is similar to that achieved in Figure 5.3, i.e. the rotor angle oscillations have been damped to ±2.5% of their post fault values within 3 seconds. For all stabilisers though, the performance in damping power oscillations is satisfactory and all stabilisers demonstrate robustness.

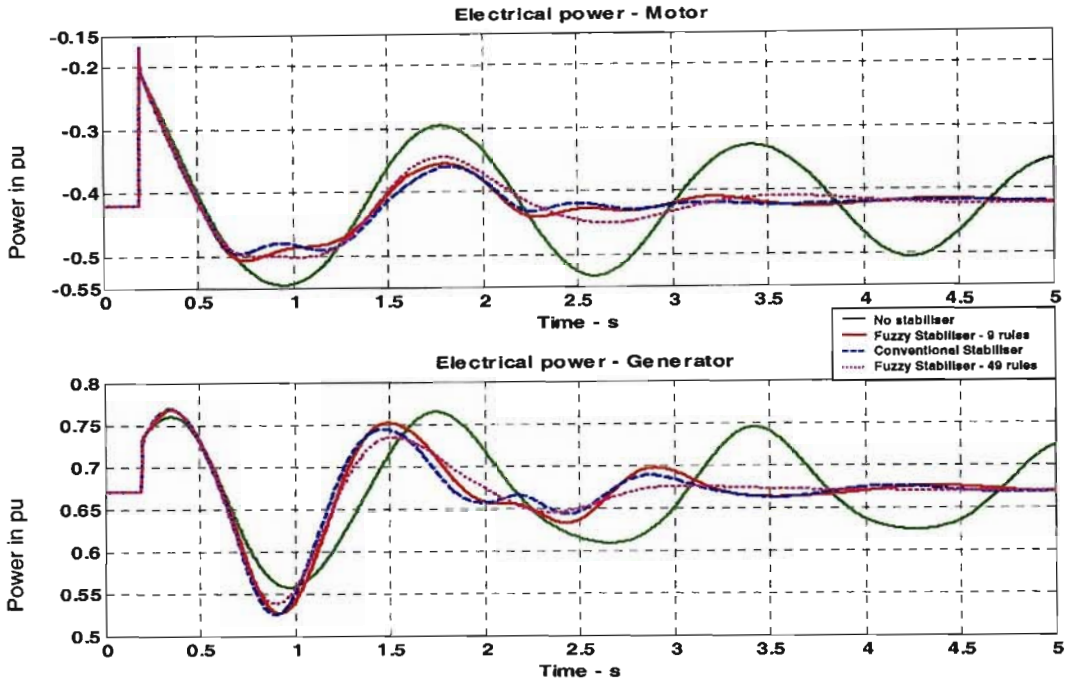

Figure 5.8 – Real electrical power at each machine's terminals when the motor is operating at leading power factor.

Figure 5.8 illustrates the electrical power at the machine's terminals, for this new initial condition. The electrical power oscillations for both the machines, with the fuzzy stabilisers in service, are damped to within ±2.5% of their post-fault values in just over 4 seconds. In this respect the performance of the 9 rule fuzzy stabiliser is similar to that in Figure 5.4 for case 1. Again the results achieved are similar to the results in Case 1, with damping of the oscillations in the rotor angles, to within acceptable margins, taking place in under 5 seconds.

This case illustrates, to a certain extent, the robustness of the fuzzy stabilisers. The conventional stabiliser also demonstrates some robustness. However no significant distinction between the robustness of the fuzzy and conventional stabilisers can be determined. The next case further demonstrates the robustness of the fuzzy stabilisers.

5.2.3 Case 3 – Motor operating with increased input electrical power

For Case 3 the system is operated at the pre-fault operating conditions indicated in Table 5.6 i.e. the motor's input real electrical power is increased from - 0.42 pu (Case 1 and 2) to -0.62 pu with the motor's terminal voltage magnitude at 1.03 pu. The motor is operating with a lagging power factor. The pre and post fault current flows in the transmission network are given in Table 5.7. A phasor representation of the voltages and currents of the machines at pre and post fault steady state conditions is shown in Figure 5.9.

Table 5.6 – Steady operating point parameters for case 3

Quantity	Pre-fault		Post-fault	
	Magnitude (pu)	Angle (degrees)	Magnitude (pu)	Angle (degrees)
Voltage - generator	1.03	6.7	1.03	-2.1
Voltage - motor	1.03	-8.9	1.03	-27.4
Current - generator	0.67	2.2	0.67	-13.0
Current - motor	-0.62	161.2	-0.62	168.0
P generator	0.67		0.67	
Q generator	0.05		0.13	
Power factor - generator	0.997		0.982	
P motor	-0.62		-0.62	
Q motor	0.10		0.17	
Power factor - motor	0.987		0.964	
Load LD_1 – real electrical power	0.05		0.05	
Load LD_2 – real electrical power	0.05		0.05	

Table 5.7 – Pre-and post fault current flows in the transmission network

From bus	To bus	Line currents – pre-fault		Line currents – post fault	
		Real	Imaginary	Real	Imaginary
1	2	0.43	0.07	0.67	0.17
1	3	0.19	0.02	-0.05	0.0
2	3	-0.24	0.03	0	0

Figure 5.9 indicates the changes to the angular position of the currents for both the machines, with the current of the generator changing by approximately 15° and that of the motor changing by 7°. A significant increase in the motor's post fault internal voltage is noticed, with a magnitude of approximately 3pu. The generator's terminal voltage angle becomes negative with respect to the infinite bus under post-fault conditions. This is due to the power now having to flow from the infinite bus towards the generator in order to compensate for the resistive losses in the transmission line between the generator and infinite bus. All the real power supplied by the generator is used to supply the loads LD_1 and LD_2, the line losses between the motor and generator and the motor's load.

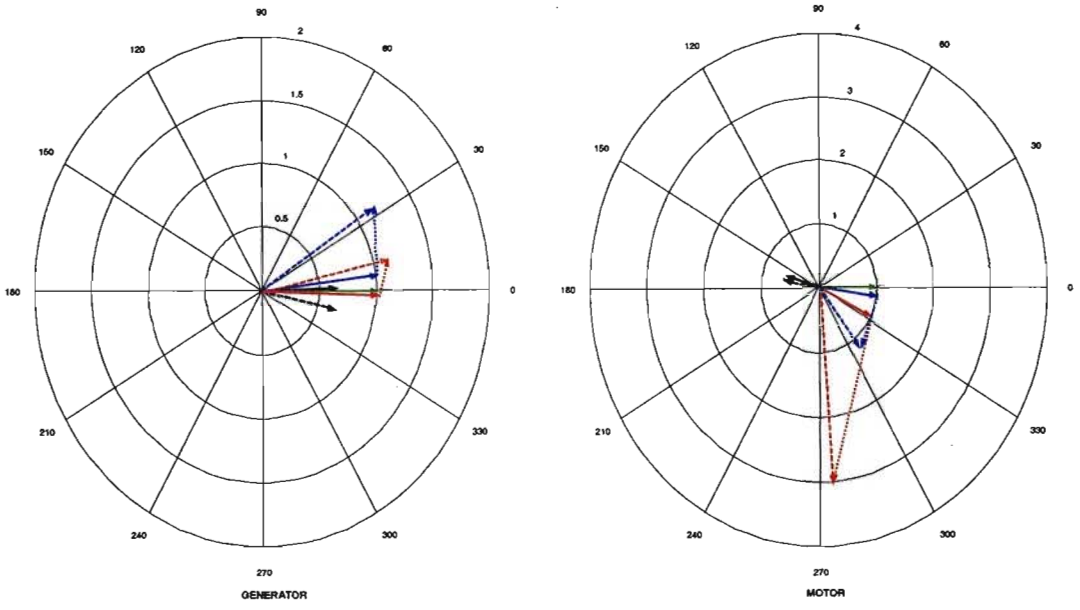

→	Terminal voltage – pre-fault	→	Terminal voltage – post-fault
- - →	Internal machine voltage – pre-fault	- - →	Internal machine voltage – post-fault
····→	Voltage due to machine inductance – pre-fault	····→	Voltage due to machine inductance – post-fault
→	Machine current – pre-fault	- - →	Machine current – post-fault
→	Infinite bus voltage		

Figure 5.9 – Phasor representation of the pre-and post fault current and voltage phasors for both machines for case 3

Figure 5.10 shows the dynamic results of the rotor angles of the machines, when the same line L_{23} as before is removed from service. For the system with no stabiliser present, the power oscillations indicate the poorly damped nature of the system model.

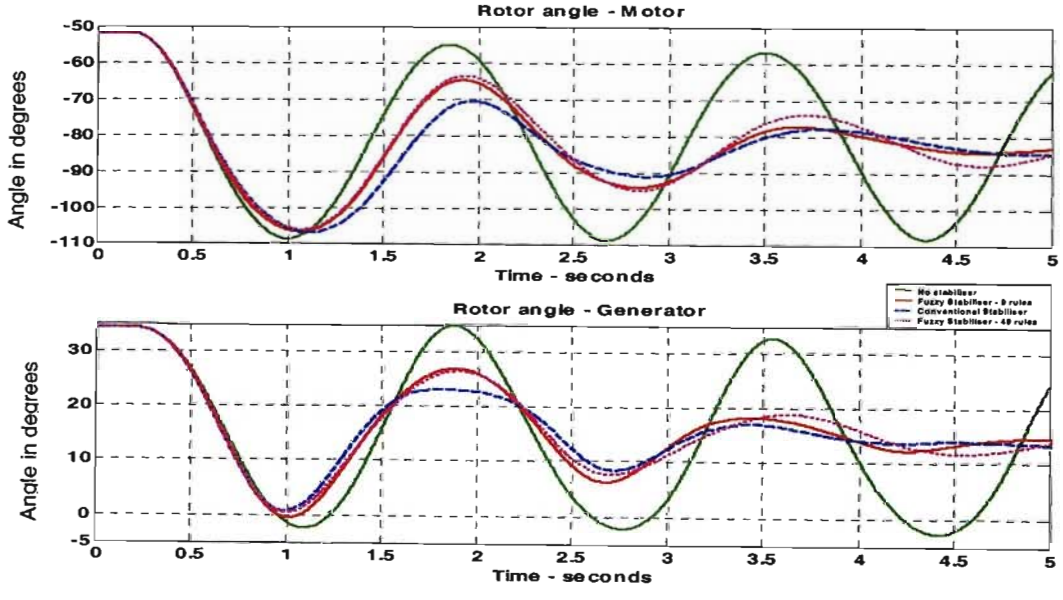

Figure 5.10 – Rotor angle of both machines for each type of stabiliser when the motor is operating with increased electrical power.

In the case of the motor, the improved damping due to the addition of a PSS is clear. Adding a stabiliser to the motor has clearly also improved the damping of the generator. The performance of the conventional stabiliser is similar to that of the fuzzy stabilisers. The fuzzy stabilisers have managed to quickly damp out the power oscillations as well as maintain system stability. The robustness of the fuzzy stabilisers is clearly demonstrated by this case. The CPSS performs just as well as the FLPSS, contrary to expectations of the performance of the CPSS degrading with a change in operating point.

Figure 5.11 shows the effects of the stabilisers on both the machines real electrical power. The conventional and fuzzy stabilisers manage to contain the increasing oscillations, thus maintaining stability. After 4.5 seconds both the fuzzy stabilisers have damped out the oscillations in both the machines to within ±2.5% of the post-fault machines' electrical power.

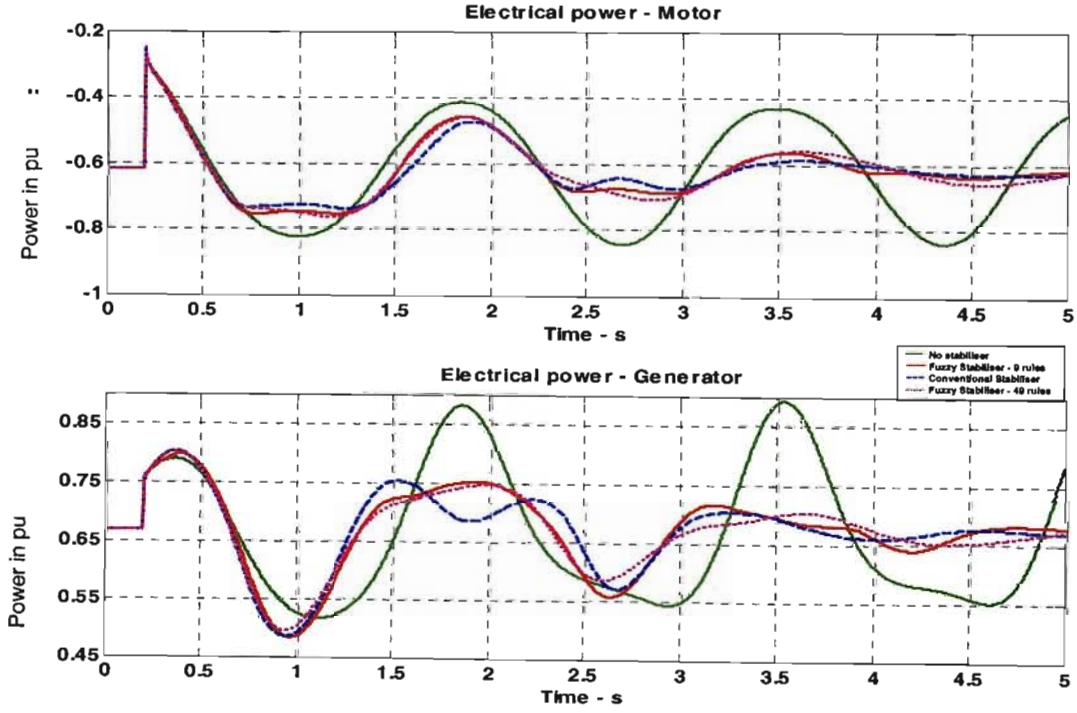

Figure 5.11 – Real electrical power at each machines terminals when the motor is operating with increased electrical power.

5.2 Conclusion

The results presented in this chapter illustrate that the 9 rule fuzzy logic stabiliser and the conventional stabilisers perform equally well in the system model for the different operating conditions. The 9 rule fuzzy stabiliser also performs equally well as the 49 rule fuzzy stabiliser even though it employs fewer rules to make control decisions. This is important, as the computational overheads of this fuzzy stabiliser (9 rules) is less than the 49 rule fuzzy stabiliser. The results also show that all the stabilisers, if properly tuned, can be robust enough to deliver acceptable performance under various operating conditions.

Chapter 6 concludes this thesis by forming conclusions on the applicability of fuzzy logic stabilisers in a multi-machine environment.

CHAPTER SIX

CONCLUSION

6.1 Introduction

Chapter One introduced the research topic and gave a historical perspective of the use of fuzzy logic stabilisers in multi-machine studies. Chapter Two presented techniques to model a synchronous machine and excitation controls in computer simulations, in a multi-machine environment. The design techniques used to tune a conventional and a fuzzy logic power system stabiliser were described in Chapters Three and Four respectively. Chapter Five presented simulation results of the performance of each of the stabilisers, under different operating conditions.

Chapter Six reviews the results of Chapter 5 and concludes about the applicability of a fuzzy logic power system stabiliser, firstly applied in a multi-machine environment and secondly, applied to a synchronous motor. Other conclusions drawn from this thesis are also presented.

6.2 Conclusions

Comparing the design procedures for the fuzzy stabiliser and the conventional stabiliser, the fuzzy stabiliser design procedure is much simpler to implement than that of the conventional stabiliser. The design and tuning method of the conventional stabiliser requires an in-depth knowledge of the power system dynamics, its parameters, and classical control theory. Such in-depth control theory knowledge is often possessed by very few skilled field personnel, thus reducing the number of people that can properly understand the operation of a conventional stabiliser and effectively tune a conventional PSS.

The fuzzy stabiliser design procedure employs logical thinking methods, thus making the understanding of the operation of a fuzzy controller more widely understood. Furthermore the fuzzy stabiliser design procedure provides a convenient method to capture expert knowledge of a system and the required performance. Such knowledge acquired from experienced system operators, cannot be easily translated into a conventional controller. It may be argued though that the fuzzy stabiliser design method tends to be more subjective than objective. This may not necessarily be a disadvantage of the fuzzy stabiliser design method as often, subtle control action required for a particular system can be implemented with a fuzzy stabiliser whereas such control action may be more difficult to implement using a conventional stabiliser.

The results presented in Chapter Five, show the performance of the fuzzy stabilisers to be similar to that of the conventional stabiliser. These results prove that the fuzzy stabiliser can be effectively used to damp out low frequency power oscillations. The results also show that the fuzzy stabiliser works well under different operating conditions. These results, prove what has already been shown by previous researchers, that the fuzzy logic power system stabiliser is a robust controller.

The robust performance of the conventional stabiliser can be attributed to the fact that the conventional stabiliser is designed to compensate for the phase lag introduced through the machine's excitation system. In order to provide the required damping, the stabiliser must produce a component of electrical torque in phase with the rotor speed deviations. In order for the stabiliser is to inject a component of electrical torque T_e in phase with the rotor speed deviations, it must compensate for the phase lag introduced by the exciter and field circuit of the machine. The effects of the network conditions on the field and excitation circuits are minimal for small changes in the network conditions thus enabling the stabiliser to be tuned around an operating point. Under large changes to the network (e.g. large change to the impedance of the network as seen from the generator terminals), the effects on the field and excitation circuits may cause the conventional stabiliser to work outside the bandwidth it was designed for. This effect can be negated by slightly "de-tuning" the conventional stabiliser and allowing for a greater bandwidth of operation. This enables the conventional stabiliser to produce the required damping over a larger operating range of the machine.

The fact that the effects of the fuzzy stabilisers in this thesis have been investigated on a synchronous motor, adds another dimension to the applicability of a fuzzy stabiliser in a multi-machine system. The results of simulations with the fuzzy stabilisers, show no adverse effects caused by the fuzzy stabiliser operating on a synchronous motor. This provides proof that a PSS can be implemented effectively on a synchronous machine that is operating in motoring mode and still influence the overall network stability. Traditionally, generators are used to inject reactive/real power into networks and can be used to improve network stability after disturbances. A motor is seen as consuming real/reactive power, and its influences on network stability, if any, needs to be quantified. Nevertheless, it has been demonstrated that the motor, under the influence of a PSS, can still be used effectively to assist with network stability, even though it may not be injecting any real/reactive power. It is more a case of varying the amount of real/reactive power the motor consumes to assist with network stability.

Comparing the 9 rule fuzzy stabiliser designed in this thesis, with the previous work done by [HASSAN1], [ZHANG], [SHI], [EL-MET1],[TOLIYAT] and [CHEN], the 9 rule fuzzy stabiliser uses significantly less membership functions than previous work done. The 9 rule fuzzy only three membership functions for each of the two input variables and three membership functions for the output

variable. The simulation results presented show similar performance of the 9 rule fuzzy stabiliser as compared to the 49 rule fuzzy stabiliser. [EL-MET1] used seven membership functions for each of the two input variables and seven membership functions for the output variable. Due to the lower number of membership functions, the 9 rule fuzzy stabiliser designed in this study will require significantly less computational overheads as compared to the 49 rule fuzzy stabiliser.

The comparison between the 9 rule fuzzy stabiliser and the 49 rule fuzzy stabiliser further illustrates that with proper membership function shape and range selection, a simple yet effective controller can be implemented. This simple controller can perform just as well as the more tried and trusted conventional stabilisers.

6.3 Recommendations for Future Studies

It is recommended that the 9 rule fuzzy stabiliser designed in this thesis be implemented in hardware and tested in a machines laboratory. [HASSAN2], [HIYAMA1], [HIYAMA2] and [EL-MET2] have demonstrated the application of a 49 rule fuzzy logic stabiliser in a machine laboratory environment. Their work can form the basis for testing the 9 rule fuzzy logic stabiliser, in a multi-machine laboratory as well as on a synchronous motor. Today, fuzzy logic controller chips are freely available to enable such a controller to be easily implemented in hardware.

A further recommendation is to test the 9-rule fuzzy logic stabiliser on a digital, real time power system simulator. This simulator will enable the researcher to create a much larger power system network model, than the one used for investigations in this thesis or in the laboratory. Furthermore, a physical excitation system of a generator can be used in the experiments, to enable realistic results to be achieved.

A further benefit of using a real time simulator is that the inter-action between different stabilisers in a power system can be investigated. Such research can prove very useful towards the design and tuning techniques of power system stabilisers (albeit conventional or fuzzy stabilisers). Furthermore, researchers will be able to identify dominant controllers in the system and take preventative measures to ensure that "stabiliser fighting" is eliminated.

The final step is to test a fuzzy logic stabiliser on an actual large multi-megawatt generating unit, that is connected to the power system. This stage may however be met with much resistance, as power station managers must run their stations as efficiently and effectively as possible. In order to implement such a stabiliser would require the power station to be either taken off the grid (as in the case for maintenance) or that the stabiliser be switched into operation, whilst the station is running, without causing any adverse effects to the station and the interconnected transmission system. In order to prove that a fuzzy

stabiliser can work efficiently and effectively, much testing in a laboratory would have to be done to prove the technique and the applicability of the technique, in order to convince the respective key role players in the electrical power system.

APPENDIX A

PER UNIT SYSTEM

A1 Sign Conventions

The sign conventions adopted in this thesis is summarised as follows;

δ is positive for a motor

$p\delta$ is positive for super-synchronous speeds

$p^2\delta$ is positive for acceleration

P_e is positive for power output from the generator

M_e is positive for generator action with mechanical power passing into the machine at positive speed.

Quantities in the ABC machine frame are transformed into the dq0 reference frame via the Park's transformation matrix given by

$$[P_\theta] = \frac{2}{3}\begin{bmatrix} \cos\theta & \cos\left(\theta - \frac{2\pi}{3}\right) & \cos\left(\theta - \frac{4\pi}{3}\right) \\ \sin\theta & \sin\left(\theta - \frac{2\pi}{3}\right) & \sin\left(\theta - \frac{4\pi}{3}\right) \\ \frac{1}{2} & \frac{1}{2} & \frac{1}{2} \end{bmatrix} \quad \text{(A.1)}$$

The angle θ is defined for the rotor reference frame as the angle between the stator phase A winding and the direct axis of the rotor [ADKINS] and is given by

$$\theta = \omega_o t - \delta \quad \text{(A.2)}$$

where ω_0 is the nominal speed and δ is the machine rotor angle.

A2 Base Quantities of the Per-Unit System

In order to normalise system variables and improve computational simplicity, a per-unit system is used to represent system variables. The per-unit quantity expresses a system quantity as a dimensionless ratio and is expressed as

$$\text{per unit quantity} = \frac{\text{actual quantity}}{\text{base value of qantity}}$$

Base quantities may be chosen arbitrarily while others may be chosen depending on fundamental relationships between system variables. Normally the base quantities are chosen such that the principal system variables are equal to one per unit under rated conditions.

Four base values for this per-unit system are chosen independently, namely the base armature power P_a^b, the base armature voltage V_a^b, the base time t^b and the base electrical angle θ_e^b. The remaining base values are derived from these four values. The base field power is fixed by the particular Park's transform used while the base field current is chosen by forcing X_{md} and X_{fd} to be equal in per-unit. The base values are summarised as follows:

Base armature power	P_a^b	=	total three phase rating in Watts
Base armature voltage	V_a^b	=	rated rms voltage per phase in AC Volts
Base armature current	I_a^b	=	$P_a^b / (3V_a^b)$ in rms AC Amps
Base armature impedance	Z_a^b	=	V_a^b / I_a^b in Ohms
Base field power	P_f^b	=	$1.5 (P_a^b / 3)$ in Watts
Base field current	I_f^b	=	$I_a^b X_{md} / X_{fd}$ in DC Amps where X_{md} and X_{fd} are in ohms
Base field voltage	V_f^b	=	P_f^b / I_f^b in DC Volts
Base field impedance	Z_f^b	=	V_f^b / I_f^b in Ohms
Base time	t^b	=	1 second (s)
Base electrical angle	θ_e^b	=	1 electrical radian (rad^e)
Base frequency	f^b	=	rated frequency (1/s)
Base electrical speed	ω^b	=	θ_e^b / t^b (rad^e/s)
Base electrical acceleration	α_e^b	=	ω_e^b / t^b (rad^e/s^2)

Base electrical torque is defined as that torque which produces base power at nominal electrical speed ω_0 (expressed in electrical radians /s).

Base electrical torque $M_e^b = P_a^b / \omega_0$

APPENDIX B

FUNDAMENTAL MACHINE CONSTANTS AND SYSTEM DATA

B1 Introduction

The following section contains the fundamental quantities of the synchronous machine that are required for the study of the practical machine. The thorough derivation of the actual quantities is dealt with in [ADKINS].

In chapter 2 it was shown that;

$$u_d = p\psi_d + \omega\psi_q + R_a i_d \tag{B.1}$$

$$u_q = -\omega\psi_d + p\psi_q + R_a i_q \tag{B.2}$$

$$M_e = \frac{\omega_o}{2}\left(\psi_d i_q - \psi_q i_d\right) \tag{B.3}$$

It can be shown [ADKINS] that the relationship between the Laplace transforms of ψ_d, I_d and u_f is of the form

$$\psi_d = \frac{X_d(p)}{\omega_0} i_d + \frac{G(p)}{\omega_0} u_f \tag{B.3}$$

and between ψ_q and i_q is

$$\psi_q = \frac{X_q(p)}{\omega_0} i_q \tag{B.4}$$

The terms $X_d(p)$, $G(p)$ and $X_q(p)$ from eqns (B.3) and (B.4) can be expressed in terms of fundamental constants as;

$$X_d(p) = \frac{\left(1+T_d'p\right)\left(1+T_d''p\right)}{\left(1+T_{d0}'p\right)\left(1+T_{d0}''p\right)} X_d \tag{B.5}$$

$$G(p) = \frac{(1 + T_{kd} p)}{(1 + T_{d0}' p)(1 + T_{d0}'' p)} \frac{X_{md}}{R_f} \tag{B.6}$$

$$X_q(p) = \frac{(1 + T_q'' p)}{(1 + T_{q0}'' p)} X_q \tag{B.7}$$

B2 Fundamental machine constants

R_a = armature resistance

R_f = field resistance

R_{kd} = direct-axis damper resistance

R_{kq} = quadrature-axis damper resistance

$X_{md} = \omega_0 L_{md}$ = direct-axis magnetising reactance

$X_{mq} = \omega_0 L_{mq}$ = quadrature-axis magnetising reactance

$X_a = \omega_0 L_a$ = armature leakage reactance

$X_f = \omega_0 L_f$ = field leakage reactance

$X_{kd} = \omega_0 L_{kd}$ = direct-axis damper leakage reactance

$X_{kq} = \omega_0 L_{kq}$ = quadrature-axis damper leakage reactance

B3 Time Constants

$$T_{d0}' = \frac{1}{\omega_0 R_f}(X_f + X_{md}) \tag{B.8}$$

= direct-axis transient open circuit time constant

$$T_d' = \frac{1}{\omega_0 R_f}\left(X_f + \frac{X_{md} X_a}{X_{md} + X_a}\right) \tag{B.9}$$

= direct-axis transient short-circuit time constant

$$T_{do}'' = \frac{1}{\omega_0 R_{kd}}\left(X_{kd} + \frac{X_{md} X_f}{X_{md} + X_f}\right) \tag{B.10}$$

= direct-axis subtransient open-circuit time constant

$$T_d'' = \frac{1}{\omega_0 R_{kd}}\left(X_{kd} + \frac{X_{md} X_a X_f}{X_{md} X_a + X_{md} X_f + X_a X_f}\right) \tag{B.11}$$

= direct-axis subtransient short-circuit time constant

$$T_{q0}'' = \frac{1}{\omega_0 R_{kq}}\left(X_{kq} + X_{mq}\right) \tag{B.12}$$

= quadrature-axis subtransient open circuit time constant

$$T_q'' = \frac{1}{\omega_0 R_{kq}}\left(X_{kq} + \frac{X_{mq} X_a}{X_{mq} + X_a}\right) \tag{B.13}$$

= quadrature-axis subtransient short-circuit time constant

$$T_{kd} = \frac{X_{kd}}{\omega_0 R_{kd}} \tag{B.14}$$

= direct-axis damper leakage time constant

B4 Derived Reactances

$$X_d = X_a + X_{md} \tag{B.15}$$

= direct-axis synchronous reactance

$$X_d' = X_d \frac{T_d'}{T_{d0}'} = X_a + \frac{X_{md} X_f}{X_{md} + X_f} \tag{B.16}$$

= direct-axis transient reactance

$$X_d'' = X_d \frac{T_d' T_d''}{T_{d0}' T_{d0}''} = X_a + \frac{X_{md} X_f X_{kd}}{X_{md} X_f + X_f X_{kd} + X_{md} X_{kd}} \tag{B.17}$$

= direct-axis subtransient reactance

$$X_q = X_a + X_{mq} \tag{B.18}$$

= quadrature-axis synchronous reactance

$$X_q'' = X_q \frac{T_q''}{T_{q0}''} = X_a + \frac{X_{mq} X_{kq}}{X_{mq} + X_{kq}} \tag{B.19}$$

= quadrature-axis subtransient reactance

When a series impedance (R_e,X_e) is connected to the machine, the series impedance is added to the internal impedance (R_a, X_a) to yield

$$R_t = R_a + R_e \quad (B.20)$$

$$X_t = X_a + X_e \quad (B.21)$$

and this would cause a corresponding change to those equations listed above that contain X_a, R_a

B5 System Data

The system base apparent power is chosen as 100 MVA and the system rated frequency is chosen as 50Hz. All parameters are given in per-unit unless otherwise stated

Table B1 *- Initial system conditions specified to the loadflow*

Quantity	Magnitude (pu)	Angle (degrees)
Voltage – generator (U_{gen})	1.03	9.3
Voltage - motor (U_{mot})	1.03	-3.9
Voltage – Infinite bus (U_{inf})	1.03	0
Real electrical power - generator (P_{gen})	0.67	
Reactive electrical power - generator (Q_{gen})	0.04	
Real electrical power - motor (P_{mot})	-0.42	
Reactive electrical power - motor (Q_{mot})	0.06	
Load LD_1 – real electrical power	0.05	
Load LD_2 – real electrical power	0.05	

Table B2 *- Transmission line impedance data*

Line	R	X
L_{12}	0.02	0.67
L_{13}	0.02	0.67
L_{23}	0.02	0.67

Table B3 *- Machine parameters and time constants.*

	Generator	**Motor**
Machine base MVA	100	100
X_d	1.96	2.09
X_q	1.75	1.98
X'_d	0.228	0.205
X'_q	0.413	0.513
$X''_d=X''_q=X''$	0.144	0.164
X_l	0.11	0.11
T_{d0}'(s)	16.8	5.3
T_{do}''(s)	0.0115	0.0331
T_{qo}' (s)	0.155	0.1405
T_{qo}'' (s)	0.0115	0.0541
H	5.1	5.57

Table B4 *– Simplified Excitation system data*

	Generator	**Motor**
T_R (s)	0.01	0.01s
K_a	250	200
T_a (s)	0.2	0.2s

Table B5 *- Time constants of the conventional power system stabiliser.*

T_w (s)	10 s
T_1 (s)	0.219 s
T_2 (s)	0.029 s
T_3 (s)	0.219 s
T_4 (s)	0.029 s
K_{stab}	35
Upper output limit	+0.2pu
Lower output limit	-0.1pu

APPENDIX C

CALCULATION OF INITIAL CONDITIONS FOR THE STATE SPACE EQUATIONS

In order to calculate the initial conditions of eqn (2.83), it is assumed that the equations at t_0 are in equilibrium. Equilibrium points are defined as those points in the state space where the derivative terms of eqn (2.64) are simultaneously equal to zero. The behaviour of any dynamic system described by a set of *n* first order non linear ordinary differential equations is of the form given in (2.63) and it follows that under equilibrium or steady state that

$$f(x_0) = 0 \tag{C.1}$$

With all the derivative terms equal to zero, eqn (2.64) can now be expressed in matrix form as

$$[0] = [A][x] + [B][u] + [F] \tag{C.2}$$

hence the initial conditions for the state variables x, for any given set of inputs u, can be given by the

$$[x] = [A]^{-1}[B][u] - [F] \tag{C.3}$$

In equation (2.83) the non-linear terms are multiplied by $\dot{\delta}$, which is zero under steady state, hence eqn (C.3) can be expressed as

$$[x] = [A]^{-1}[B][u] \tag{C.4}$$

APPENDIX D

SMALL SIGNAL STABILITY

D1 Linearisation of the state matrix

The behavior of a power system may be described by a set of n non-linear ordinary differential equations expressed in vector-matrix form as;

$$\dot{\mathbf{x}} = \mathbf{f}(\mathbf{x}, \mathbf{u}, t) \tag{D.1}$$

If the derivatives of the states are not explicit functions of time, the system is said to be autonomous and eqn D.1 can be expressed as

$$\dot{\mathbf{x}} = \mathbf{f}(\mathbf{x}, \mathbf{u}) \tag{D.2}$$

and the input variables

$$\dot{\mathbf{y}} = \mathbf{g}(\mathbf{x}, \mathbf{u}) \tag{D.3}$$

If the initial state vector is $\mathbf{x}_0$ and the input vector corresponding to the equilibrium point is $\mathbf{u}_0$, then eqn D.2 is

$$\dot{\mathbf{x}}_0 = \mathbf{f}(\mathbf{x}_0, \mathbf{u}_0) = 0 \tag{D.4}$$

The system can be perturbed at the above state by letting

$$\mathbf{x} = \mathbf{x}_0 + \Delta\mathbf{x} \qquad \mathbf{u} = \mathbf{u}_0 + \Delta\mathbf{u} \tag{D.5}$$

where the prefix Δ denotes a small deviation. The new state must satisfy eqn D.2 hence

$$\begin{aligned} \dot{\mathbf{x}} &= \dot{\mathbf{x}}_0 + \Delta\dot{\mathbf{x}} \\ &= \mathrm{f}\left[\left(\mathrm{x}_0 + \Delta\mathrm{x}_0\right), \left(\mathrm{u}_0 + \Delta\mathrm{u}_0\right)\right] \end{aligned} \tag{D.6}$$

As the perturbations are deemed to be small, the nonlinear functions can be expressed in terms of Taylor series expansion. With the terms involving second and higher order powers of Δx and Δu neglected eqn D.6 may be written as

$$\begin{aligned} \dot{x}_i &= x_{i0} + \Delta x_i = f_i\left[\left(\mathbf{x}_0 + \Delta x\right), \left(u_0 + \Delta u\right)\right] \\ &= f_i\left(x_0, u_0\right) + \frac{\partial f_i}{\partial x_1}\Delta x_1 + \ldots + \frac{\partial f_i}{\partial x_n}\Delta x_n + \frac{\partial f_i}{\partial u_1}\Delta u_1 + \ldots + \frac{\partial f_i}{\partial u_r}\Delta u_r \end{aligned} \tag{D.7}$$

Since $\dot{x}_{i0} = f_i\left(\mathbf{x}_0, \mathbf{u}_0\right)$, the derivative of the perturbed state variable is

$$\Delta \dot{x}_i = \frac{\partial f_i}{\partial x_1}\Delta x_1 + \ldots + \frac{\partial f_i}{\partial x_n}\Delta x_n + \frac{\partial f_i}{\partial u_1}\Delta u_1 + \ldots + \frac{\partial f_i}{\partial u_r}\Delta u_r \tag{D.8}$$

with i = 1,2,…,*n*. In a similar manner the equation for the perturbed input variable may be given as

$$\Delta y_i = \frac{\partial g_j}{\partial x_1}\Delta x_1 + \ldots + \frac{\partial g_j}{\partial x_n}\Delta x_n + \frac{\partial g_j}{\partial u_1}\Delta u_1 + \ldots + \frac{\partial g_j}{\partial u_r}\Delta u_r \tag{D.9}$$

with j = 1,2,…,*m*. The linearised forms of equations D.8 and D.9 are expressed as

$$\Delta \dot{\mathbf{x}} = \mathbf{A}\Delta\mathbf{x} + \mathbf{B}\Delta\mathbf{u} \tag{D.10}$$

$$\Delta \dot{\mathbf{y}} = \mathrm{C}\Delta\mathbf{x} + \mathrm{D}\Delta\mathbf{u} \tag{D.11}$$

where the state or plant matrix **A,** of size *nxn*, is given by

$$\mathbf{A} = \begin{bmatrix} \frac{\partial f_1}{\partial x_1} & \cdots & \frac{\partial f_1}{\partial x_n} \\ \vdots & \ddots & \vdots \\ \frac{\partial f_n}{\partial x_1} & \cdots & \frac{\partial f_n}{\partial x_n} \end{bmatrix} \tag{D.12}$$

The input or control matrix **B**, of size *nxr* is given by

$$\mathbf{B} = \begin{bmatrix} \frac{\partial f_1}{\partial u_1} & \cdots & \frac{\partial f_1}{\partial u_r} \\ \vdots & \cdots & \vdots \\ \frac{\partial f_n}{\partial u_1} & \cdots & \frac{\partial f_n}{\partial u_r} \end{bmatrix} \tag{D.13}$$

The output matrix **C**, of size *mxn* is given by

$$\mathbf{C} = \begin{bmatrix} \frac{\partial g_1}{\partial x_1} & \cdots & \frac{\partial g_1}{\partial x_n} \\ \vdots & \cdots & \vdots \\ \frac{\partial g_m}{\partial x_1} & \cdots & \frac{\partial g_m}{\partial x_n} \end{bmatrix} \tag{D.14}$$

and the feedforward matrix **D** of size *mxr*, which defines the portion of the input that appears directly on the output, is given by

$$\mathbf{D} = \begin{bmatrix} \frac{\partial g_1}{\partial u_1} & \cdots & \frac{\partial g_1}{\partial u_r} \\ \vdots & \cdots & \vdots \\ \frac{\partial g_m}{\partial u_1} & \cdots & \frac{\partial g_m}{\partial u_r} \end{bmatrix} \tag{D.15}$$

To obtain eqns D.10 and D.11 in the frequency domain, the Laplace transform is taken of the equations yielding

$$s\Delta\mathbf{x}(s) - \Delta\mathbf{x}(0) = \mathbf{A}\Delta\mathbf{x}(s) + \mathbf{B}\Delta\mathbf{u}(s) \tag{D.16}$$

$$\Delta\mathbf{y}(s) = \mathbf{C}\Delta\mathbf{x}(s) + \mathbf{D}\Delta\mathbf{u}(s) \tag{D.17}$$

The above equations can be represented in a block diagram as shown in Figure D1, where the initial conditions $\Delta\mathbf{x}(0)$are assumed to be zero.

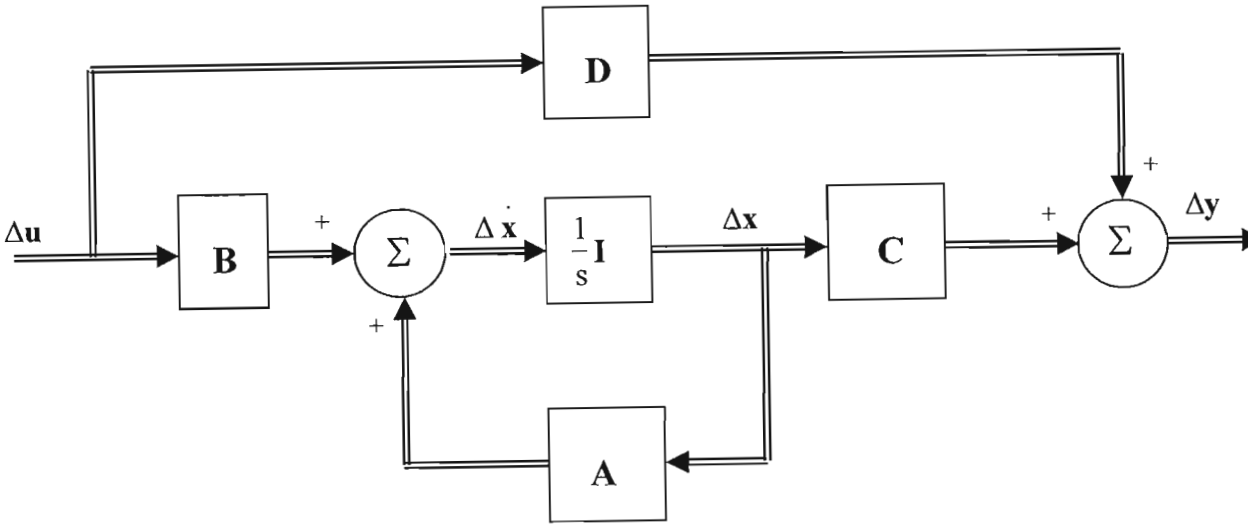

Figure D1 – Block diagram of the state-space representation

The formal solution of the state equations can be obtained by solving for $\Delta\mathbf{x}(s)$ and substituting for $\Delta\mathbf{y}(s)$. From eqn D.16

$$(s\mathbf{I}-\mathbf{A})\Delta\mathbf{x}(s)=\Delta\mathbf{x}(0)+\mathbf{B}\Delta\mathbf{u}(s) \tag{D.18}$$

Solving for $\Delta\mathbf{x}(s)$,

$$\begin{aligned}\Delta\mathbf{x}(s)&=(s\mathbf{I}-\mathbf{A})^{-1}\left[\Delta\mathbf{x}(0)+\mathbf{B}\Delta\mathbf{u}(s)\right]\\&=\frac{\text{adj}(s\mathbf{I}-\mathbf{A})}{\det(s\mathbf{I}-\mathbf{A})}\left[\Delta\mathbf{x}(0)+\mathbf{B}\Delta\mathbf{u}(s)\right]\end{aligned} \tag{D.19}$$

and solving for $\Delta\mathbf{y}(s)$ yields

$$\Delta\mathbf{y}(s)=\mathbf{C}\frac{\text{adj}(s\mathbf{I}-\mathbf{A})}{\det(s\mathbf{I}-\mathbf{A})}\left[\Delta\mathbf{x}(0)+\mathbf{B}\Delta\mathbf{u}(s)\right]+\mathbf{D}\Delta\mathbf{u}(s) \tag{D.20}$$

The poles of the $\Delta\mathbf{x}(s)$ and $\Delta\mathbf{y}(s)$ are the roots of the equation given by

$$\det(s\mathbf{I}-\mathbf{A})=0 \tag{D.21}$$

and the values of s which satisfy eqn D.21 are known as the *eigenvalues* of the state matrix **A**.

D2 Eigenproperties of the State Matrix

D2.1 Eigenvalues

The eigenvalues of a matrix are given by the value of the scalar parameter λ for which there exist non-trivial solutions, i.e. other than ϕ=0 to the equation

$$\mathbf{A}\phi = \lambda\phi \tag{D.22}$$

where

A is a *nxn* real matrix for the power system

ϕ is a *nx1* vector

To calculate the eigenvalues, eqn D.22 can be written as

$$(\mathbf{A} - \lambda\mathbf{I})\phi = 0 \tag{D.23}$$

and for a non-trivial solution

$$\det(\mathbf{A} - \lambda\mathbf{I})\phi = 0 \tag{D.24}$$

Expansion of the determinant gives the characteristic equation where the n solutions of $\lambda=\lambda_1,\lambda_2,\ldots,\lambda_v$ are called the eigenvalues of **A.** Eigenvalues may be real or complex and when the matrix is real, complex eigenvalues occur in conjugate pairs.

D2.2 Eigenvectors

The n-column vector ϕ_i which satisfies equation D.22 is called the right eigenvector of A and is associated with eigenvalue λ_i. Equation D.22 can be written as

$$\mathbf{A}\phi_i = \lambda_i\phi_i \qquad i = 1,2,\ldots,n \tag{D.25}$$

where the eigenvector ϕ_i has the form given by

$$\phi_i = \begin{bmatrix} \phi_{1i} \\ \phi_{2i} \\ \vdots \\ \phi_{ni} \end{bmatrix} \tag{D.26}$$

Since eqn D.23 is homogenous, eigenvectors are determined only to within scalar multipliers as $k\phi_i$ (where k is a scalar) is also a solution. The left eigenvector associated with eigenvalue λ_i is defined by ψ_i , a n-row vector which satisfies

$$\psi_i A = \lambda_i \psi_i \qquad i = 1,2,\ldots,n \tag{D.27}$$

The left and right eigenvectors corresponding to different eigenvalues are orthogonal, i.e. if λ_i is not equal to λ_j then

$$\psi_i \phi_i = 0 \tag{D.28}$$

However in the case of eigenvectors corresponding to the same eigenvalue, the solution is now given by

$$\psi_i \phi_i = C_i \tag{D.29}$$

where C_i is a non-zero constant. Normalized eigenvectors are given by

$$\psi_i \phi_i = 1 \tag{D.30}$$

D2.3 Modal Matrices

In order to express the eigenproperties of **A** succinctly, it is convenient to introduce the following matrices

$$\Phi = \begin{bmatrix} \phi_1 & \phi_2 & \cdots & \phi_n \end{bmatrix} \tag{D.31}$$

$$\Psi = \begin{bmatrix} \psi_1^T & \psi_2^T & \cdots & \psi_n^T \end{bmatrix}^T \tag{D.32}$$

Λ = diagonal matrix with the eigenvalues $\lambda_1, \lambda_2, \ldots, \lambda_n$ as diagonal elements (D.33)

Each of the matrices in eqns D.31 to D.33 have dimensions of nxn. Equations D.27 and D.30 can be expressed as

$$\mathbf{A}\Phi = \Phi\Lambda \tag{D.34}$$

$$\Psi\Phi = I \qquad \Psi = \Phi^{-1} \tag{D.35}$$

Equation D.34 can also be expressed as

$$\Phi^{-1}\mathbf{A}\Phi = \Lambda \tag{D.36}$$

D2.4 Free Motion of a Dynamic System

From equation D.10, the free motion of a system with no input can be expressed as

$$\Delta \dot{x} = \mathbf{A}\Delta x \tag{D.37}$$

When **A** is real, i.e. derived from physical parameters, the rate of change of each state variable is a linear combination of all state variables. As a result cross coupling between states makes it difficult to isolate the parameters that influence the motion in a significant way. In order to eliminate the effect of cross coupling between state variables, a new state vector **z** is introduced, related to the original state vector by

$$\Delta x = \Phi \mathbf{z} \tag{D.38}$$

where Φ is the modal matrix of **A** defined by eqn D.31. Using eqn D.38, eqn D.37 can be expressed as

$$\Phi \dot{\mathbf{z}} = \mathbf{A}\Phi\mathbf{z} \tag{D.39}$$

Using equations D.39 and D.36, the new state equation can be expressed as

$$\dot{\mathbf{z}} = \Phi^{-1}\mathbf{A}\Phi\mathbf{z} = \Lambda\mathbf{z} \tag{D.40}$$

The major difference between eqns D.40 and D.37 is that **A** is, generally, non-diagonal where as Λ is a diagonal matrix. Equation D.40 represents n uncoupled first order equations, given as

$$\dot{z} = \lambda_i z_i \qquad 1 = 1,2,\ldots,n \tag{D.41}$$

The solution of eqn D.41 with respect to time t is given by;

$$z_i(t) = z_i(0)e^{\lambda_i t} \tag{D.42}$$

where $z_i(0)$ is the initial value of z_i.

Expressing eqn D.38 in terms of the original state vector is given by

$$\begin{aligned}\Delta x &= \Phi z \\ &= \begin{bmatrix}\phi_1 & \phi_2 & \cdots & \phi_n\end{bmatrix}\begin{bmatrix}z_1(t)\\ z_2(t)\\ \cdots\\ z_n(t)\end{bmatrix}\end{aligned} \tag{D.43}$$

which implies that Δx can be expressed with respect to time as

$$\Delta x(t) = \sum_{i=1}^{n} \phi_i z_i(0) e^{\lambda_i t} \tag{D.44}$$

From eqn D.43, we have

$$\begin{aligned}\mathbf{z}(t) &= \Phi^{-1}\Delta x(t) \\ &= \Psi \Delta x(t)\end{aligned} \tag{D.45}$$

which implies that

$$z_i(t) = \psi_i \Delta x(t) \tag{D.46}$$

At t=0, the initial conditions of eqn D.46 can be expressed as

$$z_i(0) = \psi_i \Delta x(0) \tag{D.47}$$

by using c_1 to denote the scalar product $\psi_i \Delta x(0)$, eqn D.44 can be expressed as

$$\Delta x(t) = \sum_{i=1}^{n} \phi_i c_i e^{\lambda_i t} \tag{D.48}$$

Expanding eqn D.48, we get the time response for the ith state variable as

$$\Delta x(t) = \phi_{i1} c_1 e^{\lambda_1 t} + \phi_{i2} c_2 e^{\lambda_2 t} + \ldots + \phi_{in} c_n e^{\lambda_n t} \tag{D.49}$$

Equation D.49 expresses the free motion of a system in terms of the eigenvalues, left and right eigenvectors. The free motion response is given by a linear combination of n dynamic modes corresponding to the n eigenvalues of the state matrix. The magnitude of the excitation of the ith mode is given by the scalar product, $c_i = \psi_i \Delta x(0)$. If the vector representing the initial conditions is not an eigenvector, it can be represented by a linear combination of the n eigenvectors. The response of the system will be the sum of n responses.

The eigenvalues of the system help determine the stability of the system. A real eigenvalue corresponds to a non-oscillatory mode. A negative real eigenvalue represents a decaying mode whereas a positive real eigenvalue represents aperiodic instability. The larger the magnitude of the eigenvalue, the faster the decay or increase.

Complex eigenvalues occur in conjugate pairs, with each pair corresponding to an oscillatory mode. The real component of the eigenvalue represents the damping of the oscillation, with a negative real value indicating a damped oscillation and a positive real value representing an oscillation of increasing amplitude. The imaginary component gives the frequency of the oscillation. Thus for a complex pair of eigenvalues;

$$\lambda = \sigma \pm j\omega \tag{D.50}$$

The actual or damped frequency of oscillation in Hz is given by

$$f = \frac{\omega}{2\pi} \tag{D.51}$$

and the rate of decay f the oscillation or *damping ratio* is given by

$$\zeta = \frac{-\sigma}{\sqrt{\sigma^2 + \omega^2}} \tag{D.52}$$

D2.5 Participation Factor

When using the left and right eigenvectors individually to identify the relationship between states and the modes, the elements of the eigenvectors are dependent on the units and scaling associated with the state variables. The participation matrix is used as a measure of association between state variables and modes, and is defined by

$$\mathbf{P} = \begin{bmatrix} \mathbf{p}_1 & \mathbf{p}_2 & \cdots & \mathbf{p}_n \end{bmatrix} \tag{D.53a}$$

where

$$\mathbf{p}_i = \begin{bmatrix} p_{1i} \\ p_{2i} \\ \vdots \\ p_{ni} \end{bmatrix} = \begin{bmatrix} \phi_{1i}\psi_{i1} \\ \phi_{2i}\psi_{i2} \\ \vdots \\ \phi_{ni}\psi_{in} \end{bmatrix} \tag{D.53b}$$

where

ϕ_{ki} = the element on the *k*th row and *i*th column of the modal matrix Φ

= the *kth* entry of the right eigenvector ϕ_i

ψ_{ik} =the element on the *i*th row and *k*th column of the modal matrix Ψ

= the *k*th entry of the left eigenvector ψ_i

The element $p_{ki} = \phi_{ki}\psi_{ik}$ is termed the participation factor and is a measure of the relative participation of the *k*th state variable in the *i*th mode and vice versa. Due to the multiplication of the elements from the left and right eigenvectors, participation factors are dimensionless. In view of the eigenvector normalisation, the sum of the participation factors associated with any mode or with any state is equal to 1.

APPENDIX E

GENERAL FUZZY OPERATORS

E1 Introduction

The classical and more commonly used fuzzy operators have been defined in chapter 4. This appendix gives a more general description of fuzzy operators and the basic requirements that these operators must comply with.

E2 Fuzzy operators

The intersection of two fuzzy sets X and Y is specified in general by a function T which aggregates two degrees of membership as in eqn (E.1)

$$\mu_{X\cap Y}(x) = T(\mu_X(x),\mu_Y(x)) = \mu_X(x) \otimes \mu_Y(x) \qquad (E.1)$$

where $\otimes$ is a binary operator for the function T. These fuzzy intersection operators are usually referred to as T-norm (triangular norm) operators.

A T-norm operator is a two-place function that meets the following basic requirements;

(i) Boundary : $T(0,0) = 0,\ T(x,1) = T(1,x) = x$

(ii) Monotonicity: $T(x,y) <= T(z,p)$ if $x <= z$ and $b <= p$

(iii) Commutativity: $T(x,y) = T(y,x)$

(iv) Associativity: $T(x,T(y,z)) = T(T(x,y),z)$

Requirement (i) imposes the correct generalization to crisp sets. The second requirement implies that a decrease in the degree of membership value in X or Y cannot produce an increase in the degree of membership value in X intersection Y. The third requirement indicates that the operators are indifferent to the order of the fuzzy sets to be combined. Requirement (iv) allows the intersection of any number of sets in any order of pairwise groupings.

The fuzzy union operator is specified in general by a function S, and is given in eqn (E.2).

$$\mu_{X\cup Y}(x) = S(\mu_X(x),\mu_Y(x)) = \mu_X(x) \oplus \mu_Y(Y) \qquad (E.2)$$

where $\oplus$ is a binary operator for the function S. These fuzzy intersection operators are usually referred to as T-conorm or S-norm operators which satisfy the following basic requirements;

(i) Boundary: $S(1,1) = 1, S(x,0) = S(0,x) = x$

(ii) Monotonicity: $S(x,y) <= S(z,p)$ ia $x <= z$ and $y <= p$

(iii) Commutativity: $S(x,y) = S(y,x)$

(iv) Associativity: $S(a,S(y,z) = S(S(x,y),z)$

S-norm operators have the same justification as for T-norm operators.

REFERENCES

[ADKINS] Adkins B, Harley RG, "The General theory of Alternating Current Machines: Application to Practical Problems", Chapman and Hall, London, 1975, ISBN 0-412-12080-1.

[BOLLING] Bollinger KE, Mistr AF Jr., "PSS Tuning at the Virginia Electric and Power Co. Bath County Pumped Storage Plant", IEEE Transactions on Power Systems, Vol.4, No. 2, May 1989, Pages 566-573.

[BANDEM] Bandemer H, Gottwald S, " Fuzzy Sets, Fuzzy Logic, Fuzzy Methods with Applications", John Wiley and Sons, Chichester, 1995, ISBN 0471956368.

[CHEN] Chen GP, Malik OP, Hope GS, Qin YH, Xu GY, "*An adaptive Power System Stabilizer based on the Self-Optimizing Pole Shifting Control Strategy*", IEEE Transactions on Energy Conversion, Vol 8, No 4, December 1993, Pages 639-645.

[CHOW] Chow JH, " *Power System Toolbox, A collection of m-files for use with Matlab®*", Cherry Tree Scientific Software, 1993, RR#5, Colborne, Ontario, KOK 1S0, Canada.

[DEMELLO] Demello FP, Concordia C, "*Concepts of Synchronous machine Stability as affected by Excitation Control*", IEEE Transactions on Power Apparatus and Systems, Vol Pas-88, No 4, April 1969, Pages 316-329

[EL-MET1] El-Metwally KA, Malik OP, "*Fuzzy Logic Power System Stabiliser*", IEE Proceedings-Generation, Transmission, Distribution, Vol 142, No 3, May 1995, Pages 277-281.

[EL-MET2] El-Metwally KA, Hancock GC, Malik OP, "*Implementation of a Fuzzy Logic PSS Using Micro-controller and Experimental Results*", IEEE Transactions on Energy Conversion, Vol 11, No 1, March 1996, Pages 91-96.

[FARMER] Farmer RG, Agrawal BL, "*State-of-the-Art Technique for Power System Stabilizer Tuning*", IEEE Transactions on Power Apparatus and Systems, Vol PAS-102, No 3, March 1983, Pages 699-709.

[HASSAN1] Hassan MAM, Malik OP, Hope GS, " *A fuzzy Logic Based Self-tuned Power System Stabilizer*", Third International Conference on Power System Monitoring and Control, sponsored by IEE, London, UK, June 1991, Conference publication No. 336, Pages 146-151.

[HASSAN2] Hassan MAM, Malik OP, Hope GS, " *A Fuzzy Logic Based Stabilizer for a Synchronous Machine*", IEEE Transactions on Energy Conversion, Vol 6, No 3, Sept 1991, Pages 407-413.

[HASSAN3] Hassan MAM, Malik OP, "*Implementation and laboratory Test Results for a Fuzzy Logic Based Self-Tuned Power System Stabilizer*", IEEE Transactions on Energy Conversion, Vol 8, No 2, June 1993, Pages 221-228.

[HIYAMA1] Hiyama T, "*Real Time Control of Micro-machine System using Micro-computer based Fuzzy Logic Power System Stabiliser*", IEEE Transactions on Energy Conversion, Vol 9, No 4, December 1994, Pages 724-731.

[HIYAMA2] Hiyama T, " *Robustness of Fuzzy Logic Power System Stabilisers Applied to Multimachine Power System*", IEEE Transactions on Energy Conversion, Vol 9, No 3, September 1994, Pages 451-458.

[HSU] Hsu YY, Chen CR, "*Tuning of Power System Stablizers Using Artificial Neural Network*", IEEE Transactions on Energy Conversion, Vol 6, No 4, December 1991, Pages 612-617

[KUNDUR1] Kundur P, "*Power System Stability and Control*", McGraw-Hill, United States of America, 1994, ISBN 0-07-035958-X.

[KUNDUR2] Kundur P, Klein M, Rogers G J, Zywo MS, "*Application of power system stabilizers for enhancement of overall stability*", IEEE Transactions on Power systems, Vol 4, No. 2, May 1989, Pages 614-626

[KOSKO] Kosko B, "*Neural Networks and Fuzzy Systems. A Dynamic approach to machine intelligence*", Prentice Hall, New Jersey, 1992, ISBN 0-13-612334-1

[LARSEN1] Larsen EV, Swann DA, "*Applying Power system Stabilizers, Part I: General Concepts*", IEEE Transactions on power Apparatus and Systems, Vol PAS-100, No.6, June 1981, Pages 3017-3024

[LARSEN2] Larsen EV, Swann DA, "*Applying Power System Stabilizers, Part II: Performance Objectives and Tuning Concepts*", IEEE Transactions on power Apparatus and Systems, Vol PAS-100, No.6, June 1981, Pages 3025-3033

[LARSEN3] Larsen EV, Swann DA, "*Applying Power System Stabilizers, Part III: Practical Considerations*", IEEE Transactions on power Apparatus and Systems, Vol PAS-100, No.6, June 1981, Pages 3034-3046

[MOODLEY1] Moodley GV, Harley RG, Jennings GD, Wishart MT, " *Fuzzy Logic Power System Stabilizer in Multimachine Stability Studies*", 1996 IEEE Africon, 4th Africon Conference in Africa, Stellenbosch, Volume II, Pages 843-848, ISBN 0-7803-3019-6

[MOODLEY2] Moodley GV, Jennings GD, Harley RG, " *Comparison of Fuzzy Logic and Conventional Power System Stabilizers in a Multimachine System*", Cigre Third Southern Africa Regional Conference - New Technologies for Effective Power Systems, Johannesburg, 20-21 May 1998, Session 8, ISBN 0-620-22515-7

[OGATA] Ogata K , "*Modern Control Engineering*", Prentice-Hall , ISBN: 0130432458, 1991

[PARK1] Park RH, " Two-Reaction Theory of Synchronous Machines", Transactions A.I.E.E, Vol 48, 1929, Page 716

[PARK2] Park RH, " Two-Reaction Theory of Synchronous Machines II", Transactions A.I.E.E, Vol 52, 1933, Page 352

[ROGER] Roger Jang JS, Gulley N, "*Fuzzy Logic Toolbox User's Guide*", The Math works Inc, January 1995, http://www.mathworks.com

[SAY] Say MG, " *Alternating Current Machines – 5th edition*", Longman Scientific & Technical, , Essex, 1983, ISBN 0-582-98875-6, Chapter 10, Page 366.

[SHI] Shi J, Herron LH, Kalam A, "*Design and Implementation of a PC-based Automatic Voltage Regulator and Fuzzy Logic Power System* Stabilizer", IEE 2nd International Conference on Advances in Power System Control, Operation and Management, December 1993, Hong Kong, Pages 293-298.

[SYED] Syed A Nasar, "*Theory and problems of Electric Machines and Electromechanics*", Schaums Outline Series, United States of America, 1981, ISBN 0-07-045886-3, Chapter 6.

[TOLIYAT] Toliyat H A, Javad A, Ghazi R, "*Design of Augmented Fuzzy Logic Power System Stabilizers to Enhance Power Systems Stability*", IEEE Transactions on Energy Conversion, Vol 11, No 1, March 1996, Pages 97-103.

[ZADEH1] Zadeh LA, "*Fuzzy Sets*", Information and Control, Vol 8, 1965, Pages 338 – 353

[ZADEH2] Zadeh LA, "*The concept of a linguistic variable and its application to approximate reasoning*", Parts 1,2 and 3, Information Sciences Vol 8, Pages 199-250, Pages 301-357, Vol 9 Pages 43-80

[ZHANG1] Zhang Y, Chen GP, Malik OP, Hope GS, "*An Artificial Neural Network Based Adaptive Power System Stabilizer*", IEEE Transactions on Energy Conversion, Vol 8, No 1, March 1993, Pages 71-77

[ZHANG2] Zhang Y, Malik OP, Chen GP, "*Artificial Neural Network Power System Stabilizers in Multi-machine Power System Environment*", IEEE Transactions on Energy Conversion, Vol 10, No 1, March 1995, Pages 147-155

Additional References – Material consulted though not explicitly referred to.

Chow JH, Cheung KW, " *A Toolbox for Power system Dynamics and Control Engineering Education and Research*", IEEE Transactions on Power Systems, Vol 7, No 4, November 1992, Pages 1559-1563

Cheng SJ, Malik OP, Hope GS, " *Damping of Multi-Modal Oscillations in Power Systems Using a Dual-Rate Adaptive Stabilizer*", IEEE Transactions On Power Systems, Vol 3, No 1, February 1988, Pages 101-107

Klein M, Rogers GJ, Kundur P, "*A Fundamental Study of Inter-Area Oscillations in Power Systems*", IEEE Transactions on Power Systems, Vol 6, No 3, August 1991, Pages 914-921

Klein M, Rogers GJ, Moorty S, Kundur P, "*Analytical Investigation of Factors Influencing Power System Stabilizers performance*", IEEE Transactions on Energy Conversion, Vol 7, No 3, September 1992, Pages 382-390

Mamdani EH, "*Application of Fuzzy Logic to Approximate Reasoning Using Linguistic Synthesis*", IEEE Transactions on Computers, Vol 26, No 12, Pages 1182-1191, 1997.

Padiyar KR, "*HVDC Power transmission Systems*", John Wiley & Sons, 1990, ISBN 0-470-21706-5

Rogers G, Chow J, "*Hands-On Teaching of Power System Dynamics*", IEEE Computer Applications in Power, 1995, Pages 12-16

Venayagamoorthy GK, "*An Implementation of a Continually Online Trained Artificial Neural Network Controller for a Turbogenerator*" December 1998, University of Natal, Durban, South Africa, MScEng Thesis

Venayagamoorthy GK, "*Adaptive Critic Based Neurocontrollers for Turbogenerators in a Multimachine Power System*", March 2002, University of Natal, Durban, South Africa, Doctoral Thesis.

Venayagamoorthy GK, Harley RG, "*Two Separate Continually Online-Trained Neurocontrollers for Excitation and Turbine Control of a Turbogenerator*", IEEE Transactions on Industry Applications, Volume: 38 Issue: 3, May/June 2002, Page(s): 887 –893.

Venayagamoorthy GK, Harley RG, Wunsch DC, "*Comparison of Heuristic Dynamic Programming and Dual Heuristic Programming Adaptive Critics for Neurocontrol of a Turbogenerator*", IEEE Transactions on Neural Networks, Volume: 13 Issue: 3, May 2002, Page(s): 764 -773.

Venayagamoorthy GK, Harley RG, "*A Continually Online Trained Neurocontroller for Excitation and Turbine Control of a Turbogenerator*", IEEE PES Transactions on Energy Conversion, Volume: 16 Issue: 16, September 2001, Page(s): 261 - 269.

Vu H, Agee JC, "*Comparison of Power System Stabilizers for Damping Local Mode Oscillations*", IEEE Transactions on Energy Conversion, Vol 8, No 3, September 1993, Pages 533-538

Zhang BS, Edmunds JM, "*Self-Organising Fuzzy Controller*", IEE Proceedings-D, Vol 139, No 5, September 1992, Pages 460-464.